EORGIA INSTITUTE OF TECHNOLOGY — OFFICE OF CONTRACT ADMINISTRATION

PROJECT ADMINISTRATION DATA SHEET

[X] ORIGINAL [ ] REVISION NO. ____

Project No. A-3571 GTRI/~~GKK~~ DATE 6/17/83

Project Director: Dr. A. R. Ravishankara/Dr. P.H. Wine ~~School~~/Lab EML/PSD

Sponsor: Chemical Manufacturers Association

Type Agreement: Agreement FC 83-449

Award Period: From 6/14/83 To 6/14/84 (Performance) 9/14/84 (Reports)

Sponsor Amount:	This Change	Total to Date
Estimated:	$	$
Funded:	$ 89,941	$ 89,941

Cost Sharing Amount: $ Cost Sharing No:

Title: "Laboratory Studies of Stratospheric Reactions"

ADMINISTRATIVE DATA OCA Contact Frank Huff X4820

1) Sponsor Technical Contact:

John C. Van Horn
Program Manager
Fluorocarbon Program
Chemical Manufacturers Association
2501 M Street, N.W.
Washington, D.C. 20037

2) Sponsor Admin/Contractual Matters:

Peter Ron Agnew
Controller
Chemical Manufacturers Association
2501 M Street, N.W.
Washington, D.C. 20037
(202) 887-1100

Defense Priority Rating: Military Security Classification:
(or) Company/Industrial Proprietary:

RESTRICTIONS

See Attached Supplemental Information Sheet for Additional Requirements.

Travel: Foreign travel must have prior approval — Contact OCA in each case. Domestic travel requires sponsor approval where total will exceed greater of $500 or 125% of approved proposal budget category.

Equipment: Title vests with GIT; however see Section 11 relative to restrictions over next ten years. See also inventory reporting requirement.

COMMENTS:

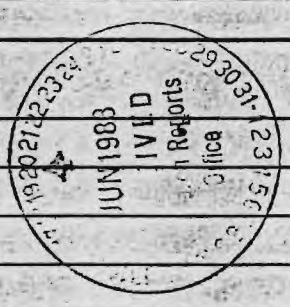

COPIES TO:

Project Director	Procurement/EES Supply Services	GTRI
Research Administrative Network	Research Security Services	Library
Research Property Management	Reports Coordinator (OCA)	Project File
Accounting	Research Communications (2)	Other I. Newton

GEORGIA INSTITUTE OF TECHNOLOGY OFFICE OF CONTRACT ADMINISTRATION

SPONSORED PROJECT TERMINATION/CLOSEOUT SHEET

Date April 9, 1985

Project No. A-3571 ~~School~~/Lab EML

Includes Subproject No.(s) —

Project Director(s) A. R. Ravishankara/ P. H. Wine GTRC /~~GIT~~

Sponsor Chemical Manufacturers Assn.

Title Laboratory Studies

Effective Completion Date: 6/14/84 (Performance) 9/14/84 (Reports)

Grant/Contract Closeout Actions Remaining:

- [ ] None
- [X] Final Invoice or Final Fiscal Report
- [ ] Closing Documents
- [ ] Final Report of Inventions
- [X] Property Inventory & Related Certificate
- [ ] Classified Material Certificate
- [ ] Other

Continues Project No. Continued by Project No. A-3886

COPIES TO:

Project Director
Research Administrative Network
Research Property Management
Accounting
Procurement/GTRI Supply Services
Research Security Services
Reports Coordinator (OCA)
Legal Services

Library
GTRC
Research Communications (2)
Project File
Other M. Heyser; A. Jones

FORM OCA 69 285

First Quarterly Progress Report on CMA Project:
"Laboratory Studies of Stratospheric Reactions"

Contract No. FC 83-449
Georgia Tech Project #A-3571

During the last three months most of our attention has been focussed on the NO_3 + NO reaction. Work on the NO_3 + NO_2 reaction has been delayed because our argon ion laser has been back at the factory since early July having a new plasma tube installed. The laser is expected to be back on-line around September 20. Dr. Craig Smith joined our group as a post-doctoral fellow on September 1. He will be working full time on NO_3 + NO_2 and measurements of temperature dependent NO_3 absorption cross sections. Hence, we expect significant progress on these fronts during the next few months.

A large number of experiments have been carried out on the NO_3 + NO reaction using laser induced fluorescence (LIF) detection of NO_3 as the kinetic probe. Two significant problems have been encountered. First, the sensitivity for detecting NO_3 by LIF is lower than we initially thought because the radiative lifetime (recently measured by Nelson, Pasternack and McDonald, J. Chem. Phys., in press) is $\sim$340 μs--a factor of 300 longer than predicted based on the known integrated absorption cross section and ground state geometry. Fluorescence quenching by He and HNO_3 is found to be very efficient which, coupled with the long radiative lifetime, leads to fluorescence quantum yields under typical flow tube conditions of less than 1%. To overcome this problem, we are attempting to further optimize our NO_3 detection sensitivity and also to

increase the overall system pumping speed. Increased pumping speed allows experiments to be carried out under pseudo first order conditions with higher initial NO_3 concentrations, since higher reactant concentrations can be employed to obtain measurable decay rates. Also, we are exploring the possibility of using LIF detection of the NO_2 product as the kinetic probe.

A second problem which has been encountered in the NO_3 + NO experiments is related to the chemistry in the F atom source. The F_2/He microwave discharge produces significant quantities of O atoms. At high initial NO_3 concentrations such as those employed in the absorption cross section measurements, O atoms are rapidly consumed by the reaction $O + NO_3 \xrightarrow{M} NO_2$. However, at the low NO_3 levels employed to study the kinetics of the fast NO_3 + NO reaction, O atoms survive down the entire length of the flow tube and into the detection zone. One problem which results is a significantly enhanced background signal which is attributable to the reaction $O+NO \xrightarrow{M} NO_2^* + h\nu$. Also, NO_3 may be removed by O and NO simultaneously, thus complicating the kinetic analysis needed to extract the desired NO_3 + NO rate coefficient. To overcome these problems, we are experimenting with two new F atom sources: (1) H atom production followed by the fast reaction $H+F_2 \rightarrow F + HF$ and (2) thermal dissociation of F_2. Neither of these sources is expected to produce significant levels of O atoms. The thermal source may also prove very useful in the $NO_3 + NO_2 + M$ study because, if successful, it would allow the desired buffer gas, M, to be employed in the source; with discharge sources, on the other hand, if N_2 is the desired buffer gas it is necessary to use He or Ar in the F atom source and then correct the $NO_3 + NO_2 + N_2$

data for the contribution from the $NO_3 + NO_2 + He$ (Ar) reaction.

During August, Dr. Wine attended the XIth International Conference on Photochemistry at the University of Maryland and presented a paper entitled "Photochemistry and Reaction Kinetics of the NO_3 Radical" by A. R. Ravishankara, A. Torabi, and P. H. Wine. CMA support was acknowledged.

Second Quarterly Progress Report on CMA Project:
"Laboratory Studies of Stratospheric Reactions"
Contract No. FC 83-449
Georgia Tech Project No. A-3571

During this quarter considerable progress has been made on the studies of the following two reactions:

$$NO_3 + NO_2 + M \rightarrow N_2O_5 + M,\ M = He,\ N_2 \qquad (1)$$

$$NO_3 + NO \rightarrow 2NO_2 \qquad (2)$$

A short description of the progress is given below.

(1) $NO_3 + NO_2 + M \rightarrow N_2O_5 + M$:

As mentioned in the previous report Dr. Craig Smith has been working on this reaction full-time as of September 1, 1983. The Argon ion laser was returned to us in September and the experiments have been proceeding smoothly. In this experiment, NO_3 is being detected using longpath laser absorption. NO_2 is maintained at a concentration much greater than NO_3 and the dependence of NO_3 concentration on reaction time is measured. From the data obtained the second order rate coefficient (k_1^{II}) for reaction (1) at a given pressure is measured. The attached graph shows the variation of k_1^{II} as a function of helium pressure. The point at 1 Torr is a composite of four separate measurements. At 1 Torr He, and at higher concentrations of NO_2, NO_2 itself acts as a third body. To account for this effect, a plot of k(first order)/$[NO_2]$ was plotted against $[NO_2]$. The

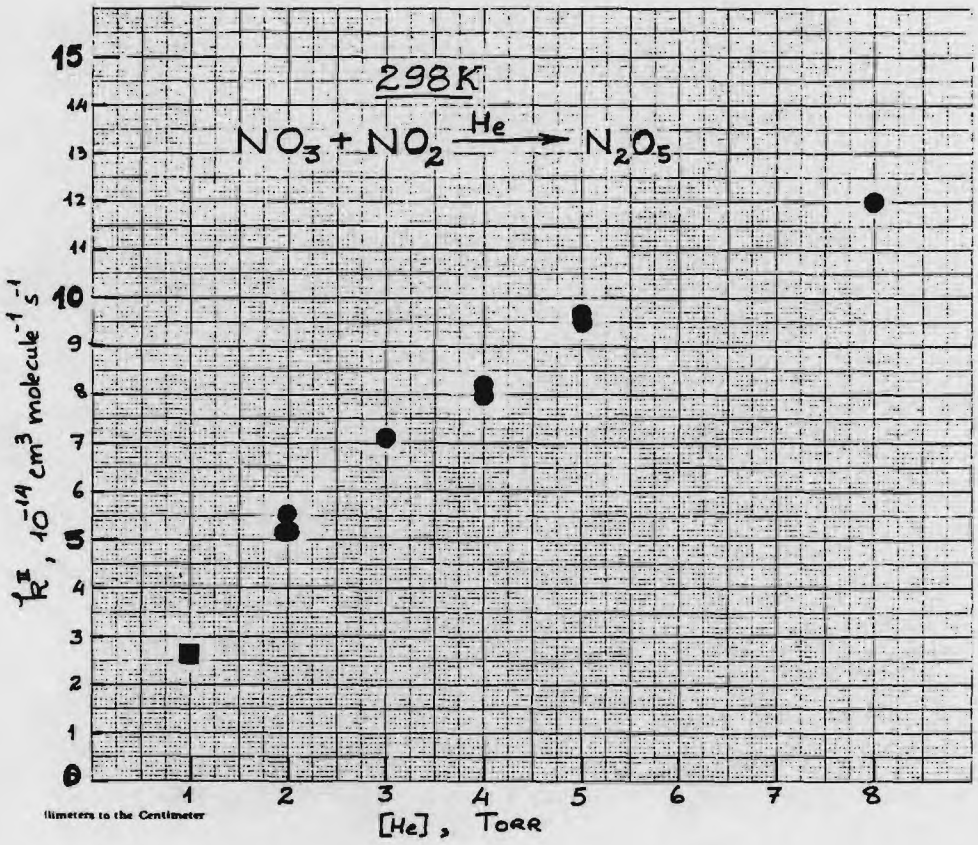

intercept gives the k_1^{II} for He while the slope gives the k^{III} (NO_2). The rectangular point is the intercept of such a plot and it reflects the value for He only. Since at higher pressures of He, k^{II} goes up and the required fraction of NO_2 goes down; consequently, this effect is not seen at pressures greater than 2 Torr. (We may treat the 2 Torr data in a fashion similar to the 1 Torr data at a later stage).

The next step is to carryout measurements of k_1^{II} with N_2 as the diluent gas. As of December 1, these

experiments will begin.

(2) $NO_3 + NO \rightarrow 2NO_2$:

The sensitivity for NO_3 detection has been improved such that 2×10^{10} cm^{-3} of NO_3 can be detected. Currently we have a problem in that the measured rate coefficient is dependent on the initial NO_3 concentration. Moreover, we see a residual signal after all NO_3 has reacted. An excitation spectrum of this species shows structure very similar to NO_2 and the lifetime is also similar. We are not certain as to where that much NO_2 is coming from. We have traced the problem to the NO_3 source. $F + HNO_3$ source works extremely well at higher NO_3 concentration where all reactive radicals are scavenged quickly. When the concentration of F is reduced to less than 10^{12} cm^{-3}, all radical-radical reactions slow down and cause the reported problem. To quantify effects of free radical reactions, we are currently detecting $O(^3P)$ resonance fluorescence. It is expected that we can track down the problem soon. Concurrently, a thermal fluorine atom source is being put together.

In addition to studies on NO_3 chemistry, in accordance with the contract modification, we have initiated the studies on $O(^3P)$ + ClO reaction. Since our source of ClO is the photolysis of a mixture of Cl_2 and O_3, it is necessary to measure the rate coefficient for $O(^3P)$ + Cl_2 reaction (as indicated in the project modification). $O(^3P)$ + Cl_2 reaction was at first studied at 298K to ensure the feasibility of the ClO production

method. The rate coefficient we obtained was approximately a factor of two slower than the literature value. In the past few weeks we have measured the temperature dependence of this reaction. The measured activation energy is much higher than previously reported. These measurements were carried out to ensure a thorough understanding of the O + ClO measurements. In addition, since the previous measurements seem to be in error, it seemed advisable to expend some time to complete this work. An Arrhenius plot of the results is shown below.

Currently, the set up for measuring O + ClO rate coefficient is operational and work is progressing smoothly.

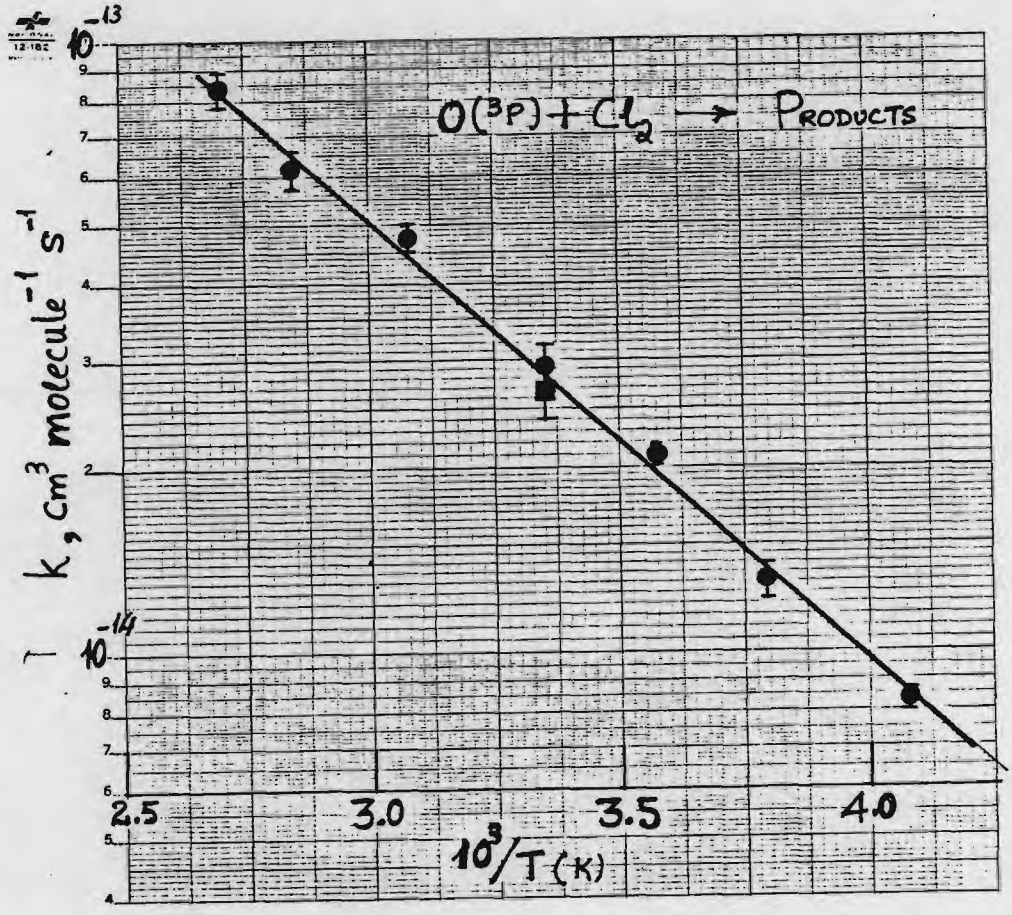

INTERIM FINAL TECHNICAL REPORT

On CMA Project

"LABORATORY STUDIES OF STRATOSPHERIC REACTIONS"

Contract No. FC-83-449
Georgia Tech Project No. A-3571

Submitted by:

Dr. A. R. Ravishankara

and

Dr. P. H. Wine

Physical Sciences Division
Electromagnetics Laboratory
Engineering Experiment Station
Georgia Institute of Technology
Atlanta, Georgia 30332

February 10, 1984

INTERIM FINAL REPORT

This report is being submitted earlier than usual and before the end of the contract period, so that it can accompany the renewal proposal. Therefore, it is only an interim report and the final version will be submitted at the end of the year. Work on the current project is progressing extremely well. Two studies are complete and two others are being carried out. Each of these studies is briefly described below:

(1) $NO_3 + NO \longrightarrow 2NO_2$

We had, for a long period, difficulty in cleanly producing the small concentrations of NO_3 necessary to measure k_1 under pseudo first conditions in NO_3. $O(^3P)$ production in the microwave discharges of F_2/He and subsequent $O(^3P)$ reactions along the flow tube was the major problem. We have completely overcome this difficulty by using thermal dissociation of N_2O_5 as a source of NO_3.

$$N_2O_5 \longrightarrow NO_3 + NO_2.$$

N_2O_5 entrained in helium is passed through a glass injector heated to ~280°C in order to completely dissociate N_2O_5 into NO_3 + NO_2. Source NO_2 does not pose any problems in these studies because of its low levels (~1 x 10^{11} cm^{-3}). NO_3 is detected via laser induced fluorescence excited at 662nm. (It is worth noting that at this pumping wavelength the sensitivity for NO_3 detection is two orders of magnitude greater than that for NO_2 at 1 torr total pressure. Thus there is only a small quantifiable interference from the presence of NO_2 in the NO_3 source.) The integrated NO_3 flourescence signal as a function of reaction time (i.e. NO injector position) is measured at various NO concentrations to obtain $k' \equiv k_1[NO]$. A plot of typical NO_3 decay curves is shown in Figure 1. The slope of a plot of k' vs. [NO]

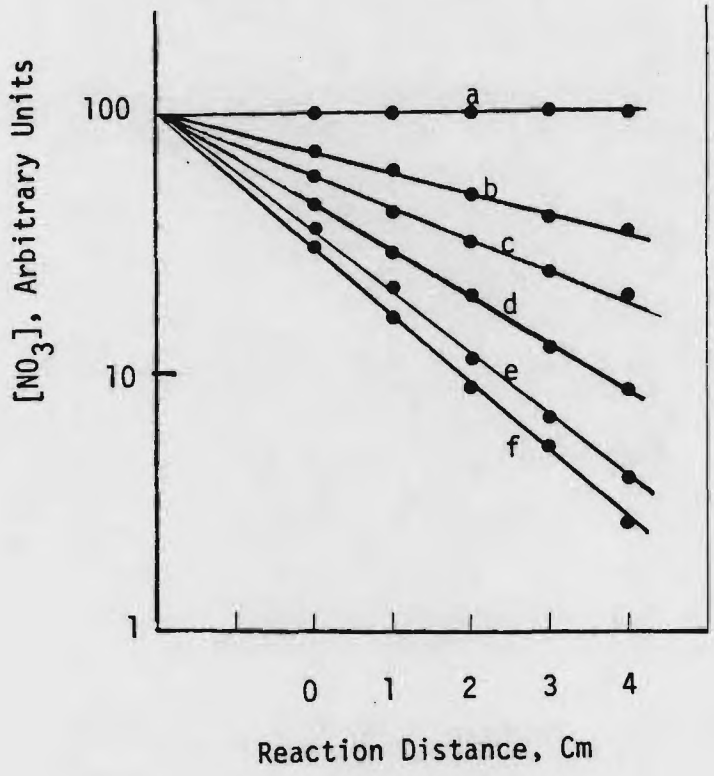

Figure 1. Plot of $[NO_3]$ function of reaction time, (i.e. reaction distance) at various concentrations of NO in units of 10^{12} cm^{-3}: a = 0; b = 0.93; c = 1.61; d = 2.49; e = 3.34; f = 3.92. Initial $[NO_3]$ = 6 x 10^{10} cm^{-3}. Linear flow velocity = 2160 cm/sec. Pressure = 1 torr of He.

yields k_1. One such plot is shown in Figure 2. k_1 has been

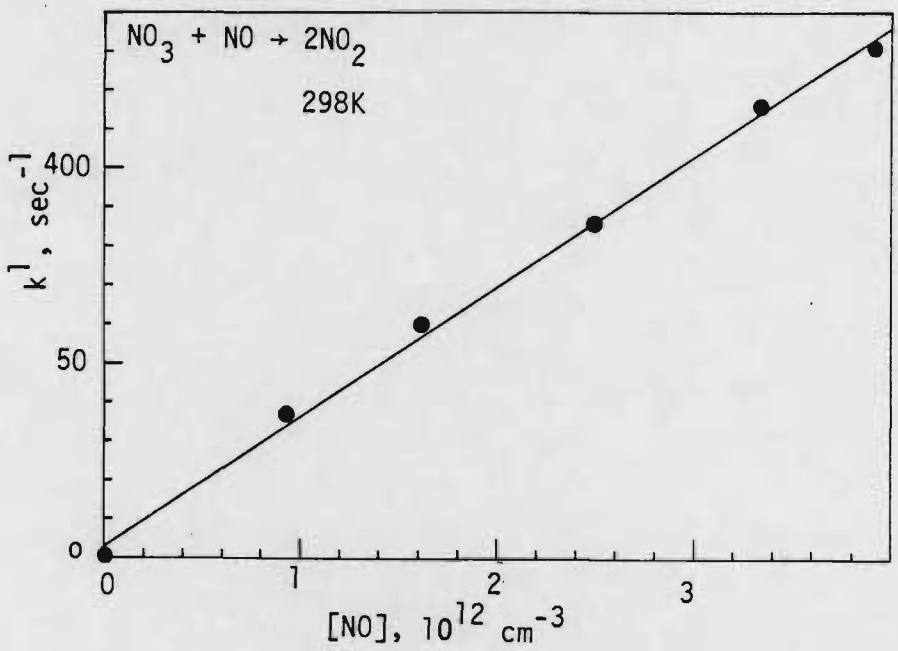

Figure 2: Plot of k' vs. [NO]. The slope of the plot gives $k_1 = (3.26 \pm 0.18) \times 10^{-11}$ cm^3 $molecule^{-1}$ s^{-1}. System pressure = 1 torr of Helium.

measured at 0.5 torr and 1 torr helium with no observable dependence on pressure. Experiments at higher pressures were precluded due to quenching of NO_3 fluorescence by He. Interestingly, NO_3 fluorescence intensity decreases by about a factor of five when the helium pressure is raised by a factor of two! Variation of the initial NO_3 concentration from 6×10^{10} to

4×10^{11} cm^{-3} had no measurable effect on k_1. The obtained value for k_1 is $(3.26 \pm 0.36) \times 10^{-11}$ cm^3 $molecule^{-1}$ s^{-1} where the error is 2σ and includes the estimated error in [NO] measurements. The above value was derived from six separate sets of experiments comprising 42 individual k' measurements. A few final touches to this work still remain to be made. One set of measurements where NO_3 is photolytically produced and monitored via long path laser absorption may be a worthwhile experiment. It is expected that these measurements will be completed in the near future. Also, it is worth noting that our results represent the first direct measurements of k_1 and they are approximately 60% faster than the currently recommended value.

(2) $NO_3 + NO_2 \longrightarrow N_2O_5$, (M = He, N_2)

k_2 has been measured as a function of pressure and diluent gas under pseudo-first order conditions in NO_3 (i.e. $[NO_3] << [NO_2]$). $[NO_3]$ was produced by the $F + HNO_3$ reaction and measured via the long path laser absorption at 662 nm. At the relatively high NO_3 concentrations employed in these experiments (compared to those used in the NO_3 + NO study), $O(^3P)$ produced in the fluorine discharge reacts rapidly with NO_3 to produce NO_2 +

O_2. The $O(^3P)$ + NO_3 reaction goes to completion in the flow tube before reactant NO_2 is added. Therefore, as long as the discharge produces significantly higher concentrations of F atoms than O atoms, the presence of $O(^3P)$ presents no problems in the study of the NO_3 + NO_2 reaction. $k_2'(\equiv k_2[NO_2])$ values were measured as in the case of reaction 1 at various concentrations of NO_2. Measurements of k_2 at 298K using helium and nitrogen as bath gases are complete; results are shown in Figure 3. As seen in

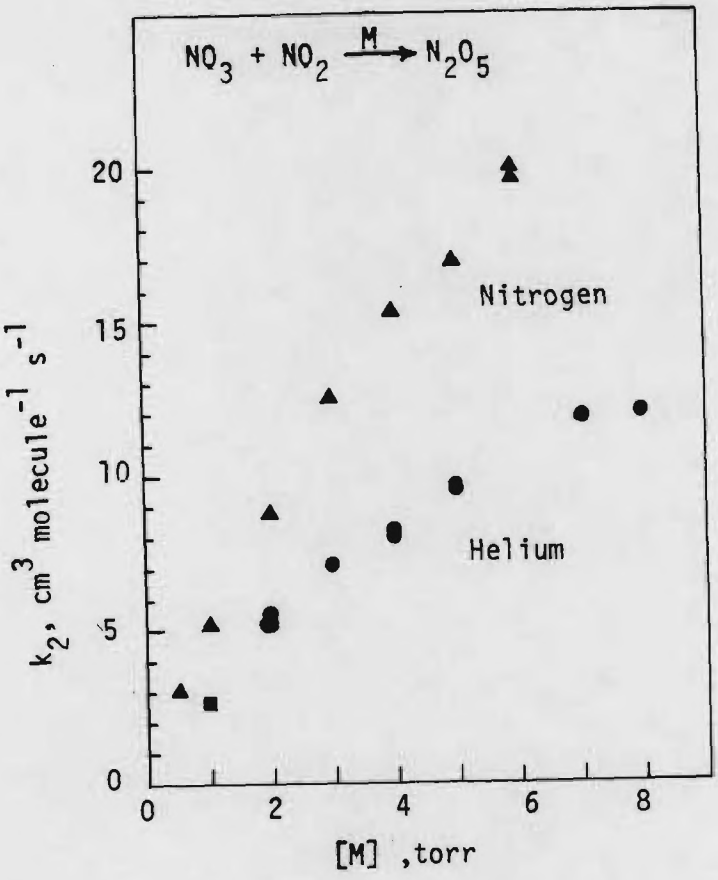

Figure 3: Plot of k_2 as a function of diluent gas pressure.

the figure, reaction (2) is in the fall-off region even at pressures as low as 1 Torr. Currently, calculations to fit the

data to a Troe formalism (such as the ones employed by NASA and CODATA Panels) are being carried out. Our measurements are the first low pressure determinations of k_2 and will help reduce uncertainties in the value of k_2 at stratospheric pressures.

(3) $O(^3P) + ClO \longrightarrow Cl + O_2$

This reaction is being studied under stratospheric pressure conditions using both He and N_2 as diluent gases. The apparatus used in this study is shown in Figure (4). ClO and $O(^3P)$ are produced via photolysis of a mixture containing Cl_2, O_3 and the

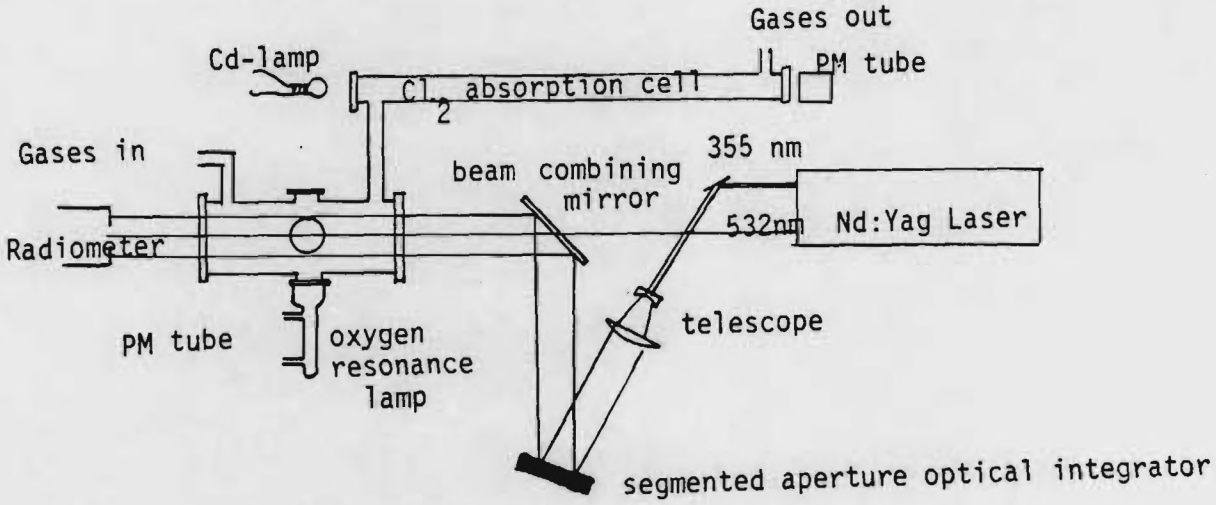

Figure 4: Schematic diagram of the apparatus used for studying reaction (3).

diluent gas. Two photolysis wavelengths, 355 nm and 532 nm, are employed simultaneously.

$$Cl_2 \xrightarrow{355\ nm} 2Cl$$

$$Cl + O_3 \longrightarrow ClO + O_2$$

$$O_3 \xrightarrow{532\ nm} O(^3P) + O_2(^3\Sigma^-g)$$

$$O(^3P) + ClO \rightarrow Cl + O_2$$

The 355 nm beam is integrated to produce a spatially uniform square beam while the 532 nm green beam is used as is. The two beams are combined using a dichroic mirror such that the green beam (which produces O atoms) is at the center of the larger 355 nm UV beam. The temporal profile of $[O(^3P)]$ is measured as a function of reaction time using the resonance fluorescence detection technique. To calculate [ClO], which is equal to the concentration of Cl atoms produced by Cl_2 photolysis, we need to know $[Cl_2]$, the absorption cross section of Cl_2 at 355 nm, and the fluence of the laser pulse at 355 nm.

$$[Cl] = 2\Phi\ \sigma_{Cl_2}^{355}\ [Cl]$$

$\sigma_{Cl_2}^{355}$ is well known. The concentration of Cl_2 is measured via UV absorption at 326 nm as the reaction mixture exits the

reactor. Φ is measured using a radiometer. To ensure the accuracy of the measured Φ , actinometery experiments were carried out. The experiments consisted of photolyzing a mixture of Cl_2 and ClNO in the apparatus shown in Figure 5a. A DC low pressure mercury lamp was used as the source of 184.9 nm light which was monitored as a function of time. Cl_2 is photolyzed under geometric conditions identical to those in the actual experiments to produce a spatially uniform density of Cl atoms.

$$Cl_2 \xrightarrow{355nm} 2Cl.$$

The chlorine atoms then react with ClNO to destroy one molecule of ClNO for each chlorine atom produced by photolysis.

$$Cl + ClNO \longrightarrow Cl_2 + NO.$$

The loss of ClNO produces an increase in the transmitted 184.9nm beam which is measured. One such measurement is shown in Figure 5b. It is seen that the ClNO loss can be measured very accurately. This measured ClNO loss is compared with the calculated concentration of Cl atoms produced. If the radiometer is accurate, then the concentration of ClNO lost should be the

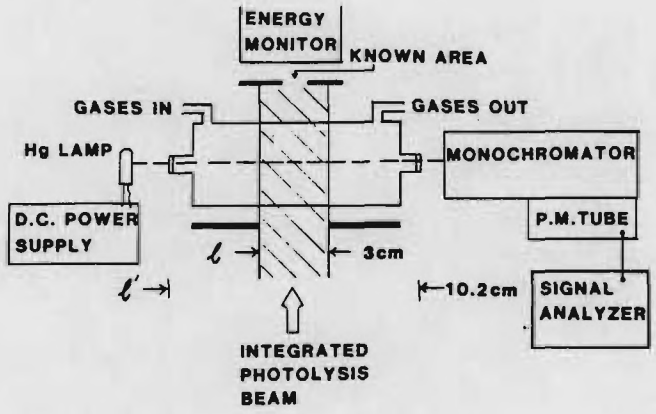

Figure 5a: Schematic diagram of the apparatus used for carrying out actinometry experiments.

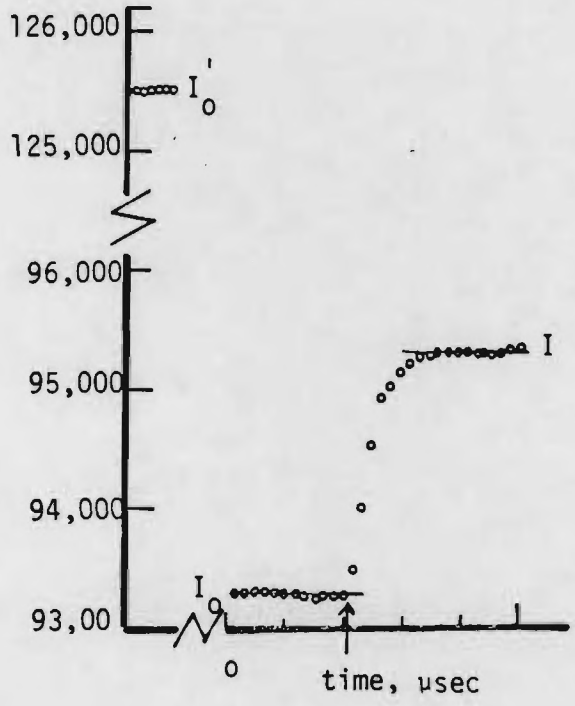

Figure 5b: A plot of the variation of the transmitted 184.9 nm light upon photolysis Cl_2/ClNO mixture at 355nm. $\ln I/I_o$ is proportional to the concentration of Cl atoms produced.

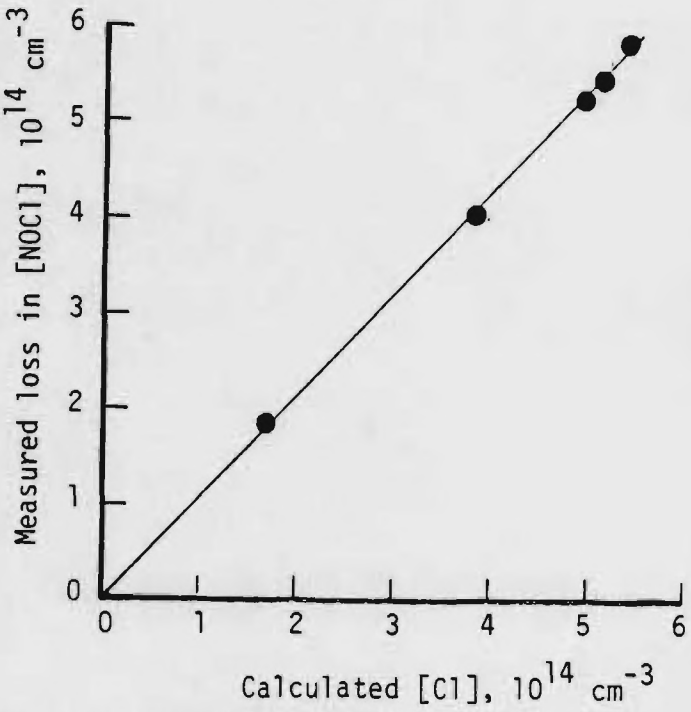

Figure 5c: Plot of the measured loss in [NOCl] (= concentration of Cl atoms produced) as a function of the calculated Cl atom concentration. Calculations were based on the fluence as measured by the radiometer.

same as the concentration of Cl atoms produced. We found that the radiometer read ~ 8% too low. Figure 5c shows a plot of [ClNO] lost vs. [Cl] produced. It was found that variations in [ClNO], $[Cl_2]$, and laser energy did not effect the calibration factor thereby indicating the validity of the method. The actinometery results have been further checked with a Scientech disc calorimeter which was purchased as part of this project and was received in late January. The Scientech measurements are 6% higher than the Actionmetery results. Attempts to further refine the laser determination are ongoing.

In the kinetics experiments, $O(^3P)$ temporal profiles are measured at various concentrations of [ClO]. Figure 6 shows a set of measurements where $[Cl_2]$ and $[O_3]$ are held constant and the fluence at 355nm is varied to change the [ClO]. The slope of these decay plots yield $k_3' \quad k_3[ClO] + k_4[Cl_2] + k_d$ where k_d is the loss rate of $O(^3P)$ due to diffusion and reaction with O_3 and k_4 is the rate coefficient for the reaction of atomic oxygen with molecular chlorine (k_4 has been measured by us recently in the same apparatus, see below). A plot of k_3' vs. [ClO] at fixed $[Cl_2]$ yields a straight line with slope = k_3. Such a plot is shown in Figure 7. k_3 has been measured at 298K as a function of and He pressure. There is no observable variation in the value of

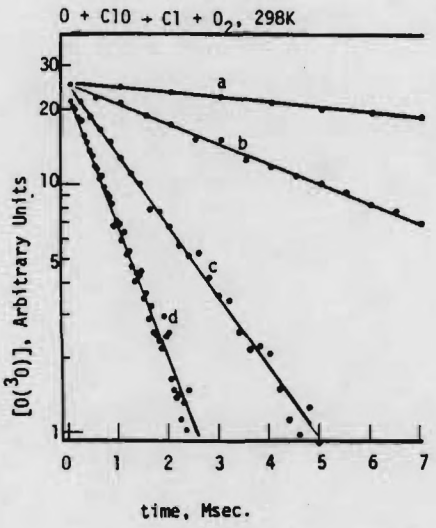

Figure 6: Plot of $[O(^3P)]$ as a function of reaction time at various concentrations of ClO. [ClO] = 0 for decays a and b. Decay a is that due to $O + O_3$ reaction while decay b is due to $O + O_3$ and $O + Cl_2$. Curve c, $[ClO]=0.85 \times 10^{13}$ cm^{-3}; curv d, $[ClO]= 1.85 \times 10^{13}$ cm^{-3}.

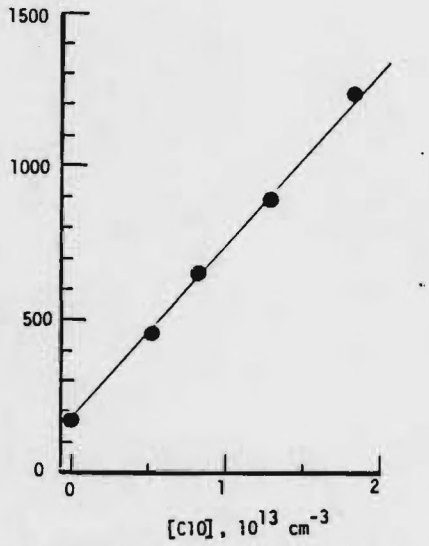

Figure 7. Plot of k' vs. [ClO]. Slope of the line yields k_3.

k_3 with $[O(^3P)]_o$, $[O_3]$, $[Cl_2]$, and the linear flow rate of gases through the reactor. Attempts are being made to extend the discharge flow tube conditions. In addition, experiments aimed at checking the possible production of $O_2(^1\ )$ in reaction (3) are being pursued. These studies are expected to be completed by the end of March so that the 298K measurement of k_3 should wrapped up during the current contract period.

(4) $O(^3P) + Cl_2 \rightarrow$ Products.

In order to study reaction (3) using the ClO production scheme described above, it is necessary to know the rate of $O(^3P)$ loss in the absence of ClO. This loss rate is dominated by the reaction of $O(^3P)$ with Cl_2. Therefore, k_4 was measured by producing $O(^3P)$ via 532 nm photolysis of O_3 in the presence of various concentrations of Cl_2 and following the rate of decay of $O(^3P)$. k_4 was measured over the temperature range 245-371K at seven temperatures. An Arrhenius plot of the data is shown in Figure 8. A linear least squares fit of the data to an Arrhenius

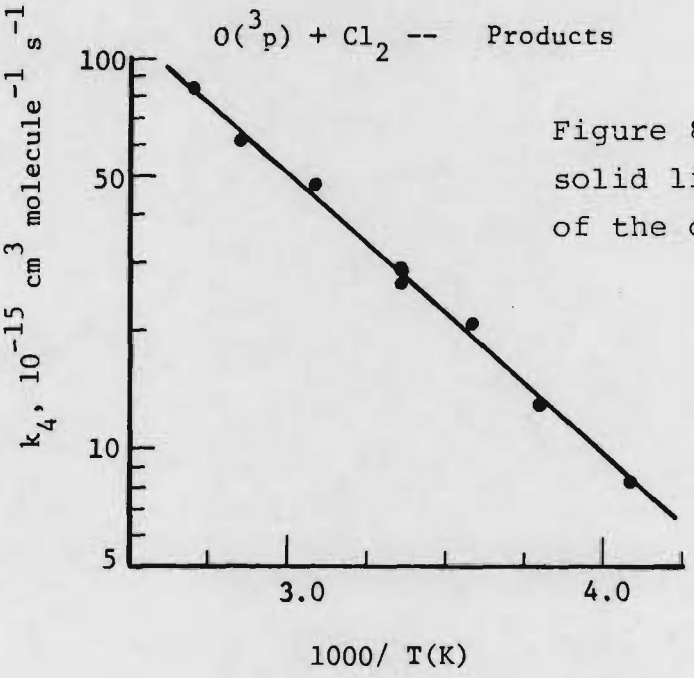

Figure 8: Plot of $\ln k_4$ vs. 1/T. The solid line is a linear least squares fit of the data.

form yields,

$$k_4 = (7.1 \pm 2.3) \times 10^{-12} \exp[-(1650 \pm 100)/T]$$

The measured 298K rate coefficient for reaction (4) is nearly 60% lower than the previously recommended value. In addition, our measured activation energy is much larger than the recommended value. Our measured values demonstrate that studies of reaction (3) can be easily carried out at temperatures less than 300K using O_3, Cl_2 reaction mixtures .

FINAL TECHNICAL REPORT
Georgia Tech Project A-3571

LABORATORY STUDIES OF STRATOSPHERIC REACTIONS

By

A. R. Ravishankara
P. H. Wine

Submitted to

CHEMICAL MANUFACTURERS ASSOCIATION
2501 M Street, N.W.
Washington, DC 20037

Under

CMA Contract FC-83-449

March 1985

GEORGIA INSTITUTE OF TECHNOLOGY
A Unit of the University System of Georgia
Atlanta, Georgia 30332

GTRI
GEORGIA TECH RESEARCH INSTITUTE

1985

LABORATORY STUDIES OF STRATOSPHERIC REACTIONS

Georgia Tech Project A-3571

CMA Contract FC-83-449

A Final Technical Report

Submitted to:

Chemical Manufacturers Association
2501 M Street, N.W.
Washington, DC 20037
Attn: Elizabeth Gormley

By:

A. R. Ravishankara and P. H. Wine
Georgia Tech Research Institute
Georgia Institute of Technology
Atlanta, GA 30332

Table of Contents

Summary

During the twelve month period of this project, emphasis was placed on studying the following three reactions:

$$NO_3 + NO_2 + M \longrightarrow \text{products} \quad (1)$$

$$NO_3 + NO \longrightarrow 2NO_2 \quad (2)$$

$$O(^3P) + ClO \longrightarrow \text{products} \quad (3)$$

All three reactions were studied at 298K only.

Reaction (1) was studied in both He and N_2 diluent gases at pressures of 0.5-8 Torr in a discharge flow system with NO_3 detected by long path laser absorption. Reaction (1) is found to be in the fall-off regime between third and second order kinetics over this pressure range. Fall-off parameters were obtained by fitting the kinetic data to the fall-off equation of Troe and co-workers. Employing a fitted fall-off expression of our data in conjunction with recently published rate coefficients for N_2O_5 decomposition, $K_{eq}(298K)$ and $\Delta H_f^o(298K)$ for NO_3 were also determined. Experimental rate coefficients, best fit fall-off parameters, and recently determined equilibrium constants are

summarized in Tables I-III of Chapter 1. Our results are compared with those reported by other investigators in Figure 4 of Chapter 1.

Reaction (2) was studied at low pressure (0.5-1.0 Torr) in a fast flow system with NO_3 detected by laser induced fluorescence (DF-LIF technique) and also at higher pressures (10-200 Torr) in a laser flash photolysis system with NO_3 detected by long path laser absorption (LFP-LPLA technique). The DF-LIF experiments gave $k_2 = (3.24 \pm 0.32)\times10^{-11}$ cm^3 molecule^{-1} s^{-1} while the LFP-LPLA experiments gave $k_2 = (2.93 \pm 0.09)\times10^{-11}$ cm^3 molecule^{-1} s^{-1}. These results are about 50% faster than the currently recommended value for k_2 (NASA panel) but in good agreement with another recent "direct" measurement by Howard and co-workers. Current recommendations are based on indirect determinations by Johnston and co-workers.

Reaction (3) was studied in a laser flash photolysis system at pressures of 8-200 Torr under pseudo-first order conditions with ClO in large excess over $O(^3P)$. ClO was prepared by 355nm pulsed laser photolysis of Cl_2 in the presence of O_3 while $O(^3P)$ was followed by resonance fluorescence spectroscopy. ClO was not directly measured, but its concentration was inferred from known photochemical parameters and careful measurements of the 355nm photolysis laser fluence. Our results are summarized in Table I of Chapter 3. There is no observable variation in the value of k_3

as a function of total pressure, $[O(^3P)]_o$, $[O_3]$, $[Cl_2]$, or the photolysis laser repetition rate. Averaging the 25 determinations gives the result $k_3 \pm 2\sigma = (5.5 \pm 1.0) \times 10^{-11}$ cm^3 molecule^{-1} s^{-1}.

As of the end of the contract period, our studies of reactions (1) and (2) are completed. However, we are obtaining a significantly faster rate constant for reaction (3) than has been reported in several recent investigations (see Table II of Chapter 3). Hence, further experimentation is required to either validate our result or find out why it is in error.

A major uncertainty in our study of reaction (3) centers around the need to measure an absolute laser photon fluence in order to determine the ClO concentration. To circumvent the need for measuring an absolute laser photon fluence and also allow direct monitoring of ClO, we have devised a modified scheme for investigating reaction (3). We expect to carry out these new experiments in the near future. Our high powered excimer laser will be used to photolyze Cl_2 at 351nm (XeF laser). Cl atoms will be produced in excess over O_3. The Cl + O_3 reaction will be allowed to go to completion, thereby converting all O_3 to ClO. After ClO production is complete, a second laser will be fired to produce $O(^3P)$ by photolysis of a small fraction of the ClO. Excess Cl atoms should not effect the temporal profiles of either

ClO or $O(^3P)$. This new reaction scheme has two important advantages: (1) the laser photon fluence need not be known in order to determine the ClO concentration--the O_3 concentration before photolysis equals the ClO concentration after photolysis, and (2) since the O + ClO reaction occurs with no O_3 present, it will be possible to directly monitor the temporal profile of ClO by UV photometry (O_3 interferes with ClO detection because it absorbs strongly in the same wavelength region as ClO).

Because of their potential involvement in our study of reaction (3), we have also investigated reactions

$$O(^3P) + Cl_2 \longrightarrow \text{products} \qquad (4)$$

$$O(^1D) + Cl_2 \longrightarrow \text{products} \qquad (5)$$

Reaction (4) represents the dominant background $O(^3P)$ removal mechanism in our studies of reaction (3). Reaction (5) represents a potential alternate source of ClO which could be employed to study reaction (3) if a significant fraction of $O(^1D)$ deactivation did not lead to $O(^3P)$. The studies of reactions (4) and (5) involved time resolved detection of $O(^3P)$ following 248nm pulsed laser photolysis of $O_3/Cl_2/N_2$ and $O_3/Cl_2/He$ mixtures. Reaction (4) was studied over the temperature range 245-371K

under conditions where the $O(^3P)$ temporal behavior was unaffected by fast secondary reactions of $O(^3P)$ with the products ClO and/or Cl_2O. The data are well described by the following Arrhenius expression: $k_4(T) = (7.4 \pm 2.4)\times10^{-12} \exp[(-1650 \pm 100)/T]$ cm^3 $molecule^{-1}$ s^{-1}. Our results demonstrate that reaction (4) is somewhat slower than previously believed. Hence, reaction (4) represents less of an interference in studies of reaction (3) than estimates based on current recommendations suggested. To study reaction (5) the appearance of $O(^3P)$ resulting from $O(^1D)$ deactivation was monitored as a function of the Cl_2 concentration. The rate coefficient for total removal of $O(^1D)$ by Cl_2 was determined to be $(2.81 \pm 0.42)\times10^{-10}$ cm^3 $molecule^{-1}$ s^{-1} at 298K. 24 ± 10% of the $O(^1D) + Cl_2$ quenching interactions result in formation of $O(^3P)$. The $O(^3P)$ yield is too large for reaction (5) to be a viable ClO source for a kinetics study of reaction (3).

Our studies of reactions (1)-(3) are discussed in detail in separate chapters of the report. The studies of reactions (4) and (5) are discussed in a fourth chapter.

Chapter 1

The NO_3 + NO_2 Reaction

A paper describing our study of the NO_3 + NO_2 reaction has been accepted for publication in The Journal of Physical Chemistry. This chapter consists of a preprint of the paper. It should be noted that the numbering of reactions and equations in the preprint is different from that in other sections of the report.

KINETICS OF THE REACTION $NO_2 + NO_3 + M$ AT LOW PRESSURES AND 298K

C. A. Smith, A. R. Ravishankara,* and P. H. Wine

Molecular Sciences Group
Engineering Experiment Station
Georgia Institute of Technology
Atlanta, Georgia 30332

*Author to whom correspondence should be addressed

Abstract

Utilizing a discharge flow-long path laser absorption apparatus, absolute rate constants have been measured for the recombination reaction, $NO_2 + NO_3 + M \rightarrow N_2O_5 + M$, at 298K over the pressure ranges of 0.5-6.0 torr N_2 and 1.0-8.0 torr He. The title reaction is found to be in the fall-off regime between third and second order kinetics over this pressure range. Fall-off parameters were obtained by fitting the kinetic data to the fall-off equation of Troe and co-workers. Employing a fitted fall-off expression of our data in conjunction with recently published rate coefficients for N_2O_5 decomposition, K_{eq} (298) and ΔH_f^o(298K) for NO_3 were also determined.

INTRODUCTION

The oxides of nitrogen have long been recognized as major constituents of both the stratosphere and the troposphere. In these parts of the atmosphere they engage in various reactions which control the concentrations of important species such as O_3, OH, and HO_2. Since NO_3 is one of these nitrogen species, a thorough understanding of its chemistry is of importance. NO_3 is produced mainly via the reaction of O_3 with NO_2 and is photochemically destroyed during sunlight hours. At night however, it reacts with NO_2 to produce N_2O_5, a temporary reservoir. In the troposphere, the ambient temperature can be high enough for the thermal decomposition of N_2O_5 to be competitive with this formation such that an equilibrium is set up.

$$NO_3 + NO_2 + M \underset{k_{-1}}{\overset{k_1}{\rightleftharpoons}} N_2O_5 + M \qquad (1)$$

To evaluate the concentration of N_2O_5 that is produced and the rate at which it is produced, the rate coefficient k_1 for Reaction (1) is needed. However, until now it has been calculated from the thermochemical data in conjunction with the rate coefficient for N_2O_5 decomposition, k_{-1}. k_{-1} has been experimentally measured by Viggiano et al.[1] and Connell and Johnston.[2]

In addition to the above mentioned need for atmospheric chemistry, Reactions (1) and (-1) have been considered for a long time as an example of classic association reactions. All the species involved in this reaction are well identified. Both forward and reverse reactions are pressure and temperature dependent in regimes that are easily accessible in the laboratory. Therefore, a complete set of rate data on this system will provide a proving ground for association reaction theories.

Since the initiation of this study, two other groups have

measured k_1 using the pulsed photolysis-absorption technique. In the first of these studies, Kircher et al.[3] measured k_1 in the pressure regime of 20 to 700 torr between 236 and 358K. The study by Croce de Cobos et al.[4] has been aimed at extracting the high pressure limiting rate coefficient by measuring k_1 between 2 and 200 atm at 298K.

In the present study a discharge flow-long path laser absorption apparatus has been employed to directly determine the absolute rate constants for Reaction (1) at 298K over the pressure range of .5 to 8 torr He and N_2. In addition, semi-empirical calculations such as those described by Malko and Troe[5] have been carried out for estimating the rate constant for Reaction (1) as a function of pressure in the fall-off regime.

EXPERIMENTAL

The experimental apparatus used in this investigation is shown schematically in Figure 1. The discharge flow-long path absorption apparatus consisted of a conventional 2.5 cm i.d. discharge flow tube connected to a 4.8 cm by 3.5 cm absorption cell.

A characterization of the NO_3 production method used in this study has been discussed in detail previously.[6] Briefly, a constant source of NO_3 radicals was produced by passing a 1% mixture of F_2 in He through a microwave discharge to produce F atoms that subsequently reacted with an excess of HNO_3:

$$F + HNO_3 \text{-------} > HF + NO_3. \qquad (2)$$

HNO_3 was introduced into the flow tube 5 cm upstream of the microwave discharge inlet port by passing He through a bubbler containing several milliliters of the pure acid. The HNO_3 concentration was at least five-times larger than that of F atoms in all experiments. Excess HNO_3 prevents the secondary

reaction F + NO_3 → FO + NO_2 from consuming NO_3. Microwave power to the discharge tube was always kept below 5 watts to minimize the production of $O(^3P)$ atoms. The presence of $O(^3P)$ atoms in the flow system results in a background source of NO_2 due to the reaction of $O(^3P)$ atoms with NO_3:

$$O(^3P) + NO_3 \text{ -------> } NO_2 + O_2 \qquad (3)$$

However, the amount of NO_2 produced through Reaction (3) was negligible compared to the concentration of NO_2 added during these studies.[6] A minimum time of 27 ms (i.e. a minimum distance of 40 cm) was provided to insure that Reactions (2) and (3) went to completion before the introduction of NO_2.

NO_3 radical concentrations were monitored as a function of injector displacement along the flow tube by measuring the absorption at 662 nm. The NO_3 absorption cell was equipped with 1/2 inch thick anti-reflection coated windows and was positioned near the focal point of a modified "white cell" that consisted of three concave dielectric coated mirrors as shown in Figure 1. The CW 662 nm probe beam was provided by a Spectra-Physics 380 C tunable ring dye laser that was pumped by the all-lines output of a 4 W Lexel argon ion laser. In order to generate a wavelength in the region where NO_3 has its strongest absorption feature, the ring dye laser was run using DCM dye. The wavelength of the probe beam was periodically checked by employing a calibrated 0.75 m Spex monochromator. The probe beam was multipassed through the absorption cell between 140 and 170 times providing path lengths between 670 and 820 cm. By utilizing this multipassing configuration, we could reduce the detection zone length in the direction of flow to ~ 1 cm thus making it a very small fraction of the reaction length. Before entering the multipass cell, a small fraction of the incident beam was diverted and measured at photodiode A. Upon exiting, the transmitted probe beam was

measured at photodiode B and the outputs from the two photodiodes were ratioed using an analog divider having a response time of 10^{-5} s. The purpose of this ratioing technique was to normalize fluctuations in the dye laser power. The resulting output from the divider was sampled every 500 s by a transient digitizer. Integration times were typically around 50 s for the measurements of each NO_3 concentration. By this method, ~5 x 10^{10} NO_3 cm^{-3} could be detected with S/N = 1 for 50 s integration.

The concentration of NO_3 in the absorption cell as determined by

$$[NO_3] = \ln(I_o/I)/\sigma\ell$$

where I is the measured output of the analog divider in the presence of NO_3 and I_o is the output of the divider in the absence of NO_3. I_o was routinely checked before and after each run by adding excess NO slightly upstream of the absorption cell, thus titrating away all NO_3. The I_o values determined utilizing this method were shown to give identical values with those determined by shutting off the microwave discharge. The absorption cross section of NO_3, σ, used at 662 nm to determine the NO_3 concentration was 1.78 x 10^{-17} cm^2/molec.[6] The path length of the absorption cell, ℓ, was calibrated using known amounts of O_3 and the absorption cross section of O_3 at 662 (2.1 x 10^{-21} cm^2/molec.[7]) The initial concentration of NO_3, typically between 0.5 - 1.0 x 10^{13} molecule/cm^3 was checked at each injector position by shutting off the NO_2 flow and measuring the absorbance of NO_3.

In order to minimize vibrational perturbations in the experimental system, the entire apparatus was mounted on an optical table equipped with a vibration isolation system. The mechanical pump was connected to the experimental system through a set of bellows to decouple any vibrations between the pump and

isolation table.

NO_2 mixed with He or N_2 was passed from a 12 ℓ bulb through a 70 cm absorption cell before entering the injector of the flow tube. The flow tube was designed such that the reaction-zone portion of the injector was never exposed to ambient air, thus minimizing possible contamination and the subsequent changes in wall loss rate of NO_3. The concentration of NO_2 was continuously monitored using the 366 nm line from a Hg pen-ray lamp that was isolated by a bandpass filter and detected by a RCA 1P28 photomultiplier tube. The output current from the photomultiplier tube was measured by an electrometer. The incident light intensity from the Hg lamp was checked before and after each run by shutting off the NO_2 flow and flushing the absorption cell with diluent gas. The NO_2 concentrations were calculated using an absorption cross section of 5.75×10^{-19} cm^2/molecule at 365 nm.[8] In no case did the amount of NO_2 tied up as N_2O_4 exceed 1.2%. By using this procedure, we could determine the concentration of NO_2 with an absolute accuracy of 5%.

The inside surface of the entire apparatus (i.e. inside of the flow tube and the outer wall of the injector) was coated with halocarbon wax in order to reduce the loss of NO_3 to the walls. The wall loss rate has been estimated to be $<1s^{-1}$. The pressure inside the flow tube was measured (after the absorption cell) by a MKS capacitance manometer. The pressure gradient between the NO_3 absorption cell and the pressure port was always less than 5% of the measured pressure. The flow rates of all gases into the experimental system were measured utilizing calibrated mass flow transducers. HNO_3 (Baker, reagent grade) was purified by distilling a mixture of HNO_3 and concentrated H_2SO_4 (Fischer, reagent grade) at 298K and collecting HNO_3 at 77K. NO_2 (99%, Matheson Gas Products) was mixed with UHP O_2 and cryopumped at 77K then degassed. F_2 (1% in He, Spectra Gases), He (UHP, Matheson Gas Products), N_2 (UHP, Spectra Gases), and NO (99%,

Matheson Gas Products) were all used without further purification.

Results ad Discussion

I. Chemical Kinetics

All experiments were carried out under pseudo-first order conditions with $\frac{[NO_2]}{[NO_3]}$ always greater than 10, but typically 50. The pseudo-first order loss of NO_3 is described by the following integrated rate equation:

$$\ln[NO_3]_o/[NO_3]_t = (k_1[NO_2])\ (d/v + C)$$
$$= k't$$

where d is the injector displacement along the flow tube, v is the average flow velocity in the flow tube, and C is a constant representing the time delay between the injector position at zero displacement and the NO_3 detection zone. This "end-effect" or time delay results from the injector position zero being upstream of the detection zone and the different cross-sectional areas of the flow tube and absorption the cell. The above equation assumes that all NO_3 decay processes are pseudo-first order in NO_3 and the surface removal of NO_3 is independent of NO_2 added. k', the pseudo-first order rate constant is determined from the slopes of $\ln[NO_3]_t/[NO_3]_o$ versus d plots (examples of which are shown in Figure 2). The intercept of these plots gives C. Even though the consequence of the injector in the flow system upon $[NO_3]$ is usually negligible, all experiments were corrected for its presence by measuring $[NO_3]_o$ at each injector position. The bimolecular rate constants, k_1, are determined from the slope of k' versus $[NO_2]$ plots using a linear least-squares analysis. A typical k' versus $[NO_2]$ plot is shown in Figure 3. For the rate constant determinations at .5 torr N_2 and 1 torr He, the effect

of NO_2 as a third body was significant and had to be accounted for. Under these conditions, the measured k' is given by the equation

$$k' = k_1^{M}[M]\ [NO_2] + k_1^{NO_2}[NO_2]\ [NO_2]$$

which can be rearranged to give

$$\frac{k'}{[NO_2]} = k_1[M] + k_1^{NO}\ [NO_2]$$

where k_1^{M} and $k_1^{NO_2}$ are the termolecular rate constants for M and NO_2 as third bodies respectively. This analysis assumes that the loss rate of NO_3 to the walls is very small as shown by zero intercepts in plots of k' vs. $[NO_2]$ at higher pressures. Thus, a plot of $k'/[NO_2]$ versus $[NO_2]$ yields the bimolecular rate constant at the respective pressure of M as the intercept; in addition, the termolecular rate constant can be determined from the slope of this plot. The termolecular rate constant for M = NO_2, $k_1^{NO_2}$ was found to be 1.68 ($\pm$ .63) x10^{-29} $cm^6/molec^2$-s and 3.8 ($\pm$ 2.4) x 10^{-29} $cm^6/molec^2$-s at 1 torr He and 0.5 torr N_2 respectively.

The linearity of the logarithmic decays of NO_3 as a function of injector position over typically 2 1/e times validated the existence of first order kinetics in NO_3 and showed that any interferences from competing reactions were negligible. As a further check for complications from possible secondary and/or biradical reactions, the initial $[NO_3]$ was varied by more than a factor of three in several experiments and no significant changes were observed in the pseudo-first order rate constant (k').

The rate constant for Reaction (1) was studied at 298K over the pressure range of 0.5-6 torr N_2 and 1-8 torr He with average flow velocities ranging between 500 and 1500 cm/s. The results

for this investigation are shown in Table 1 where the listed uncertainties represent two standard deviations. Since the $[NO_2]$ was measured directly, these error limits depict the accuracy of the measurements. The present rate constant data clearly shows that even at the low pressures of our study Reaction (1) is in the fall-off region between third and second order kinetics, (as anticipated from previous kinetic data for the thermal unimolecular decomposition of N_2O_5). [1,2,5]

II. Fall-off Parameters

Troe and co-workers[5,9-12] have developed a semi-empirical method based on statistical theories for approximating bimolecular rate constants for association reactions in the fall-off regime. The utilization of such a theory helps provide, within the framework of current understanding of association reactions, an analytical expression useful in experimental studies as well as atmospheric modeling to predict the behavior of such reactions as a function of pressure and temperature. In order to obtain a reasonable comparison for our rate constant data with those of other investigations at higher pressures, we have utilized the following expression[5,9-12] (an approximate form) to fit our data:

$$k[M,T] = \frac{k_o[M]}{1 + \frac{k_o[M]}{k_\infty}} \cdot F_c \left\{1 + \left(\log \frac{k_o[M]}{k_\infty}\right)^2\right\}^{-1} \qquad \text{I}$$

where $k_o(M,T)$ is the third order low-pressure limiting rate constant, for bath gas M at temperature T, $k_\infty(T)$ is the second order high-pressure limiting rate constant at temperature T, and $F_c(M,T)$ is the fall-off curve broadening factor at the center of the curve (i.e. when $k_o[M] = k_\infty$.) Definitions of the adjustable parameters given in equation I have been described in detail previously. [5,9-14]

Using a non-linear least-squares program, we have fit our data along with the higher pressure results of Kircher et al.[3] and Croce de Cobos et al.[4] for M=N_2, and along with the results of Kircher et al.[3] for He to equation I. The values of k_o, k_∞, and F_c at 298K were determined by floating all three parameters and iterating until the best fit of equation I to the input data was achieved. The results are indicated in Table II and fall-off curves calculated from these values are shown in Figure 4. For the purposes of atmospheric modeling, the fall-off parameters given in Table II are recommended.

In addition to calculating the fall-off parameters for Reaction (1) in the above fashion, k_o and k_∞at 298K were determined by non-linear curve fitting of the input data to equation I using calculated values for F_c similar to the calculations undertaken by Patrick and Golden.[14]

The thermal decomposition data of Viggiano et al.[1] was used in conjunction with the results of this study, Croce de Cobos et al.[4], and Kircher et al.[3] in determining the equilibrium constant, K_{eq}, at 298K. A value $k_{-1}/k_1 = 2.5 \times 10^{10}$ molecule/cm^3 at 298K was obtained over the pressure range of 10-700 torr N_2. (A comparison of the K_{eq} derived in this study with those determined in other studies is shown in Table III.) From the equilibrium constant, the enthalpy of reaction was determined to be $\Delta H_f^o(298K) = 22.43$ kcal/mole. Combining this enthalpy result with the tabulated values[14] for the heats of formation for NO_2 and N_2O_5, the heat of formation for NO_3 was determined to be $\Delta H_f^o(298K) = 17.22$ kcal/mole. Both these values are in good agreement with those recently obtained by Kircher et al.[8] Similarly if Connell and Johnston's[2] value for k_{-1} is used, then the calculated value of k_{eq} at 298K = 4.85×10^{10} molecule/cm^3 and the $\Delta H_f(298) = 16.83$ kcal/mole for NO_3.

Heat capacities calculated according to formalisms provided in the JANAF thermochemical tables[15] were used in determining

$E^{\circ}_{o} = \Delta H_{o}^{\circ}$, the critical energy for dissociation of N_2O_5. The vibrational frequencies[16] given in Table IV along with E°_{o} and the calculated values for Z_{LJ}, k_o^{sc}, and K_{eq} given in Table V (part A and B) were used in theoretically calculating F_c. In addition, the low vibrational frequencies of the adduct were treated as free rotors in one case and as hindered rotors in the other. The values for k_o, and k_∞ were then determined by fixing F_c to the calculated value and iterating until the best fit of equation I to the input data was obtained. The results are summarized in Table VI (part A) and a comparison of the fall-off parameters for Reaction (1) determined in other recent studies is given in Table VI (part B). It is necessary to point out that we have used a fixed value of F_c with no allowance given for its variation with pressure. Such treatments have been carried out by Troe and co-workers[11,12]. However, within the uncertainties of K_{eq}, and experimental errors in k_1, it seems superfluous to use an elaborate analysis.

Since this work represents the only measurements at pressures below 10 torr, a direct comparison with other rate constant data in this pressure regime is not possible. However, from the examination of Table VI and Figure 4, several observations can be made. There is reasonable unanimity in the fall-off parameters determined for Reaction (1) by the various investigations shown in Table VI. The divergence in the specific values appears acceptable given the range of adjustable parameters utilized in the calculations. The differences between the calculated F_c values (listed in Table VIA) and the fitted F_c values (listed in Table II) can be attributed largely to the uncertainty in the low vibrational frequencies for N_2O_5. The F_c values seem to be quite low for a molecule (N_2O_5) having seven atoms. Using the fall-off parameters in Figure 4, there is good agreement in the extrapolation of our kinetic data to the higher pressure results of Kircher et al.[3] (20-700 torr He, N_2). Thus,

the pressure dependency of the rate constant for Reaction (1) has now been determined over an extremely large pressure range with relatively good agreement between the three studies. In order to reasonably complete the kinetic data base on Reaction (1), an examination of the temperature dependence of k_1 at pressures below 20 torr is clearly needed. This information would be extremely pertinent in further elucidating the stratospheric chemistry of NO_3.

Acknowledgement

This work was supported by the Fluorocarbon Program Panel of the Chemical Manufacturer's Association.

REFERENCES

1. A. A. Viggiano, J. J. Davidson, F. C. Fehsenfeld, and E. F. Ferguson, J. Chem. Phys., 74, 6113 (1981).

2. P. Connell and H. S. Johnston, Geophys. Res. Lett., 6, 553 (1979).

3. K. C. Kircher, J. J. Margitan, and S. P. Sander, J. Phys. Chem., submitted for publication.

4. A. E. Croce de Cobos, H. Hippler, and J. Troe, J. Phys. Chem., submitted for publication.

5. M. W. Malko and J. Troe, Int. J. Chem. Kinetics, 14, 399 (1982).

6. A. R. Ravishankara and P. H. Wine, Chem. Phys. Lett., 101, 73 (1983).

7. M. Nicolet, Etude des reactions chimiques de lozone dans la Stratosphere.

8. P. H. Wine, N. M. Kreutter,and A. R. Ravishankara, J. Phys. Chem. 83, 3191 (1979).

9. J. Troe, J. Phys. Chem., 83, 114 (1979).

10. K. Luther and J. Troe, Proc. 17th Int. Symp. on Combustion, 535 (1978).

11. J. Troe, Ber Bunsenges Phys. Chem., 87, 161 (1983).

12. R. G. Gilbert, K. Luther, and J. Troe, Ber Bunsenges. Phys. Chem. 87, 169 (1983).

13. P. H. Wine, R. J. Thompson, A. R. Ravishankara, D. H. Semmes, C. A. Gump, A. Torabi, and J. M. Nicovich, J. Phys. Chem., 80, 2095 (1984).

14. R. Patrick and D. M. Golden, Int. J. Chem. Kinetics, 15, 1189 (1983).

15. JANAF Thermochemical Tables, 2nd edition, 1970.

16. I. C. Hisatune, J. P. Devlin, and J. Wada, Spectrochim. Acta., 18, 1641 (1962).

17. R. A. Graham and H. S. Johnston, J. Phys. Chem., 82, 254 (1978).

18. W. B. Demore, M. J. Molina, R. T. Watson, D. M. Golden, R. F. Hampson, M. J. Kurylo, C. J. Howard, and A. R. Ravishankara, JPL publication 83-62, Jet Propulsion Laboratory, California Institute of Technology, Pasadena, California (1983).

TABLE I. Rate Constants for the Reaction of

$NO_3 + NO_2 + M \rightarrow N_2O_5 + M$

at 298K as a Function of Pressure and Diluent Gas.

PRESSURE (torr)	k_1 ($\pm 2\sigma$) ($\times 10^{-14}$ cm^3/molecule-s)	
	M=He	M=N_2
0.5*		3.6 (± 2.0)
1.0*	2.58 (± 0.70)	4.5 (± 1.0)
2.0	5.29 (± 0.20)	8.7 (± 1.4)
2.0	5.27 (± 0.14)	8.8 (± 0.8)
2.0	5.73 (± 0.28)	
	5.43 (± 0.38)	8.75 (± 1.3)
3.0	7.20 (± 1.40)	12.5 (± 2.4)
4.0	8.78 (± 0.98)	15.6 (± 3.4)
4.0	8.46 (± 0.94)	
	8.62 (± 1.36)	
5.0	9.50 (± 1.60)	16.8 (± 3.6)
5.0	9.55 (± 2.28)	
	9.53 (± 1.86)	
6.0		20.3 (± 2.8)
6.0		19.7 (± 1.8)
		20.0 (± 3.2)
7.1	11.9 (± 0.4)	
8.0	12.7 (± 1.8)	

*extrapolated values

TABLE II. Fall-off parameters derived by fitting Equation I to the rate constant data of this study along with Kircher et al. for M=He and with Croce de Cobos et al. and Kircher et al. for $M=N_2$

M	F_c	k_o (cm^6/molecule^2-s)	k (cm^3/molecule-s)
He	.55	9.5×10^{-31}	1.45×10^{-12}
N_2	.47	2.12×10^{-30}	1.85×10^{-12}
N_2 (a)	.40	2.32×10^{-30}	1.84×10^{-12}
N_2 (b)	.60	1.97×10^{-30}	1.40×10^{-12}

(a) Parameters fitted with rate constant data of this study and that of Croce de Cobos, et al. (Refrence 4).

(b) Parameters fitted with rate constant data of this study and that of Kircher, et al. (Reference 3).

TABLE III. A summary of recent measurements of K_{eq} for $N_2O_5 + M \rightleftarrows NO_3 + NO_2 + M$ at 298K.

Investigation	K_{eq} (298K) (x 10^{10} molecule/cm^3)
Patrick and Golden[16]	6.93
Graham and Johnston[17]	4.28
Connell and Johnston[10]	4.26
NASA[18]	5.24
Kircher et al.[3]	3.07
This Work	2.50[a] ; 4.85 ; 3.64

a. using C. Viggiano et. al.'s data for k_{-1}

b. using Connell and Johnston's data for k_{-1}

c. using a combination of Viggano's and Connell and Johnston's for k_{-1}

TABLE IV. Estimated Vibrational Frequencies for N_2O_5

MODE	FREQUENCY (cm^{-1})
NO_2 antisym stretch	1728
NO_2 sym stretch	1338
NO_2 deformation	743
NO_2 rock (in-plane)	614
NO sym stretch (N-O-N)	353
N-O-N deformation	85
NO_2 wag (out-of-plane)	614
NO_2 twist	55
NO_2 antisym stretch	1728
NO_2 sym stretch	1247
NO antisym stretch (N-O-N)	860
NO_2 deformation	743
NO_2 rock (in-plane)	353

TABLE V. Calculated Values at 298K for Z_{LJ} and $k_{o_{rec}}^{sc}$. $k_{o_{rec}}^{sc}$ was calculated from Equation IX

Using E_o = 22.28 kcal/mole and Keq = 2.50 x 10^{10} molecule/cm^3.

A. Low vibrational frequencies of adduct treated as hindered rotors

M	Z_{LJ} (x 10^{14} cm^3/molecule-s)	$k_{o_{rec}}^{sc}$ (x10^{29} cm^6/molecule-s)
He	2.97	3.19
N_2	2.15	2.31

B. Low vibrational frequencies of adduct treated as free rotors

M	Z_{LJ} (x10^{14} cm^3/molecule-s)	$k_{o_{rec}}^{sc}$ (x10^{-29} cm^6/molecule-s)
He	2.97	6.00
N_2	2.15	4.36

TABLE VI. Summary of Calculated Fall-Off Parameters at 298K

A. Derived in This Study

M	(3) k_o ($\times 10^{-30}$ cm^6/molec-s)	k_∞ ($\times 10^{-12}$ cm^3/molec-s)	F_c ($S_k^{(4)}=S_{eff}$)	F_c ($S_k^{(4)}=S_{eff}+1$)
He	.036	1.15	2.50	.30 (1)	----
N_2	.114	2.64	1.98	.35 (1)	----
He	.036	1.03	2.65	----	.21 (1)
N_2	.145	3.34	2.07	----	.26 (1)
He	.019	1.13	2.15	----	.34 (2)
N_2	.055	2.40	1.92	----	.39 (2)
He	.017	1.04	1.70	.45 (2)	----
N_2	.049	2.15	1.52	.52 (2)	----

B. Determined in Other Studies

M	β (3)	F_c	k_o ($\times 10^{-30}$ cm^6/molec-s)	k_∞ ($\times 10^{-12}$ cm^3/molec-s)	Referenc
He	--	.60	1.2 ($\pm$ 0.4)	1.40 ($\pm$ .14)	3
N_2	--	.60	2.0 ($\pm$ .5)	1.40 ($\pm$ .14)	3
N_2	--	.36	3.0 ($\pm$ 1.5)	2.2 ($\pm$ .5)	4
N_2	.13	.33	2.2	---	16
N_2	--	.60	2.2 ($\pm$ .1)	1.0 ($\pm$ .8)	2

(1) low adduct frequencies as hindered rotors

(2) low adduct frequencies as free rotors

(3) $\beta = k_o^{wc}/k_o^{sc}$

(4) $S_k = S_{eff} + \frac{(E_a - E_o)}{RT}$ where $E_{a\infty}$ is the Arrhenius activation-energy for adduct decompostion in high-pressure limit and E_o is the critical energy for adduct decomposition.

FIGURE CAPTIONS

Figure 1. Schematic diagram of discharge flow-long path absorption apparatus.

Figure 2. Pseudo first-order decays in the presence of excess NO_2 at 298K and a total pressure of 6 torr N_2. (a) $[NO_2]$ = 11.4 x 10^{13} molecule/cm^3; (b) $[NO_2]$ = 17.3 x 10^{13} molecule/cm^3; (c) $[NO_2]$ = 2.19 x 10^{14} molecules/cm^3; (d) $[NO_2]$ = 3.16 x 10^{14} molecule/cm^3; (e) $[NO_2]$ = 4.2 x 10^{14} molecule/cm^3.

Figure 3. k' versus $[NO_2]$ plot for $NO_2 + NO_3 + M(N_2)$ at 298K. (a) 6 torr N_2; (b) 5 torr N_2; (c) 4 torr N_2; (d) 3 torr N_2; (e) 2 torr N_2.

Figure 4. Fall-off curves for M = He and N_2 at 298K. For M = He, rate constant data of this study is plotted along with the higher pressure results of Kircher et al. For M = N_2 our data is plotted along with the higher pressure results of Kircher et al. and Croce de Cobos et al. The low pressure limiting rate coefficients, $k_o[M]$, and high pressure limiting rate coefficients, k_∞, given in Table II are shown as dashed lines.

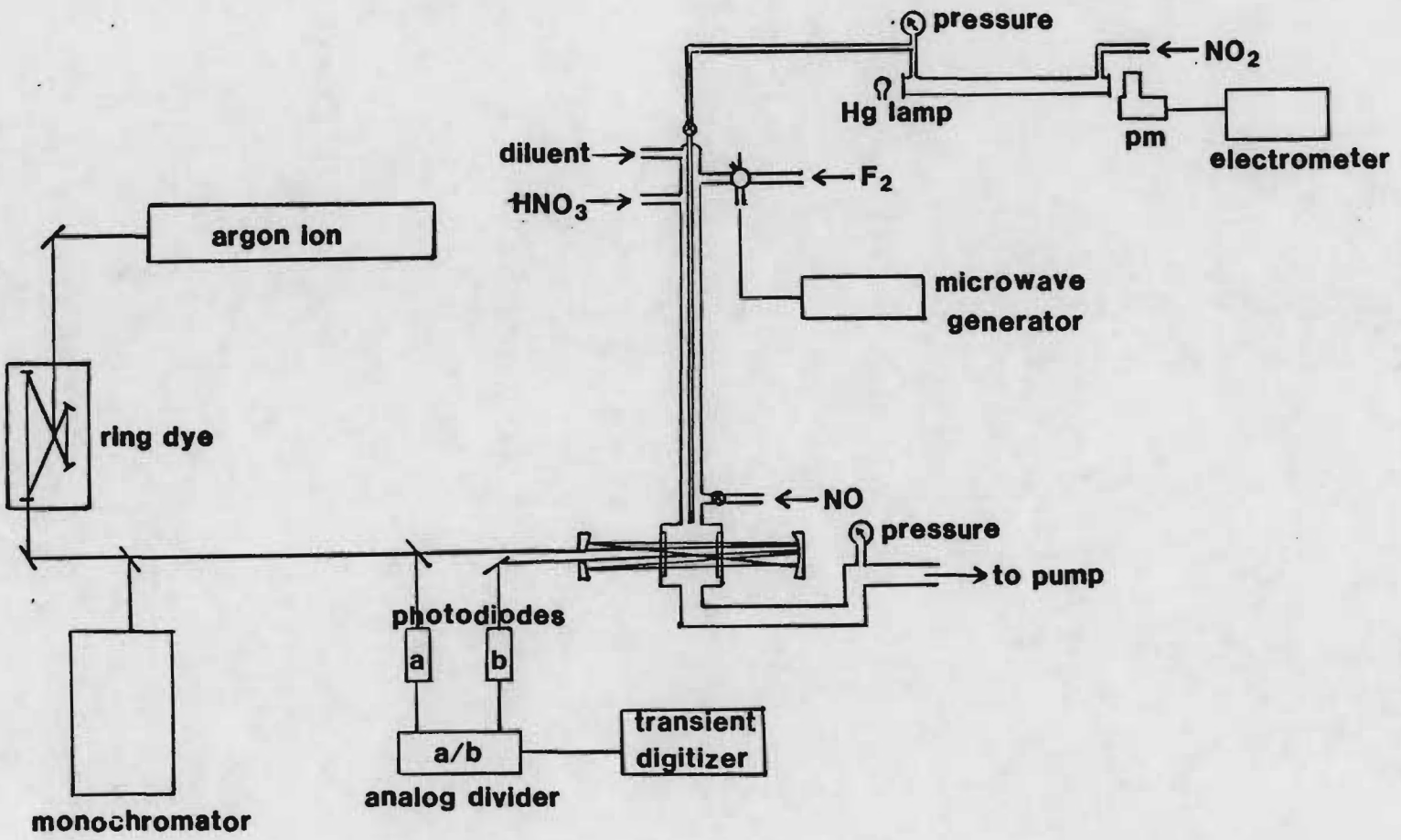
pressure
NO_2
Hg lamp
pm
electrometer
diluent
F_2
HNO_3
argon ion
microwave generator
ring dye
NO
pressure
to pump
photodiodes
a
b
transient digitizer
a/b
analog divider
monochromator

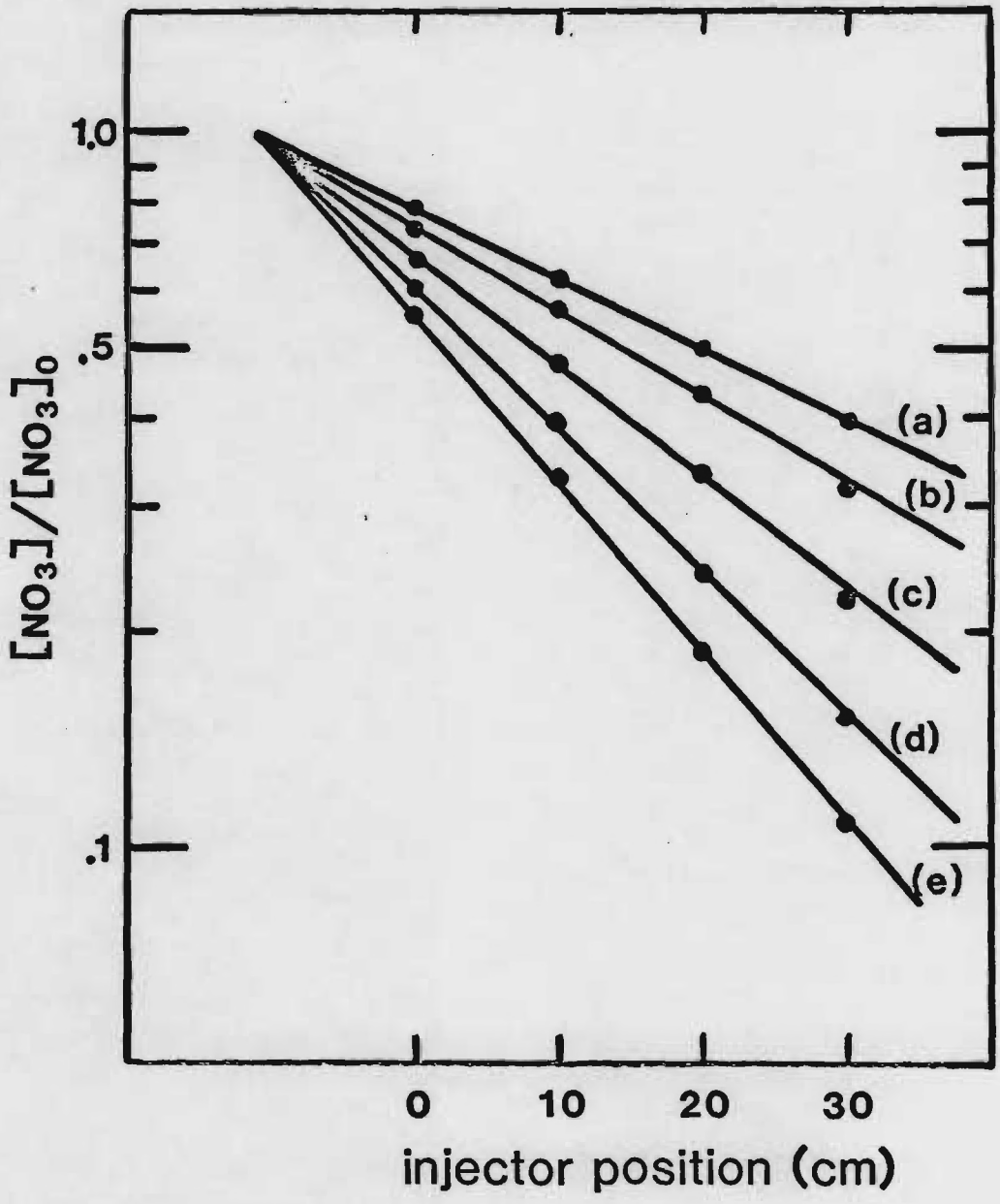
1.0
.5
.1
$[NO_3]/[NO_3]_o$
(a)
(b)
(c)
(d)
(e)
0
10
20
30
injector position (cm)

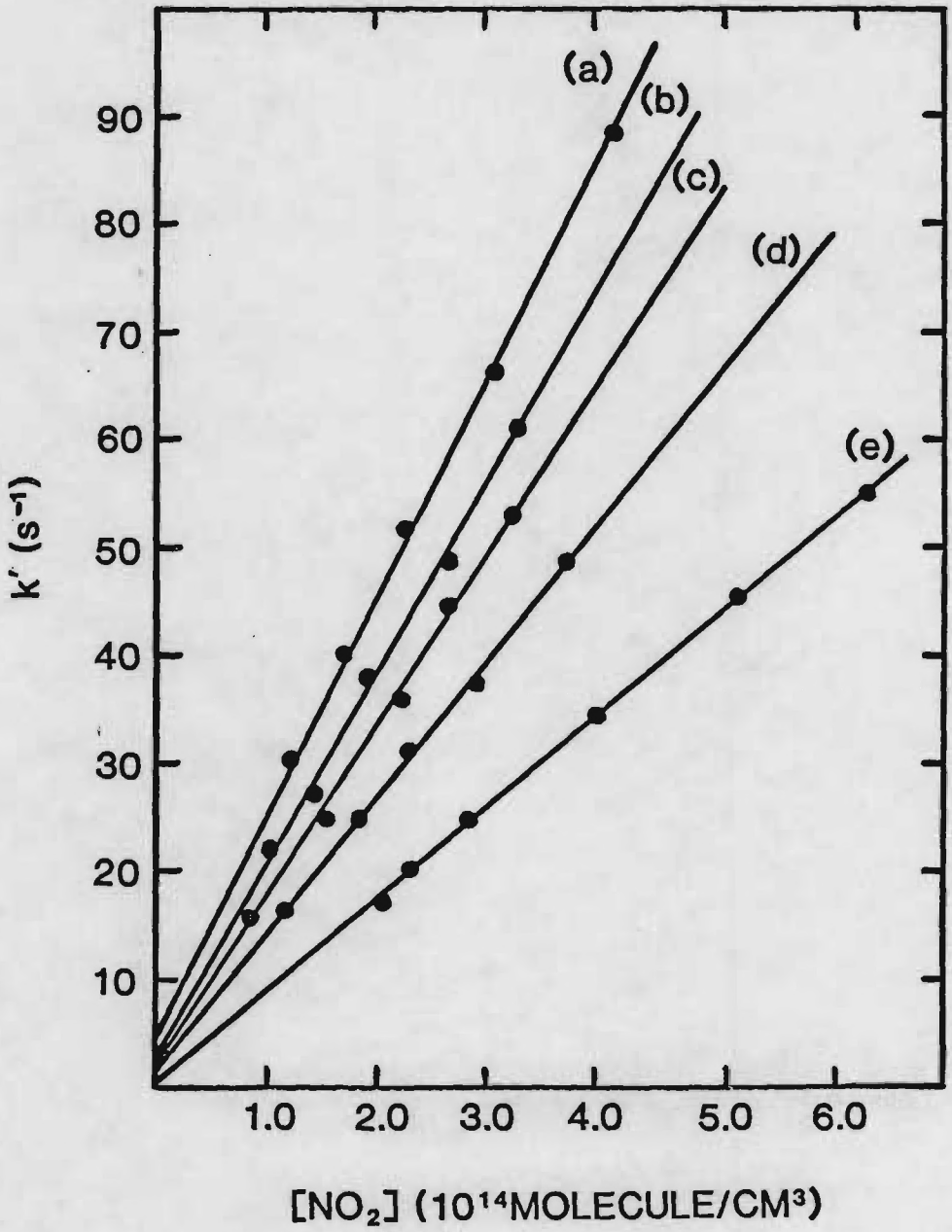
(a)
(b)
(c)
(d)
(e)
90
80
70
60
50
40
30
20
10
k' (s⁻¹)
1.0
2.0
3.0
4.0
5.0
6.0
[NO₂] (10¹⁴MOLECULE/CM³)

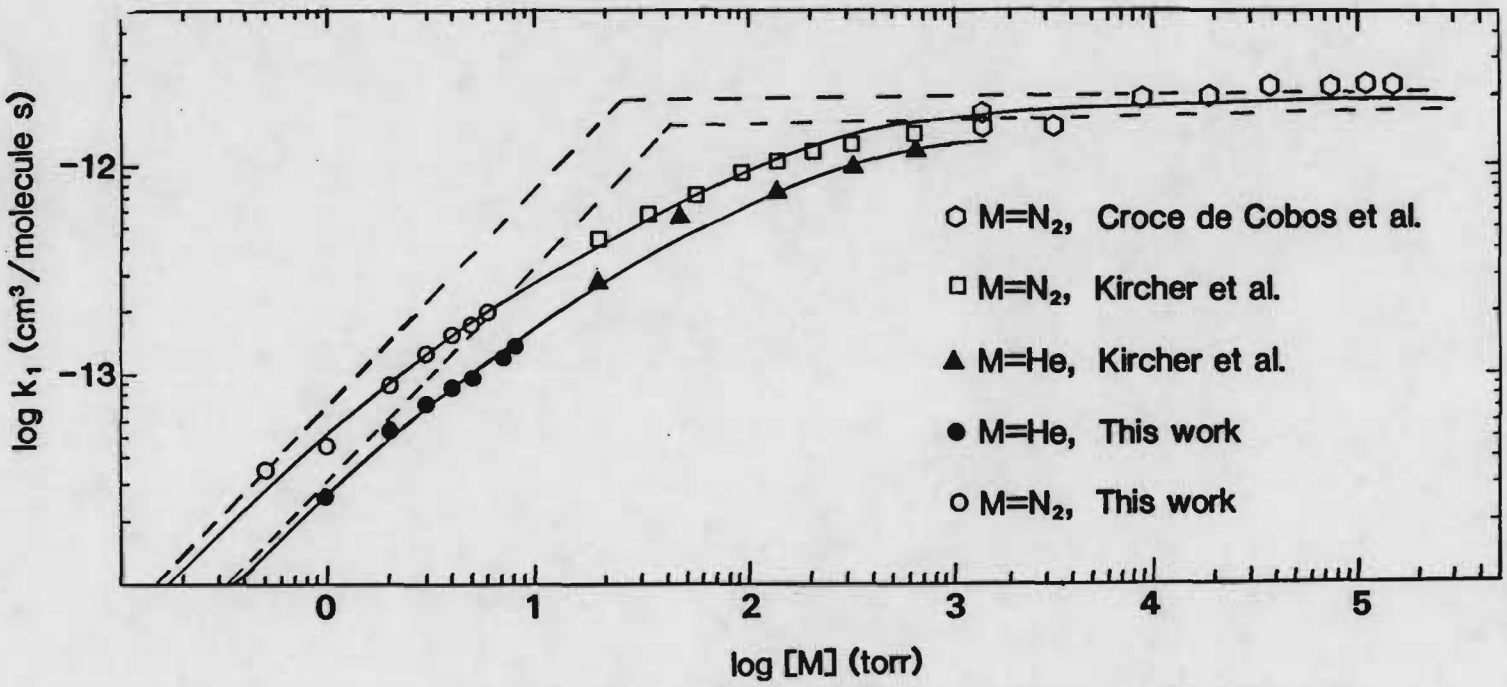
log k_1 (cm^3/molecule s)
−12
−13
0
1
2
3
4
5
log [M] (torr)
M=N_2, Croce de Cobos et al.
M=N_2, Kircher et al.
M=He, Kircher et al.
M=He, This work
M=N_2, This work

Chapter 2

The NO_3 + NO Reaction

Reaction (2),

$$NO_3 + NO \longrightarrow 2NO_2 \qquad (2)$$

was studied in two different experimental systems. A graduate student, Abbas Torabi, carried out this study as part of his Ph.D. thesis research. In a fast flow system, NO_3 was produced by thermolysis of N_2O_5 and detected by laser induced fluorescence. Experiments were carried out at pressures of 0.5-1.0 Torr in helium. A rate constant of $(3.24 \pm 0.32)\times10^{-11}$ cm^3 $molecule^{-1}$ s^{-1} was obtained; this rate constant is about 50% higher than those reported in two other recent studies[1,2] where k_2 was inferred by modeling complex system chemistry but in good agreement with another recent "direct" measurement.[3] To confirm that the results obtained in the fast flow experiments were free of systematic errors, particularly those involving wall catalyzed removal of NO_3, a second set of experiments were carried out where NO_3 was produced in a flash photolysis system by 193nm pulsed laser photolysis of N_2O_5 and monitored in real time by long path laser absorption. The pulsed photolysis experiments were carried out at pressures of 10-200 Torr in three different buffer gases. The

rate constant obtained from the pulsed photolysis experiments was $(2.93 \pm 0.09)\times10^{-11}$ cm^3 $molecule^{-1}$ s^{-1}. Experimental techniques and results are described in detail below.

The Flow System Experiments

Two major difficulties had to be overcome to carry out the fast flow experiments. First, since reaction (2) is very fast (about one eighth of gas kinetic) and our flow system has limited pumping speed, very low NO_3 levels had to be employed in order to attain pseudo first order conditions with NO in excess over NO_3. Under low pressure flow tube conditions, pulsed laser induced fluorescence was found to be about 100 times more sensitive than long path laser absorption. The radiative lifetime of electronically excited NO_3 is very long[4] (340 μs), so fluorescence quenching limits sensitivity even at very low pressures. For this reason, all fast flow experiments were carried out at total pressures of 1 Torr or less. A second major difficulty encountered in carrying out the fast flow experiments centered around cleanly producing the required small concentrations of NO_3. Initially, microwave discharges of F_2/He and CF_4/He were tried:

$$\mu\text{wave discharge through } F_2/He \text{ or } CF_4/He \longrightarrow F \quad (2.1)$$

$$F + HNO_3 \longrightarrow NO_3 + HF. \quad (2.2)$$

Large amounts of $O(^3P)$ were produced in these discharges, and the reaction

$$O(^3P) + NO_3 \longrightarrow NO_2 + O_2 \quad (2.3)$$

competed with reaction (2) down the length of the flow tube. A microwave discharge through an H_2/He mixture was also tried:

$$\mu\text{wave discharge through } H_2/He \longrightarrow H \quad (2.4)$$

$$H + F_2 \longrightarrow HF + F \quad (2.5)$$

$$F + H_2 \longrightarrow HF + H \quad (2.6)$$

$$F + HNO_3 \longrightarrow NO_3 + HF \quad (2.7)$$

However, large $O(^3P)$ levels were also produced when this method was employed. The approach which proved successful in eliminating problems from reaction (2.3) was thermal decomposition of N_2O_5:

$$N_2O_5 \xrightarrow{\Delta} NO_3 + NO_2 \quad (2.8)$$

N_2O_5 entrained in helium was passed through a glass injector heated to ~280°C in order to completely dissociate N_2O_5 into NO_3 + NO_2. The temperature of the injector was chosen to obtain complete dissociation of N_2O_5 while minimizing secondary dissociation of NO_3. Source NO_2 did not pose any problems because at 662nm, the fluorescence excitation wavelength, the sensitivity for NO_3 detection is about two orders of magnitude greater than the sensitivity for NO_2 detection (at 1 Torr total pressure).

A schematic of the fast flow apparatus is shown in Figure 2-1. NO_3 enters the flow tube through a side injector where it is entrained in the main helium flow. NO is added through a moveable injector. The integrated NO_3 fluorescence signal as a function of reaction time (i.e. NO injector position) is measured at various NO concentrations to obtain $k' \equiv k_2[NO]$. Typical NO_3 decay curves are shown in Figure 2-2. The slope of a plot of k' versus [NO] yields k_2. One such plot is shown in Figure 2-3. Six separate sets of experiments involving 42 individual k' measurements were carried out. In these experiments, the total pressure was varied by a factor of two and the NO_3 concentration in the absence of NO, $[NO_3]_o$, was varied by a factor of 8. The NO concentration in the NO/He storage bulk was checked before and after each set of experiments by converting NO quantitatively to NO_2 (through

reaction with O_2) and measuring [NO_2] by UV photometry. The results are summarized in Table 2-I. A weighted average of the six determinations gives the value $k_2 \pm 2 = (3.24 \pm 0.32) \times 10^{-11}$ cm^3 $molecule^{-1}$ s^{-1}.

The Laser Flash Photolysis Experiments

A schematic diagram of the laser flash photolysis-long path laser absorption apparatus (LFP-LPLA) is shown in Figure 2-4. The 193nm output from an ArF excimer laser was expanded, made spatially uniform via reflection off a segmented aperture optical integrator (SAOI), then passed through a 3 cm x 3 cm aperture and through the reaction cell. 662nm cw radiation from an Argon ion laser pumped ring dye laser was multipassed through the reaction cell at right angles to the photolysis beam. Using a modified White cell arrangement, we typically achieved 150 passes (i.e. a path length of 450 cm). The 662nm beam exiting the White cell was carefully filtered to remove all background radiation, diffused, and detected by a photomultiplier. The photomultiplier signal was then amplified and fed into a transient digitizer. Attenuation of the 662nm beam by NO_3 absorption was monitored as a function of time. The NO_3 detection sensitivity in these experiments was

about a factor of 10 poorer than in the fast flow experiments. However, resolution was about a factor of 100 better, so pseudo first order conditions could readily be attained.

Typical NO_3 temporal profiles observed in the LFP-LPLA experiments are shown in Figure 2-5. A pseudo-first order rate constant, k_1' is obtained as the slope of a plot of $\ln[\ln(I/I_o)]$ versus t where I_o is the signal immediately before the photolysis laser fires and I is the signal at time t after the laser fires. The slope of a plot of k' versus [NO] yields k_2. One such plot is shown in Figure 2-6. The negative intercept in the k' versus [NO] plot results from the fact that a steady state background NO_3 concentration was present due to N_2O_5 decomposition in the reactor. Hence, some of the added NO was removed by reaction with background NO_3 before the photolysis laser fired. To minimize this effect, the path from the cooled N_2O_5 reservoir to the reactor was made as short as possible, the flow rate through the reactor was made very fast, and N_2O_5 was added to the reaction mixture immediately before the mixture entered the reactor.

A total of twenty sets of experiments involving measurement of 96 individual pseudo-first order rate constants were carried out. In these experiments, He, Ar, and N_2 were used as buffer gases and the total pressure was varied by a factor of 20. The

initial NO_3 concentration, $[NO_3]_o$, was also varied by a factor of 20. The results are summarized in Table 2-II. A weighted average of the twenty rate constant determinations gives the result $k_2 \pm 2\sigma = (2.93 \pm 0.09) \times 10^{-11}$ cm^3 molecule^{-1} s^{-1}.

Comparison with Previous Work

Our results are compared with those reported by other investigators in Table 2-III. Our rate constants are in excellent agreement with the only other direct measurement, a very recent flow tube study by Hammer, et al.[3] The agreement with indirect measurements is not as good. However, if some of the results reported in the indirect studies are reanalyzed using currently accepted rate constants, better agreement is obtained. For example, Harker and Johnston[5] generated NO_3 by photolysis of NO_2 and considered eight simultaneously occurring reactions to deduce $k_2 = 8.7 \times 10^{-12}$ cm^3 molecule^{-1} s^{-1}. To obtain k_2, they measured k_2/K_{eq} where

$$NO_2 + NO_3 + M \longrightarrow N_2O_5 + M \qquad (2.9)$$

$$N_2O_5 + M \longrightarrow NO_2 + NO_3 + M \qquad (2.8)$$

$$K_{eq} \longrightarrow k_{2.9}/k_{2.8}. \qquad (2.10)$$

They used K_{eq} = 1.24 x 10^{-11} cm^3 $molecule^{-1}$ from the older literature. Their value for k_2/K_{eq} is 0.71 s^{-1}. Using K_{eq} = 3.35 x 10^{-11} cm^3 $molecule^{-1}$, the average of two recent determinations,[6,7] one obtains k_2 = 2.38x10^{-11} cm^3 $molecule^{-1}$ s^{-1}.

Graham and Johnston[1] measured K_{eq} and used Harker and Johnston's data to deduce k_2 = (1.89 ± 0.41)x10^{-11} cm^3 $molecule^{-1}$ s^{-1}. The work of Graham and Johnston does not represent an independent determination of k_2 and, of course, correction of their K_{eq} to the currently accepted value also gives k_2 = 2.38 x 10^{-11} cm^3 $molecule^{-1}$ s^{-1}. Another early determination of k_2 was reported by Husain and Norrish.[8] They produced NO_3 by the following mechanism:

$$NO_2 \longrightarrow NO + O(^3P) \qquad (2.11)$$

$$O(^3P) + NO_2 + M \longrightarrow NO_3 + M. \qquad (2.12)$$

Husain and Norrish used a seven reaction scheme to model their system chemistry including a value of 2.75 x 10^{-31} cm^6 $molecule^{-2}$ s^{-1} for $k_{2.12}$; they obtained k_2 = 13.8-20 x10^{-11} cm^3 $molecule^{-1}$ s^{-1}. However, if the currently recommended[10] value for $k_{2.12}$, 6.76 x 10^{-32} cm^6 $molecule^{-2}$ s^{-1}, is used to model Husain and Norrish's results, the value k_2 = 3.0-4.4 x 10^{-11} cm^3 $molecule^{-1}$ s^{-1} is obtained.

References

1. R. A. Graham and H. S. Johnston, J. Phys. Chem. 82, 254 (1978).

2. A. E. Croce de Cobos, H. Hippler, and J. Troe, J. Phys. Chem. 88, 5083 (1984).

3. P. D. Hammer, E. J. Dlugokencky, and C. J. Howard, to be published.

4. H. H. Nelson, L. Pasternack, and J. R. McDonald, J. Chem. Phys. 79, 4279 (1983).

5. A. B. Harker and H. S. Johnston, J. Phys. Chem. 77, 1153 (1973).

6. E. C. Tuazon, E. Sanhueza, R. Atkinson, W. P. L. Carter, A. M. Winer, and J. N. Pitts, Jr., J. Phys. Chem. 88, 3098 (1984).

7. C. C. Kircher, J. J. Margitan, and S. P. Sander, J. Phys. Chem. 88, 4370 (1984).

8. D. Husain and R. G. W. Norrish, Proc. Roy. Soc. A 273, 165 (1963).

9. H. W. Ford and N. Endow, J. Chem. Phys. 27, 1156 (1957).

10. W. B. DeMore, M. J. Molina, R. T. Watson, D. M. Golden, R. F. Hampson, M. J. Kurylo, C. J. Howard, and A. R. Ravishankara, "Chemical Kinetics and Photochemical Data for Use in Stratospheric Modeling", JPL publication 83-62, 1983.

Table 2-I. Rate constants for the NO_3 + NO reaction at 298K obtained using a fast flow apparatus with laser induced fluorescence detection of NO_3. Helium was used as the buffer gas in all experiments.

P(Torr)	$[NO_3]_o$ (10^{11} cm^{-3})	$k_2 \pm 2\sigma$ (10^{-11} cm^3 $molecule^{-1}$ s^{-1}
1.0	1.4	3.11 ± 0.15
1.0	0.6	3.42 ± 0.25
0.5	4.0	3.38 ± 0.38
0.5	1.0	3.60 ± 0.28
1.0	2.0	2.79 ± 0.30
1.0	5.0	3.33 ± 0.20

Table 2-II. Rate constants for the NO_3 + NO reaction at 298K obtained using a laser flash photolysis apparatus with long path laser absorption detection of NO_3.

M	P(Torr)	$[NO_3]_o$ (10^{12} cm^{-3})	$k_2 \pm 2\sigma$ (10^{-11} cm^3 $molecule^{-1}$ s^{-1})
He	10	6	2.76 ± 0.18
	15	20	2.79 ± 0.27
	20	25	3.17 ± 0.51
	36	23	3.63 ± 0.43
	40	16	2.87 ± 0.28
	45	14	3.72 ± 0.59
	53	30	3.02 ± 0.59
	100	16	2.79 ± 0.19
	200	10	3.08 ± 0.66
Ar	50	1.5	3.33 ± 0.51
	50	7	3.50 ± 0.42
	51	9	2.90 ± 0.28
	54	4	3.58 ± 0.70
	60	6	2.77 ± 0.64
	200	6	2.75 ± 0.46
	200	3	2.96 ± 0.20
N_2	50	8	2.75 ± 0.27
	50	22	2.84 ± 0.14
	200	10	3.49 ± 0.37
	200	20	2.70(a)

(a) based on only two data points, so no standard deviation can be quoted.

Table 2-III. Comparison of our rate constants for the NO_3 + NO reaction with those measured by other investigators.

Investigators	$k_2(10^{-11}cm^3molecule^{-1}s^{-1})$ Original analysis	Updated analysis[a]	Ref.
Husain & Norrish	13.8-19.9	3.0-4.4	8
Harker & Johnston	0.87 ± 0.06	2.38	5
Graham & Johnston	1.9 ± 0.4		1
Croce de Cobos, et. al.	2 ± 1		2
Hammer, et al.	2.9	direct measurement	3
This work			
flow system	3.24 ± 0.32	direct measurements	
flash phot. system	2.93 ± 0.09		

(a) see text for details

Figure Captions

2-1. Schematic of the fast flow apparatus.

2-2. Typical plots of $[NO_3]$ observed at the detector versus injector position, d. $[NO_3]_o = 1.4 \times 10^{11}$ cm^{-3}. [NO] in units of 10^{12} cm^{-3}=(a) 0, (b) 1.55, (c) 3.07, (d) 4.23, (e) 5.78, (f) 7.02, (g) 8.35. Solid lines are obtained from linear least squares analyses and give the following pseudo first order rate constants: (a) 0 s^{-1}, (b) 63 ± 11 s^{-1}, (c) 109 ± 5 s^{-1}, (d) 138 ± 9 s^{-1}, (e) 190 ± 7 s^{-1}, (f) 226 ± 24 s^{-1}, (g) 267 ± 28 s^{-1}. Errors are 2σ and represent precision only.

2-3. Plot of k' vs. [NO] for the data shown in Figure 2. Solid line is obtained from a linear least squares analysis which gives $k_2 \pm 2\sigma = (3.11 \pm 0.15) \times 10^{-11}$ cm^3 molecule^{-1} s^{-1}.

2-4. Schematic of the laser flash photolysis apparatus.

2-5. Typical NO_3 temporal profiles observed in the laser flash photolysis experiments. P = 51 Torr, buffer gas = Argon, $[NO_3]_o = 9 \times 10^{12}$ cm^{-3}, [NO] in units of 10^{15} cm^{-3} = (a) 1.43, (b) 1.73, (c) 2.00. Solid lines are obtained from linear least squares analyses and give the following pseudo first order rate constants: (a) 30600 s^{-1}, (b) 37100 s^{-1}, (c) 48300 s^{-1}.

2-6. Typical k' vs. [NO] plot for the laser flash photolysis experiments. P = 51 Torr, buffer gas = Argon, $[NO_3]_o = 9 \times 10^{12}$ cm^{-3}. Solid line is obtained from a linear least squares analysis which gives $k_2 \pm 2\sigma = (2.90 \pm 0.28) \times 10^{-11}$ cm^3 molecule^{-1} s^{-1}.

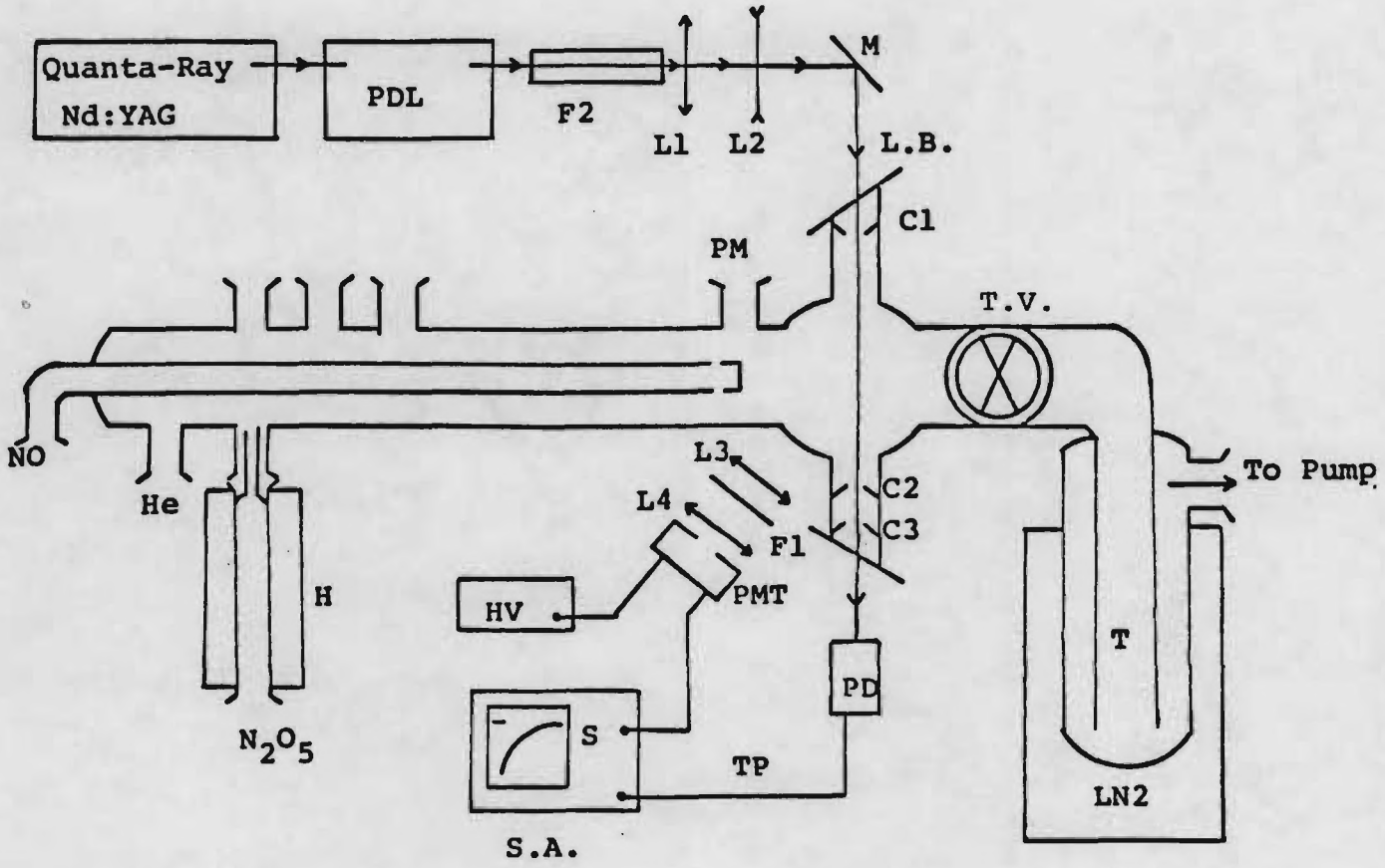

C_1, C_2, C_3 = Collimators

F1 = Colored Glass Filter

F2 = NO_2 Absorption Filter

H = Heater

HV = High Voltage

L1, L2, L3, L4 = Lenses

L.B. = Laser Beam

PD = Photodiode LN_2, Liquid Nitrogen

PDL = Pulsed Dye Laser

PM = Pressure Monitor

S = Signal

S.A. = Signal Analyzer

T = Trap

TP = Trigger Pulse

TV = Throttle Valve

Figure 2-1

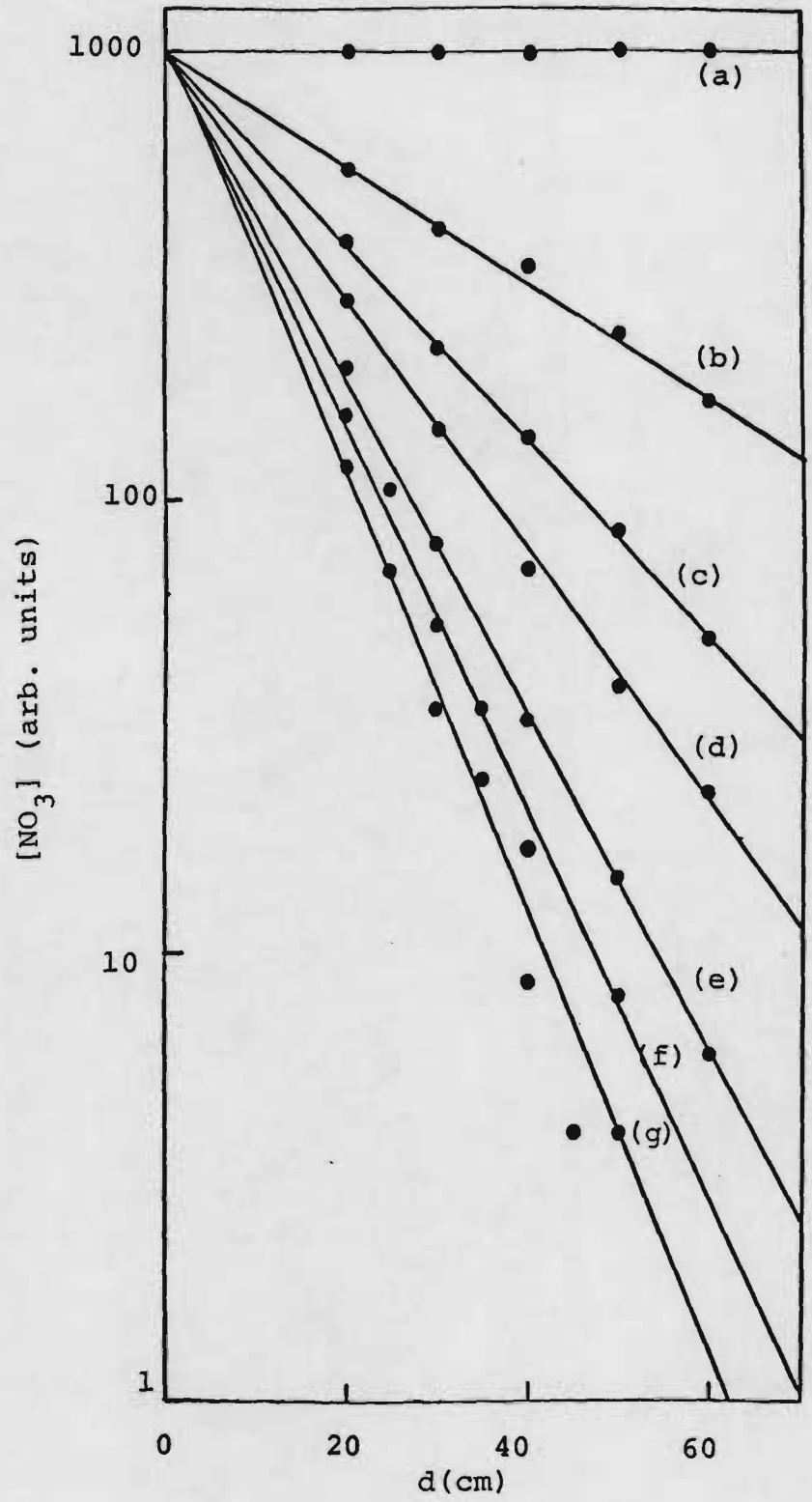

Figure 2-2

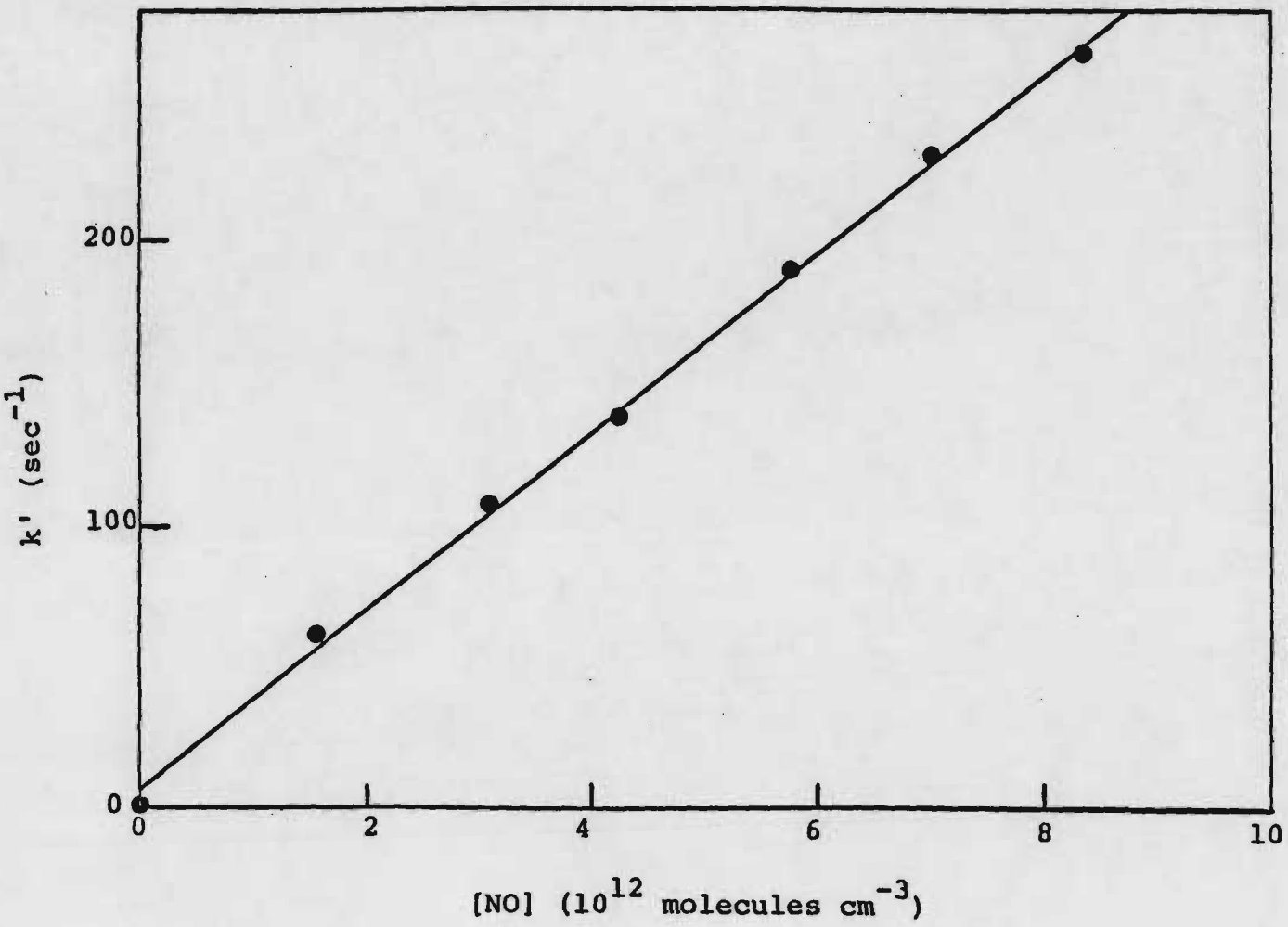

Figure 2-3

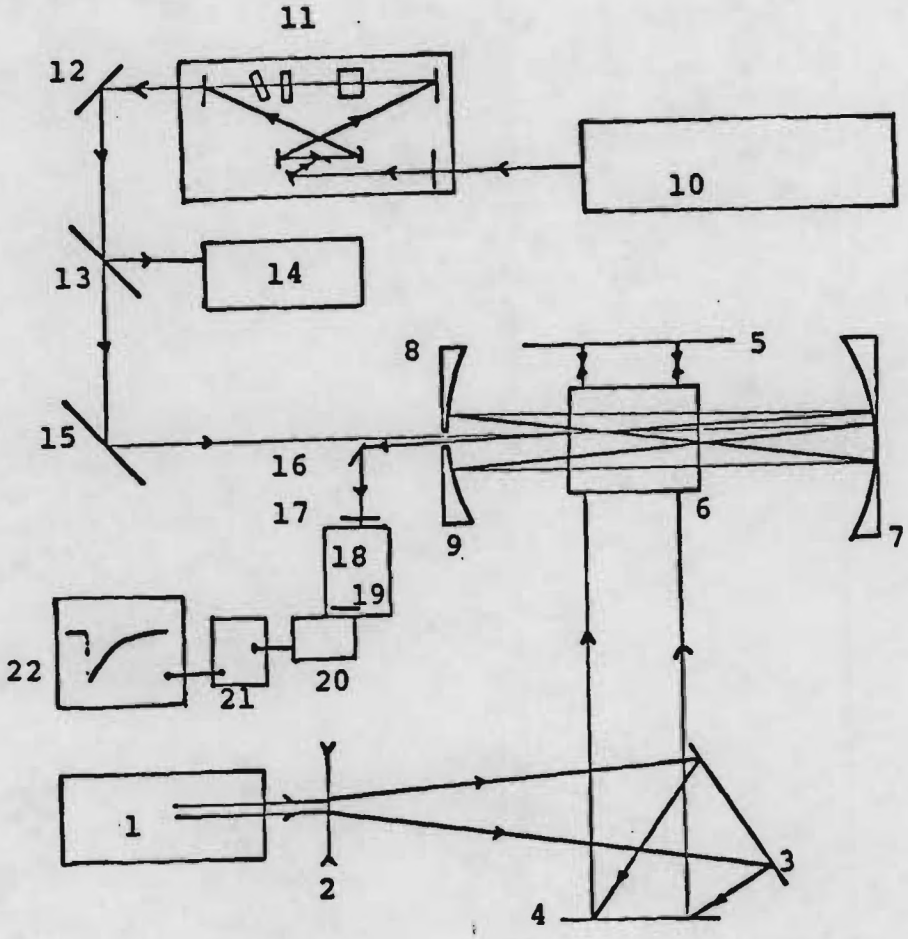

1. Ar-F Excimer Laser
2. Cylindrical Lens
3. U.V. Coated Mirror
4. SAOI
5. U.V. Coated Mirror
6. The Reaction Cell
7, 8, and 9. Concave Mirrors
10. Ar Ion Laser
11. Ring Dye Laser
12. Coated Mirror
13. Focusing Lens
14. Monochromator
15. Coated Mirror
16. Coated Mirror
17. Neutral Density Filter
18. Grating
19. Diffuser
20. PMT
21. Amplifier
22. Signal Analyzer

Figure 2-4

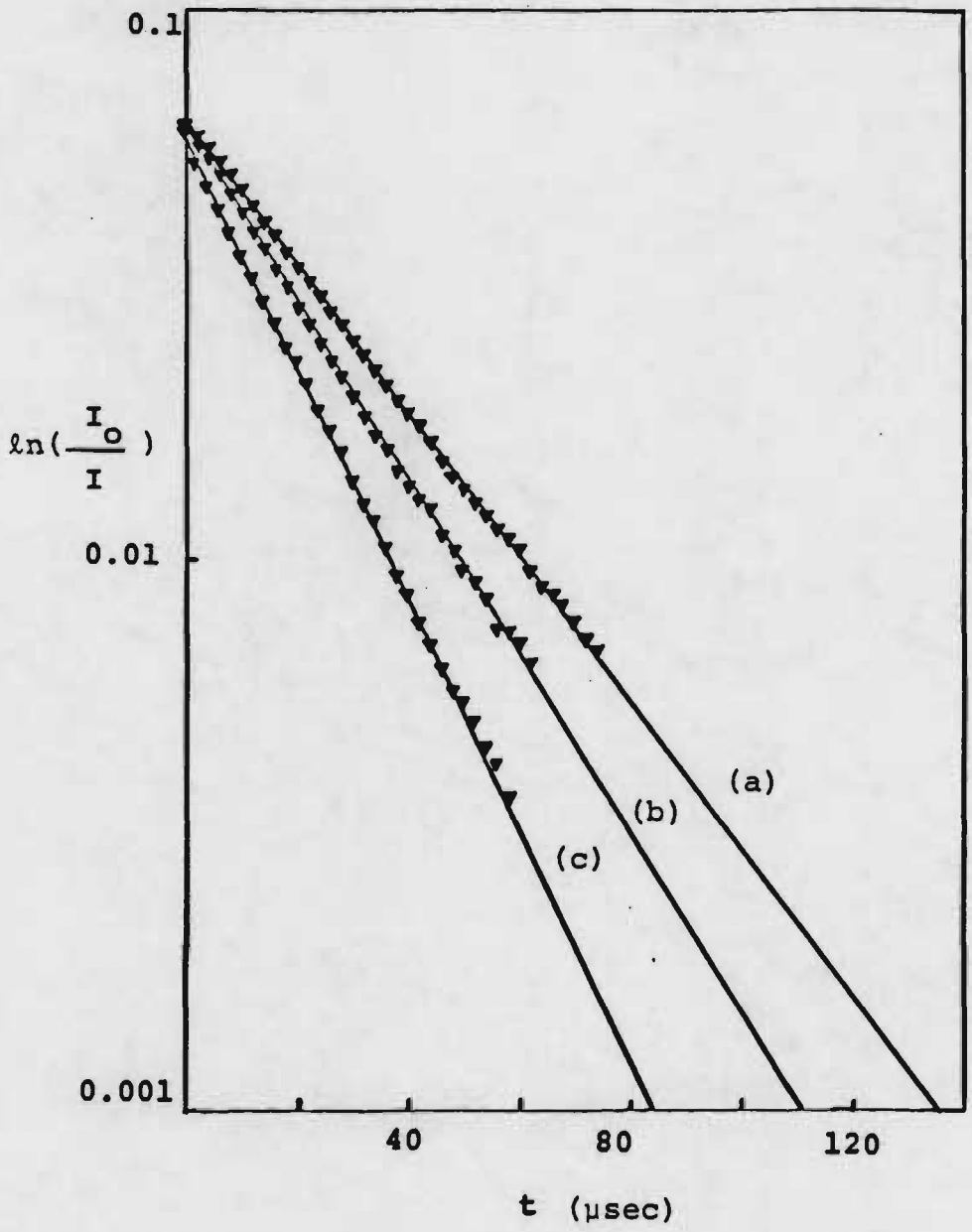

Figure 2-5

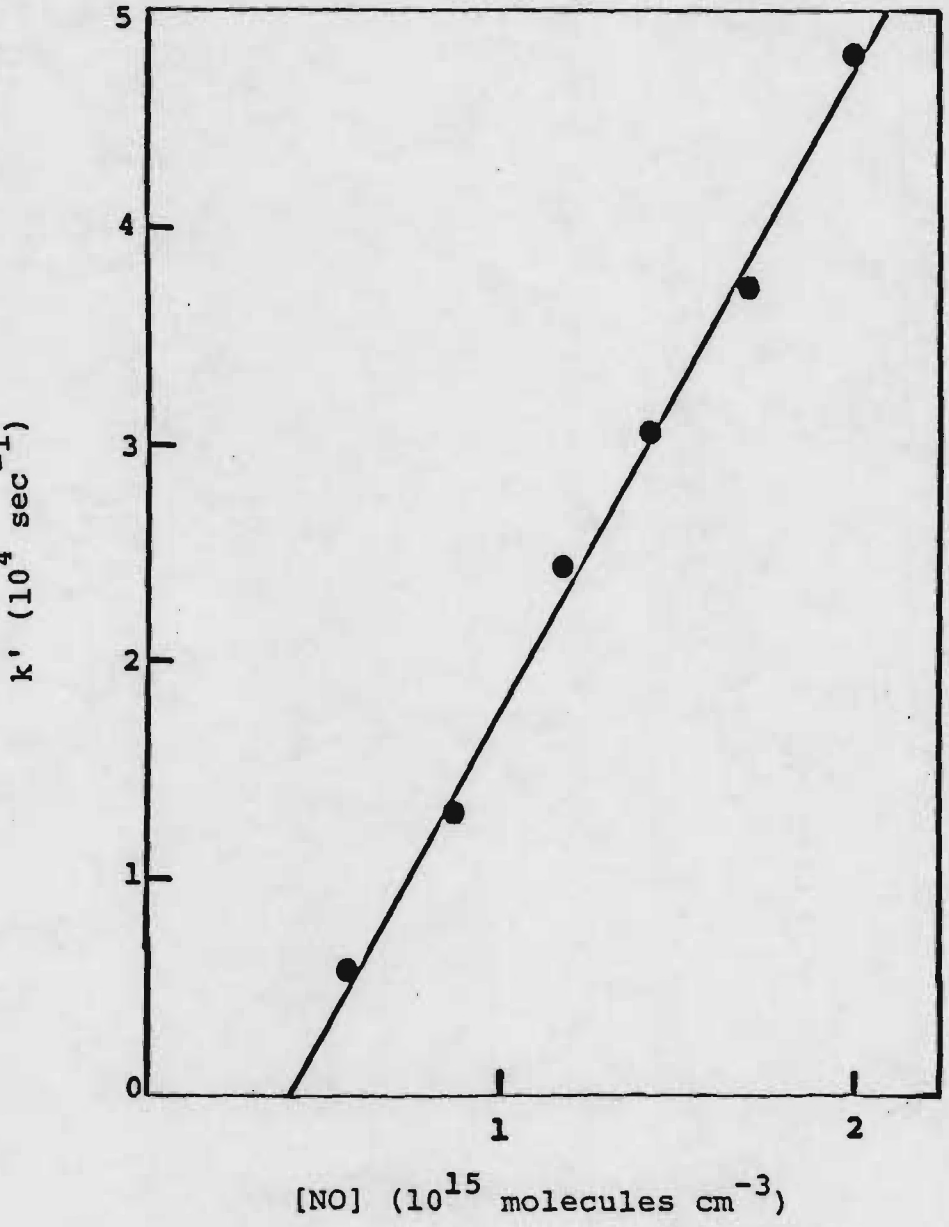

Figure 2-6

Chapter 3

The O + ClO Reaction

Reaction (3) is of great interest because of its role as the rate limiting step in the chlorine catalyzed destruction of stratospheric ozone:

$$O(^3P) + ClO \longrightarrow Cl + O_2 \qquad (3)$$

$$Cl + O_3 \longrightarrow ClO + O_2. \qquad (3.1)$$

The currently recommended[1] 298K rate constant for reaction (3), 5.0×10^{-11} cm^3 $molecule^{-1}$ s^{-1}, is based on the pre-1984 work of Bemand, et al.[2], Clyne and Nip[3], and Zahniser and Kaufman.[4] Recently, there have been four studies of reaction (3)[5-8] which report $k_3(298K)$ values 15-30% below the recommended value. All four of the recent studies were conducted in the low pressure regime of discharge flow systems. Our study of reaction (3) employs a laser flash photolysis technique recently developed in our laboratory[9] for studying radical-radical reaction kinetics at high pressure. The goal of the experiments is to check the validity of the recent studies and examine the pressure

dependence of k_3 up to several hundred Torr.

The apparatus used to study reaction (3) is shown in Figure 3-1. ClO and $O(^3P)$ were produced via photolysis of a mixture containing Cl_2, O_3, and the diluent gas (He or N_2). Two photolysis wavelengths, 532nm and 355nm (i.e. the 2nd and 3rd harmonics of the Nd:YAG fundamental), were employed simultaneously.

$$Cl_2 \xrightarrow[355nm]{h\nu} 2Cl \qquad (3.2)$$

$$Cl + O_3 \quad ClO + O_2 \qquad (3.1)$$

$$O_3 \xrightarrow[532nm]{h\nu} O(^3P) + O_2\ (X^3\Sigma) \qquad (3.3)$$

$$O(^3P) + ClO \longrightarrow \text{products.} \qquad (3)$$

The 355nm UV beam was optically integrated[9] to produce a spatially uniform square beam while the 532nm green beam was used as is. The two beams were combined using a dichroic mirror such that the green beam was at the center of the much larger UV beam. The temporal profile of $O(^3P)$ was measured as a function of reaction time using the resonance fluorescence detection technique. Experiments were carried out under pseudo-first order conditions with ClO in large excess over $O(^3P)$. Based on our knowledge of ClO chemistry, we expected the ClO concentration to

be constant during the period of $O(^3P)$ decay. To calculate [ClO], which is equal to the concentration of Cl atoms produced by Cl_2 photolysis, it is necessary to know $[Cl_2]$, the absorption cross section for Cl_2 at 355nm ($\sigma_{Cl_2}^{355nm}$), and the photon fluence of the 355nm laser pulse (Φ):

$$[Cl] = 2\Phi\sigma_{Cl_2}^{355nm}[Cl_2]. \qquad (3.4)$$

$\sigma_{Cl_2}^{355nm}$ is well known.[1] The Cl_2 concentration was measured by UV photometry at 326nm *in situ* in the slow flow system. Φ was measured using an EG&G radiometer. To ensure the accuracy of the measured Φ, actinometry experiments were carried out. The experiments consisted of photolyzing a Cl_2, NOCl mixture in the apparatus shown in Figure 3-2a. A DC low pressure mercury lamp was used as the source of 185nm radiation. The lamp intensity was monitored as a function of time. Cl_2 was photolyzed under geometric conditions identical to those in the actual experiments to produce a spatially uniform density of Cl atoms. The Cl atoms then reacted with NOCl to destroy one atom of NOCl for each chlorine atom produced by photolysis:

$$Cl + NOCl \longrightarrow Cl_2 + NO. \qquad (3.5)$$

The loss of NOCl produced an increase in transmitted 185nm radiation, an example of which is seen in Figure 3-2b. It is clear that the measured NOCl loss could be measured very accurately. The measured NOCl loss is compared with the calculated concentration of Cl atoms produced. If the radiometer is accurate, then the concentration of NOCl lost should equal the calculated concentration of Cl atoms produced. We found that the radiometer read ~ 8% too low. Figure 3-2c shows a plot of [NOCl] lost versus calculated [Cl] produced. It was found that variations in [NOCl], [Cl_2], and laser energy did not effect the calibration factor. The actinometry results were also checked against a Scientech disc calorimeter and were found to be 6% lower than the calorimeter measurements.

In the kinetics experiments, $O(^3P)$ temporal profiles were measured at various concentrations of ClO. Figure 3-3 shows a set of measurements where [Cl_2] and [O_3] were held constant and the photon fluence at 355nm was varied to change [ClO]. The slope of these decay plots yield

$$k_3' \equiv k_3[ClO] + k_4[Cl_2] + k_d, \qquad (3.6)$$

where k_d is the rate of loss $O(^3P)$ due to diffusion from the

detector field of view, reaction with O_3, and reaction with background impurities. A plot of k_3' vs. [ClO] at fixed $[Cl_2]$ and $[O_3]$ yields a straight line with slope k_3. A typical k' vs. [ClO] plot is shown in Figure 3-4. A total of 25 determinations of k_3 involving measurement of 234 individual k_3' values have been carried out. The results are summarized in Table 3-I. There is no observable variation in the value of k_3 as a function of total pressure, $[O(^3P)]_o$, $[O_3]$, $[Cl_2]$, or the photolysis laser repetition rate. Averaging the 25 determinations gives the result $k_3 \pm 2\sigma = (5.5 \pm 1.0) \times 10^{-11}$ cm^3 molecule^{-1} s^{-1}.

Our results are compared with those reported by other investigators in Table 3-II. Our value for $k_3(298K)$ is in good agreement with the early measurements of Clyne and co-workers[2,3] but somewhat higher than the values reported in the five most recent studies.[4-8] There do not seem to be any secondary chemistry complications in our experiments which could account for this difference. If ClO were being depleted by some unidentified background reaction, then our measured rate constant would be lower than the actual value. Similarly, if reaction (3) produced some $O_2(^1\Sigma)$, then $O(^3P)$ would be rapidly regenerated under our experimental conditions via the reaction

$$O_2(^1\Sigma) + O_3 \longrightarrow O(^3P) + 2O_2. \qquad (3.7)$$

This complication would also result in measurement of a rate constant which was lower than the actual value. Some of the recent determinations of k_3 could have overestimated [ClO] due to unaccounted for losses in the source region of the discharge flow system. However, the experiments of Schwab, et al.[7], where kinetic data were obtained with both O and ClO in excess and both radicals were directly measured in all experiments, are difficult to dispute.

Due to interference from O_3, we were not able to directly monitor ClO by UV photometry. Instead, the ClO concentration was inferred from the measured 355nm laser photon fluence and the known photochemistry of the Cl_2/O_3 system. The laser photon fluence measurement was carried out using a calibrated radiometer, a disc calorimeter, and a chemical actinometry method. The actinmetry results, which were 8% higher than the radiometer results and 6% lower than the calorimeter results, were used to calculate [ClO]. Hence, it seems unlikely that the measured photon fluence was in error by more than ± 10%. Nonetheless, the laser photon fluence remains the parameter which is most likely to be in error.

To circumvent the need for measuring an absolute laser

photon fluence and also allow direct monitoring of ClO, we have devised a modified scheme for investigating reaction (3). We expect to carry out these new experiments in the near future. Our new high powered excimer laser will be used to photolyze Cl_2 at 351nm (XeF laser). With a photon fluence of 20 mjoules per cm^2, 1% of the Cl_2 in the path of the laser beam will be photolyzed, i.e. photolysis of 10^{16} Cl_2 per cm^3 will yield $2x10^{14}$ Cl per cm^3. In the presence of 5×10^{13} O_3 per cm^3, reaction (3.1) will proceed at a first order rate of 3400 s^{-1} and will result in conversion of all O_3 to ClO. After reaction (3.1) has gone to completion, a second laser will be fired to photolyze a small fraction of ClO and produce $O(^3P)$. $O(^3P)$ will decay by reacting with ClO ($k' \sim 2000\ s^{-1}$ under the specified conditions) and Cl_2 ($k' \sim 300\ s^{-1}$ under the specified conditions). Excess Cl atoms should not effect the temporal profiles of either ClO or $O(^3P)$. This reaction scheme has two important advantages: (1) the laser photon fluence need not be known in order to determine the ClO concentration - the O_3 concentration before photolysis equals the ClO concentration after photolysis, and (2) since the O+ ClO reaction will occur with no O_3 present, it will be possible to directly monitor the temporal profile of ClO by UV photometry.

In closing, we would like to emphasize that our present

value for k_3 is very tentative; we do not yet consider it a publishable result. Hopefully, the new experiments described above will help to clarify the reasons for the discrepancy between our result and other recent measurements.

References

1. W. B. DeMore, M. J. Molina, R. T. Watson, D. M. Golden, R. F. Hampson, M. J. Kurylo, C. J. Howard, and A. R. Ravishankara, "Chemical Kinetics and Photochemical Data for Use in Stratospheric Modeling", JPL publication 83-62, 1983.

2. P. P. Bemand, M. A. A. Clyne, and R. T. Watson, J. C. S. Far. Trans. I 69, 1356 (1973).

3. M. A. A. Clyne and W. S. Nip, JCS Far. Trans. I 72, 2211 (1976).

4. M. S. Zahniser and F. Kaufman, J. Chem. Phys. 66, 3673 (1977).

5. M. T. Leu, J. Phys. Chem. 88, 1394 (1984).

6. J. J. Margitan, J. Phys. Chem. 88, 3638 (1984).

7. J. J. Schwab, D. W. Toohey, W. H. Brune, and J. G. Anderson, J. Geophys. Res. 89, 9581 (1984).

8. A. P. Ongstad and J. W. Birks, J. Chem. Phys. 81, 3922 (1984).

9. A. R. Ravishankara, P. H. Wine, and J. M. Nicovich, J. Chem. Phys. 78, 6629 (1983).

Table 3-I. Kinetic data for the reaction $O(^3P) + ClO \rightarrow$ products. T = 298K. Except where otherwise indicated, 355nm photolysis of Cl_2, O_3, M mixtures was used as the source of ClO and the laser repetition rates were 0.58 Hz. 532nm photolysis of O_3 was the source of $O(^3P)$ in all experiments.

P(Torr)	M	$[Cl_2]$ (10^{15} cm^{-3})	$[O_3]$ (10^{14} cm^{-3})	No. of Experiments[a]	Range of $k'(s^{-1})$	$10^{11} k_{bi}$[b] (cm^3 $molecule^{-1}$ s^{-1}
8	N_2	3.3	6.2	17	270-1370	6.17 ± 0.38
16	N_2	3.7	11	4	159-1040	5.02 ± 0.55
16	N_2	3.7	10	7	232-1510	6.11 ± 0.36
35	He	3.1	2.1-6.5	9	206-893	5.49 ± 0.82
35	N_2	3.2	7.3	4	334-911	4.72 ± 0.43
35	N_2	3.2	6.6	9	165-948	5.35 ± 0.34[a]
35	N_2	3.6	10-31	9	185-921	5.45 ± 0.11
35	N_2	3.2	2.6-11	6	137-661	5.51 ± 0.38
35	N_2	3.6	7.0	10	177-1080	5.66 ± 0.47
35	N_2	3.6	3.1-6.0	9	172-879	4.79 ± 0.34[d]
35	N_2	3.7	3.9	6	177-1240	5.60 ± 0.38
35	N_2	3.7	15	5	164-1160	5.18 ± 0.11
35	N_2	1.8	10	8	120-1100	5.82 ± 0.26
35	N_2	3.7	12	8	169-703	5.49 ± 0.64[e]
35	N_2	3.8	12	6	186-749	5.60 ± 0.35[e]
35	N_2	3.9	11	8	207-715	6.43 ± 0.50[e][f
35	N_2	3.5	11	7	192-641	5.62 ± 0.26[e]
35	He	3.3	11	9	260-771	6.12 ± 0.39

Table 3-I (continued)

P(Torr)	M	$[Cl_2]$ (10^{15} cm^{-3})	$[O_3]$ (10^{14} cm^{-3})	No. of Experiments[a]	Range of $k'(s^{-1})$	$10^{11} k_{bi}$[b] (cm^3 $molecule^{-1}$ s^{-1})
50	He	3.2	9.7	8	227-1190	5.56 ± 0.49
50	He	2.7	8.3	11	148-963	4.42 ± 0.31[g]
100	N_2	3.6	10-31	11	161-784	6.09 ± 0.95
190	N_2	3.5	18	19	152-920	4.64 ± 0.43
190	N_2	3.2	10-24	13	143-909	5.45 ± 0.35[d]
200	N_2	3.5	10	12	181-924	5.74 ± 0.64[d]
200	He	3.4	3.0-5.0	19	141-1300	5.27 ± 0.29[g]

(a) Experiment ≡ determination of one pseudo first order rate constant

(b) Errors are 2σ and represent precision only

(c) Laser repetition rate: 0.2 Hz

(d) Very low $[O(^3P)]$

(e) 355nm beam expanded more than in other experiments to give a more uniform beam, but with lower photon fluence.

(f) 0.5 Torr H_2O added to reaction mixture.

(g) 351nm XeF laser photolysis used to produce ClO.

Table 3-II. Summary of reported rate constants for the O + ClO reaction at 298K.

Investigators	Method[a),(b)]	k_3 (10^{-11} cm^3 $molecule^{-1}$ s^{-1})	Reference
Bemand, Clyne, & Watson	DF-RF(O) DF-MS(ClO)	5.3 ± 0.8 5.7 ± 2.3	2
Clyne and Nip	DF-RF(O)	5.2 ± 1.6	3
Zahniser and Kaufman	DF-RF(Cl)[c]	4.4 ± 0.9	4
Leu	DF-RF(O)	3.6 ± 0.7	5
Margitan	LFP-RF(O)[d]	4.2 ± 0.8	6
Schwab, Toohey, Brune, & Anderson	DF-LMR(ClO) DF-RF(O)	3.5 ± 0.5	7
Ongstad & Birks	DF-CL(O)[e]	3.5 ± 0.6	8
This Work	LFP-RF(O)	5.5 ± 1.0[f]	

(a) DF ≡ discharge flow; LFP ≡ laser flash photolysis; RF ≡ resonance fluorescence, MS ≡ mass spectrometry; LMR ≡ laser magnetic resonance; CL ≡ chemiluminescence.

(b) The monitored species is given in parentheses

(c) O + ClO rate constant measured relative to Cl + O_3 rate constant

(d) ClO produced in DF system, i.e. experiments limited to low pressures

(e) NO added to produce chemiluminescence via $O + NO + M \rightarrow NO_2^* \rightarrow h\nu + NO_2$

(f) Further experimentation is needed to verify this result.

Figure Captions

3-1. Schematic of the apparatus used in the O + ClO study.

3-2. a) Schematic of the apparatus used in the actinometry experiments.
b) Plot of the variation of transmitted 185nm light following photolysis of a Cl_2/NOCl mixture at 355nm. ln (I/I_o) is proportional to the concentration of Cl atoms produced. I_o' is the transmitted intensity before addition of NOCl.
c) Plot of the measured loss in NOCl as a function of the calculated Cl atom concentration (based on fluence measured using the radiometer.

3-3. Typical $O(^3P)$ temporal profiles. Experimental Conditions: 35 Torr N_2; 3.9×10^{14} O_3 per cm^{-3}; [ClO] = (a) & (b) 0, (c) 0.85×10^{13} cm^{-3}, (d) 1.88×10^{13} cm^{-3}. k' values derived from the data are (a) 46 s^{-1}, (b) 178 s^{-1}, (c) 651 s^{-1}, (d) 1240 s^{-1}.

3-4. Typical k' vs. [ClO] plot. Experimental Conditions: 35 Torr N_2, 3.9×10^{14} O_3 per cm^3, 3.7×10^{15} Cl_2 per cm^3. Solid line is obtained from a linear least squares analysis and gives the bimolecular rate constant. Open circles are points obtained from temporal profiles (b)-(d) in Figure 3.3.

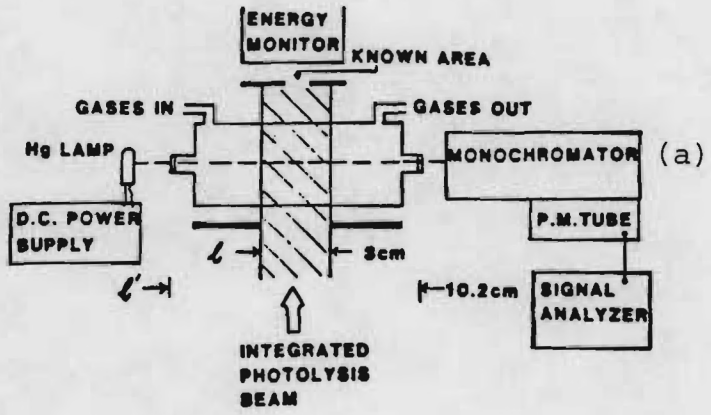
ENERGY MONITOR
KNOWN AREA
GASES IN
GASES OUT
Hg LAMP
MONOCHROMATOR
(a)
D.C. POWER SUPPLY
P.M.TUBE
ℓ
3cm
ℓ'
10.2cm
SIGNAL ANALYZER
INTEGRATED PHOTOLYSIS BEAM

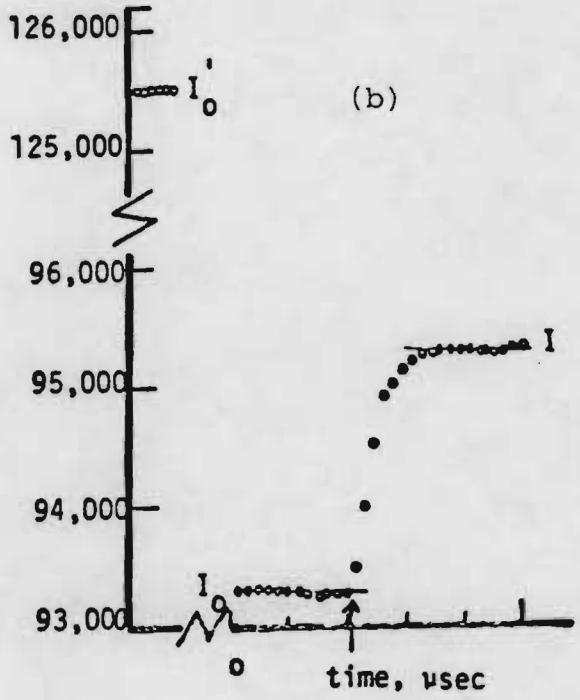
126,000
I_o'
(b)
125,000
96,000
95,000
94,000
I
I_o
93,000
0
time, μsec

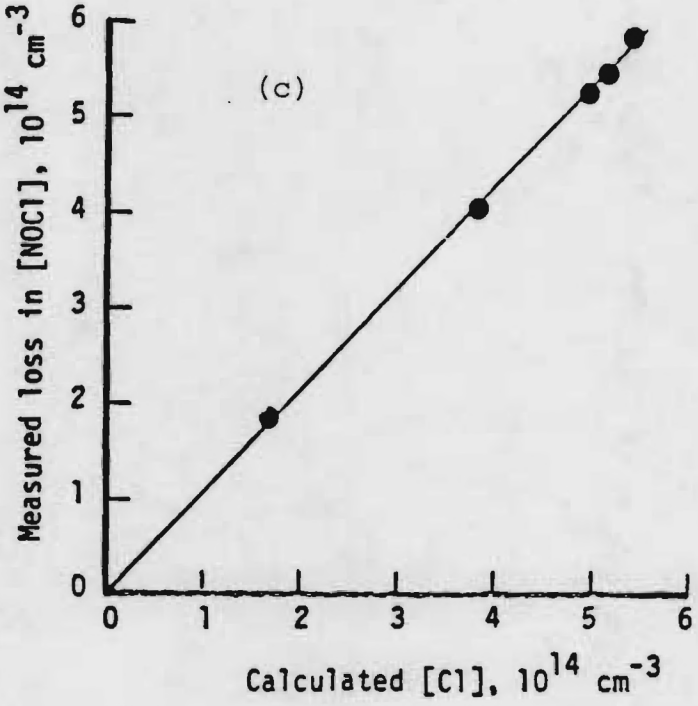
(c)
Measured loss in [NOCl], 10^{14} cm^{-3}
0
1
2
3
4
5
6
Calculated [Cl], 10^{14} cm^{-3}

Figure 3-2

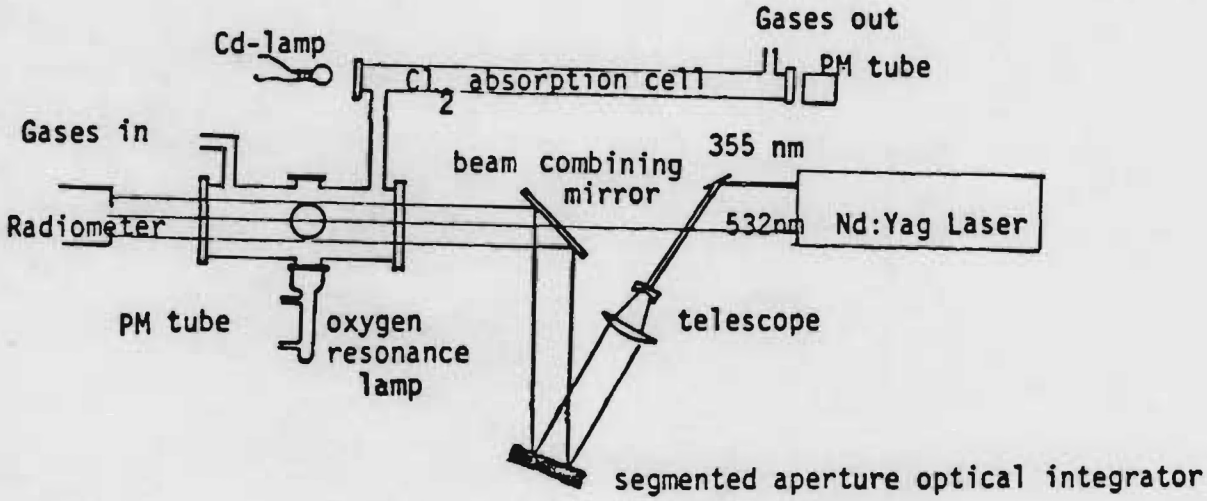
Gases out
Cd-lamp
PM tube
Cl_2 absorption cell
Gases in
355 nm
beam combining mirror
Radiometer
532nm
Nd:Yag Laser
PM tube
oxygen resonance lamp
telescope
segmented aperture optical integrator

Figure 3-1

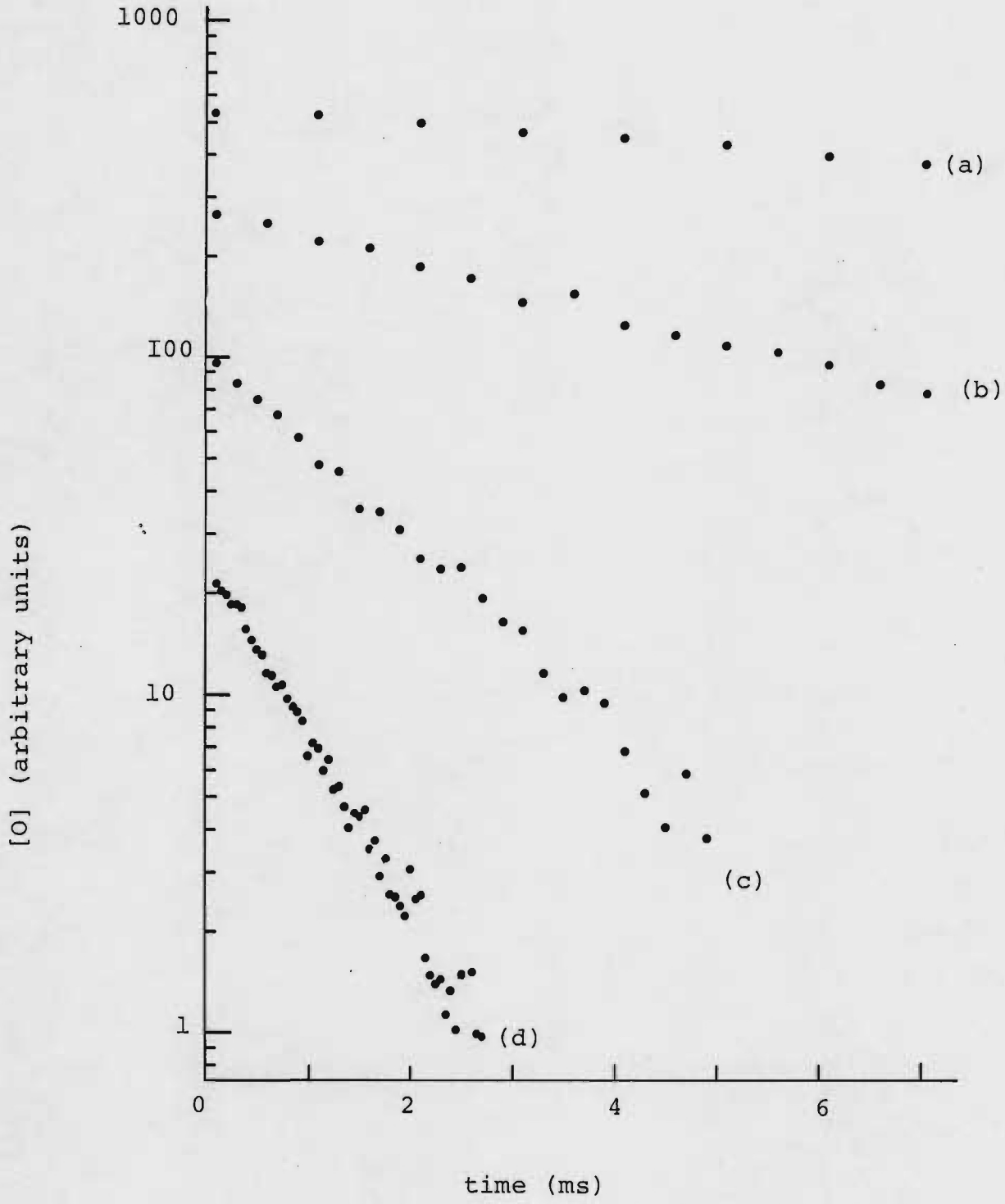

Figure 3-3

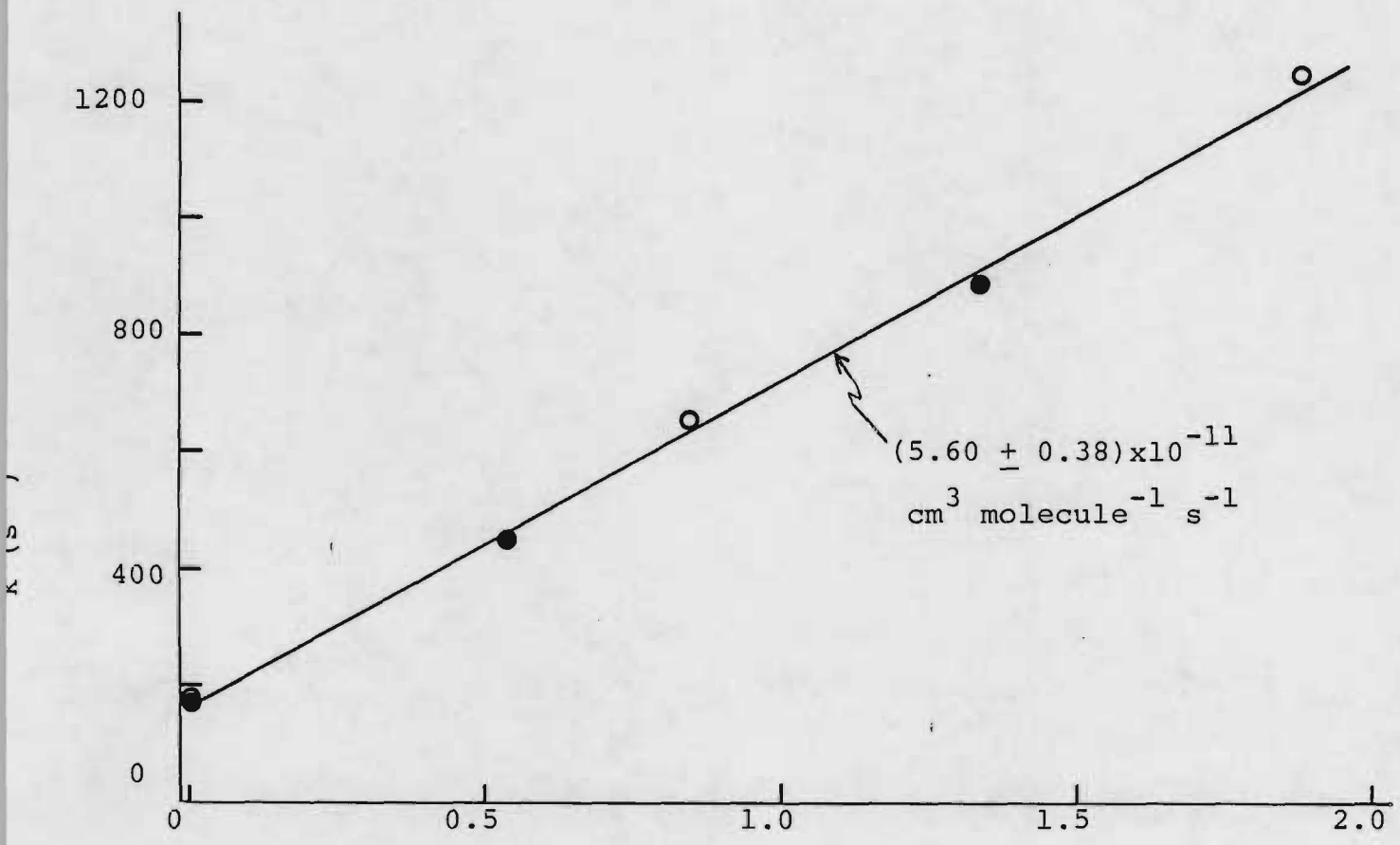
1200
800
400
0
0
0.5
1.0
1.5
2.0
(5.60 ± 0.38)x10^-11
cm^3 molecule^-1 s^-1
[ClO] (10^13 cm^-3)

Figure 3-4

Chapter 4

The Reactions of $O(^3P)$ and $O(^1D)$ with Cl_2

The reactions of $O(^3P)$ and $O(^1D)$ with Cl_2, i.e. reactions (4) and (5), were investigated because of their potential involvement in our study of the $O(^3P)$ + ClO reaction, i.e. reaction (3). In order to study reaction (3) using the ClO production scheme described in the last chapter, it is necessary to know the rate of $O(^3P)$ loss in the absence of ClO. This loss rate is expected to be dominated by reaction (4). Reaction (5) represents a potential alternate source of ClO which could be employed to study reaction (3) if a significant fraction of $O(^1D)$ deactivation did not lead to $O(^3P)$ production. Unfortunately, our results suggest that nearly one out of every four $O(^1D)$ atoms removed by Cl_2 is converted to $O(^3P)$.

A paper describing our studies of the reactions of $O(^3P)$ and $O(^1D)$ with Cl_2 has been submitted to The Journal of Physical Chemistry. The remainder of this chapter consists of a copy of the manuscript. It should be noted that the numbering of reactions and equations in the manuscript is different from that in other sections of the report.

KINETICS OF THE REACTIONS OF $O(^3P)$ AND $O(^1D)$ WITH Cl_2

P. H. Wine,* J. M. Nicovich, and A. R. Ravishankara+

Molecular Sciences Branch, Georgia Tech Research Institute,
Georgia Institute of Technology, Atlanta, GA 30332

*Author to whom correspondence should be addressed

+Present address: Aeronomy Laboratory, NOAA/R/E/AL-2,
325 Broadway
Boulder, CO 80303

Submitted to The Journal of Physical Chemistry

ABSTRACT

$O(^3P)$ has been monitored using time resolved resonance fluorescence spectroscopy following 248nm pulsed laser photolysis of $O_3/Cl_2/N_2$ and $O_3/Cl_2/He$ mixtures. Rate coefficients for the reaction $O(^3P) + Cl_2 \xrightarrow{k_1}$ products have been measured over the temperature range 245-371K under conditions where the $O(^3P)$ temporal behavior was unaffected by fast secondary reactions of $O(^3P)$ with products. The data are well described by the following Arrhenius expression: $k_1(T) = (7.4 \pm 2.4) \times 10^{-12} \exp[(-1650 \pm 100)/T]$ cm^3 $molecule^{-1}$ s^{-1}. By monitoring the appearance of $O(^3P)$, the rate coefficient for total removal of $O(^1D)$ by Cl_2 has been determined to be $(2.81 \pm 0.42) \times 10^{-10}$ cm^3 $molecule^{-1}$ s^{-1} at 298K. 24 ± 10% of the $O(^1D) + Cl_2$ quenching interactions result in formation of $O(^3P)$.

KINETICS OF THE REACTIONS OF $O(^3P)$ AND $O(^1D)$ WITH Cl_2

Introduction

The reactions of ground state and electronically excited oxygen atoms with molecular chlorine,

$$O(^3P) + Cl_2 \longrightarrow Cl + ClO + 6.5 \text{ kcal/mole} \quad (1a)$$

$$O(^3P) + Cl_2 \xrightarrow{M} Cl_2O + 39 \text{ kcal/mole} \quad (1b)$$

$$O(^1D) + Cl_2 \longrightarrow Cl + ClO + 52 \text{ kcal/mole} \quad (2a)$$

$$O(^1D) + Cl_2 \xrightarrow{M} Cl_2O + 84 \text{ kcal/mole} \quad (2b)$$

$$O(^1D) + Cl_2 \longrightarrow O(^3P) + Cl_2 + 45 \text{ kcal/mole} \quad (2c)$$

are of interest to kineticists both as examples of simple three atom systems where experimental rate coefficients and branching ratios can be used to test the validity of reaction rate theories, and also as laboratory sources of the important stratospheric

radical ClO. While kinetic data for both reaction (1)[1-6] and reaction (2)[7,8] are reported in the literature, neither k_1 nor k_2 is firmly established. Kinetics investigations of reaction (1) are subject to interferences from the fast secondary reactions

$$O(^3P) + ClO \text{ ----> products} \quad (3)$$

$$O(^3P) + Cl_2O \text{ -----> products.} \quad (4)$$

None of the studies carried out to date employed sufficiently large Cl_2 to $O(^3P)$ concentration ratios to avoid this complication. The only direct measurement of k_2 reported to date[7] employed an experimental approach which, based on comparison with results from several laboratories for a number of $O(^1D)$ reactions, seems to systematically overestimate $O(^1D)$ reaction rates by more than a factor of two.

In this paper we report the results of a temperature dependent kinetics study of reaction (1). Also, we report a 298K study of reaction (2) where both the overall rate coefficient and the branching ratio for reactive versus non-reactive quenching were determined. Both reactions were studied under experimental conditions where secondary removal or formation of $O(^3P)$, the monitored species, was unimportant.

Experimental

The experimental approach is described elsewhere.[9-11] It involves time resolved resonance fluorescence detection of $O(^3P)$ following 248nm pulsed laser photolysis of O_3. All experiments were carried out under slow flow conditions with the concentration of each component in the reaction mixture determined from measurements of the appropriate mass flow rates and the total pressure. In studies of reaction (1), where Cl_2 levels were relatively high, the Cl_2 concentration was measured directly by UV photometry at 326.1nm; the Cl_2 absorption cross section at the monitoring wavelength was taken to be 2.58×10^{-19} cm^2.[12] The light source for the absorption measurement was a cadmium pen ray lamp and the absorption cell, plumbed in series with the reaction cell, was 60 cm in length. Experiments were carried out with the reaction mixture traversing the absorption cell both before and after flowing through the reactor. The observed kinetics were independent of the relative positions of the absorption cell and reactor.

The gases used in this study had the following stated minimum purities: He - 99.999%, N_2 - 99.995%, O_2 - 99.99%, Cl_2 - 99.96%. He, N_2, and O_2 were used as supplied while Cl_2 was subjected to repeated freeze(77K)- pump-thaw cycles before use.

O_3 was prepared by passing UHP O_2 through a commercial ozonator and stored on silica gel at 197K. Before use it was degased at 77K to remove O_2.

Results and Discussion

1. $O(^3P) + Cl_2$

In studies of reaction (1), nitrogen was used as the buffer gas at a pressure of 150 Torr. In all experiments $[N_2] > 50$ $[Cl_2]$. Since $k_2 \sim 10\ k_5$, more than 80% of the photolytically produced $O(^1D)$ was deactivated by N_2.

$$O(^1D) + N_2 \text{ -----> } O(^3P) + N_2. \qquad (5)$$

$k_5 = 2.6 \times 10^{-11}$ cm^3 $molecule^{-1}$ s^{-1},[12] so conversion of $O(^1D)$ to $O(^3P)$ was complete in 50ns, which is instantaneous on the time scale for $O(^3P)$ decay. All experiments were carried out under pseudo-first order conditions with $[Cl_2] >> [O(^3P)]$. Reaction of $O(^3P)$ with O_3 was negligibly slow under our experimental conditions. Therefore, in the absence of complicating secondary reactions, the $O(^3P)$ temporal profile should be controlled by

$O(^3P) + Cl_2 \text{ -----> products}$ (1)

$O(^3P) \text{ -----> }$ loss by diffusion from the detector field of view and reaction with background impurities, (6)

and simple first order kinetics should be obeyed:

$$\ln\{[O(^3P)]_o/[O(^3P)]_t\} = (k_1[Cl_2] + k_6)t \equiv k't. \quad (I)$$

As predicted by equation (I), exponential $O(^3P)$ decays and linear dependencies of k' on $[Cl_2]$ were observed under nearly all experimental conditions investigated. The only exceptions were a few preliminary experiments where the ratio $[Cl_2]/[O(^3P)]_o$ was intentionally made low. Under these conditions the $O(^3P)$ decay rate increased with increasing time after the photolysis flash due to reaction of $O(^3P)$ with ClO and/or Cl_2O generated as products of reaction (1). Only experiments where $[Cl_2]/[O(^3P)]_o > 2.5 \times 10^4$ were used to obtain values for $k_1(T)$. Under such conditions, large variations in $[O(^3P)]_o$ and $[O_3]$ had no effect on measured rate coefficients.

Typical $O(^3P)$ temporal profiles observed under conditions of high $[Cl_2]/[O(^3P)]_o$ are shown in Figure 1 and typical k' vs. $[Cl_2]$ plots are shown in Figure 2. The rate data for reaction (1) are summarized in Table I. Errors quoted in Table I are 2σ and represent the precision of the slope of the k' vs. $[Cl_2]$ plots. The absolute accuracy of each $k_1(T)$ is affected by uncertainties in the Cl_2 concentration measurement as well as the precision of the data and is estimated to be ±12%. An Arrhenius plot of the results for reaction (1) is shown in Figure 3. An unweighted linear least squares analysis of the ln k_1 vs. 1/T data gives the following Arrhenius expression:

$$k_1(T) = (7.4 \pm 2.4) \times 10^{-12} \exp[(-1650 \pm 100)/T] \text{ cm}^3 \text{ molecule}^{-1} \text{ s}^{-1}.$$

Errors in the Arrhenius parameters are 2σ and refer to precision only ($\sigma_A \equiv A\, \sigma_{\ln A}$).

Our results for reaction (1) are compared with those obtained in other laboratories in Figure 3. We obtain a somewhat larger activation energy and larger A factor than currently recommended[13]. At 298K and below, our data suggest that k_1 is significantly slower than previously believed. All previous investigations of reaction (1) employed discharge flow systems

and most used relatively insensitive detection schemes. Consequently, in all previous studies it was necessary to correct the raw kinetic data for contributions from the rapid secondary reactions of $O(^3P)$ with ClO and/or Cl_2O. Our experiments employed such large Cl_2:$O(^3P)$ concentration ratios that the contribution of secondary removal to the observed $O(^3P)$ kinetics was negligible.

Our results provide little information concerning the relative importance of channels (1a) and (1b). In experiments where the $[Cl_2]/[O(^3P)]_o$ ratio was intentionally made low, the $o(^3P)$ decay rate was found to be time dependent, increasing with increasing time after the photolysis flash. However, since both ClO and Cl_2O react rapidly with $O(^3P)$, the above observation does not allow one to distinguish between the two reaction channels. A few preliminary experiments were carried out at a total N_2 pressure of 50 Torr--a factor of three lower than the pressure used in a vast majority of the experiments. Within experimental error, $k_1(298K)$ was found to be the same at 50 Torr as at 150 Torr. k_{1b} would probably be pressure dependent at N_2 pressures below 150 Torr, so this observation can be considered weak evidence that Cl + ClO are the major products of reaction (1). However, a significant addition channel should not be ruled out,

particularly since Parrish and Herschbach[14], in a molecular beam study of reaction (1), found evidence for a long lived Cl_2O intermediate.

2. $O(^1D) + Cl_2$

In studies of reaction (2), helium was used as the buffer gas at a pressure of 25 Torr. The concentration of O_3 photolyte was typically 7×10^{12} per cm^3 and the photolysis laser power was kept low enough that less than 10% of the O_3 in the beam was photolyzed. Photolytically produced $O(^1D)$ interacted with O_3, He, background impurities, and Cl_2 to produce some $O(^3P)$. In the absence of rapid secondary $O(^3P)$ production or removal processes, measurement of the $O(^3P)$ appearance rate constitutes a measurement of the total $O(^1D)$ removal rate. Since the primary photolysis yield of $O(^3P)$ is accurately known,[10] measurement of the ratio of instantaneously produced $O(^3P)$ to that produced as a result of $O(^1D)$ deactivation provides information concerning the branching ratio for non-reactive versus reactive quenching. More precise information about the branching ratio can often be obtained from comparison of fluorescence signals obtained in excess Cl_2 with those obtained in excess N_2 [N_2 deactivates $O(^1D)$

to $O(^3P)$ with unit yield].

Over the range of experimental conditions employed to measure k_2, $O(^3P)$ formed directly from O_3 photolysis appeared as an instantaneous signal synchronous with the laser firing while $O(^3P)$ formed from collisional deactivation of $O(^1D)$ appeared as an exponentially rising signal with a time constant of 36-260 μs. Since secondary production of $O(^3P)$ should be negligible on the time scale for reaction (2), the $O(^3P)$ temporal profile is described by the following relationship:

$$[O(^3P)]_t = \frac{k_a[O(^1D)]_o\Theta}{k_d - k_a}\{\exp(-k_a t) - \exp(-k_d t)\} + [O(^3P)]_o \exp(-k_d t) \qquad \text{(II)}$$

where k_a and k_d are pseudo-first order rate coefficients for the appearance and decay of $O(^3P)$, $[O(^1D)]_o$ and $[O(^3P)]_o$ are the initial concentrations of photolytically produced atoms, and Θ is the number of $O(^3P)$ formed for each $O(^1D)$ removed. k_d was directly measured by monitoring the $O(^3P)$ decay after $O(^1D)$

deactivation was complete, and was found to be ~ 50 s^{-1} in all experiments. k_d was significantly faster than in the $O(^3P) + Cl_2$ experiments (Table I) because the experiments were carried out at lower pressure in helium buffer gas and because much faster flow rates were employed in order to minimize reactions of $O(^1D)$ with background impurities.

Typical $O(^3P)$ temporal profiles are shown in Figure 4. To obtain k_a from the data, it is necessary to determine S_{max}^{corr}, the maximum signal which would have been obtained if no $O(^3P)$ loss occurred before $O(^1D)$ removal was complete. The iterative procedure used to obtain S_{max}^{corr} from the measured S_{max} has been described previously.[9] Because, k_a was more than 70 times k_d in all experiments, the required corrections were small and S_{max}^{corr} was determined quite accurately. Values for k_a were obtained from linear least squares analyses of $\ln(S_{max}^{corr} - S_t)$ versus t plots. The results are plotted as a function of $[Cl_2]$ in Figure 5. A linear least squares analysis of the k_a versus $[Cl_2]$ data gives the rate coefficient $k_2 = (2.81 \pm 0.13) \times 10^{-10}$ cm^3 $molecule^{-1}$ s^{-1}, where the uncertainty is 2σ and represents precision only. Based on estimates of possible systematic errors and uncertainties in the determination of the Cl_2 concentration, we feel that the absolute accuracy of our determination of k_2 is

± 15%.

The kinetic data used to determine k_2 were also used to estimate the fraction of $O(^1D)$ deactivation which proceeds via non-reactive quenching, i.e. k_{2c}/k_2. First, β , the ratio of $O(^3P)$ produced by photolysis to that produced by $O(^1D)$ deactivation, was determined for each temporal profile measured:

$$\beta \equiv \frac{[O(^3P)]_o}{[O(^1D)]_o\Theta} = \frac{S_o}{S_{max}^{corr} - S_o} \qquad \text{(III)}$$

In the above equation S_o represents the fluorescence signal immediately after the laser fires. The β versus f_{Cl_2} data were then simulated for different choices of k_{2c}/k_2 ($f_{Cl_2} \equiv$ the fraction of $O(^1D)$ removed by Cl_2). The following equations govern the f_{Cl_2} versus β dependence:

$$f_{Cl_2} = k_2[Cl_2]/k_a = (k_a - k_a^o)/k_a \qquad \text{(IV)}$$

$$\beta^* = \beta\Theta \qquad \text{(V)}$$

$$\Theta = (k_Q + k_{2b})/k_a \qquad \text{(VI)}$$

$$k_Q + k_R = k_a^o \qquad \text{(VII)}$$

$$k_Q/k_a^o = \beta^*/\beta^o. \qquad \text{(VIII)}$$

In the above equations, β^* represents β under conditions where $O(^1D)$ is deactivated to $O(^3P)$ with unit yield ($\beta^* = 0.103 \pm 0.031$[10]) while k_a^o and β^o represent k_a and β when $[Cl_2] = 0$. The rate coefficients k_Q and k_R cannot be associated with a particular physical process, but serve to operationally separate $O(^1D)$ deactivation in the absence of Cl_2 into a component which results in $O(^3P)$ production (k_Q) and a component which results in no $O(^3P)$ production (k_R). Analysis of our two experiments with $[Cl_2] = 0$ gives $\beta^o \sim 0.217$, which, according to equation (VIII), gives $k_Q/k_a^o = 0.48$. Since $O(^1D)$ removal by O_3 is thought to produce $O(^3P)$ with near unit yield[15,16] and, under our experimental conditions, O_3 removes $O(^1D)$ at a rate of ~ 1600 s^{-1}, it appears that removal of $O(^1D)$ by background impurities in our experiments is dominated by chemical reaction rather than physical quenching. The β versus f_{Cl_2} data are shown in Figure 6. The best reproduction of the data was obtained in the simulation which assumed $k_{2c}/k_2 = 0.23$. For comparison, simulations which assume $k_{2c}/k_2 = 0$ and 1 are also shown in the figure. Considering the uncertainty of β^* and potential systematic errors in the

determination of β , we estimate that the accuracy of this branching ratio determination is about 40%, i.e. $k_{2c}/k_2 = 0.23 \pm 0.09$.

A potentially more accurate, though slightly less direct, determination of k_{2c}/k_2 was performed using reaction mixtures where Cl_2 was added in sufficient quantity ($>10^{16}$ per cm^3) to completely dominate $O(^1D)$ removal. Experiments were carried out on a time scale (50 μs per channel) where the $O(^3P)$ appearance was essentially instantaneous but the $O(^3P)$ decay was temporally resolved. The signal at time t' (= a time shortly after the laser fired when $O(^3P)$ formation had gone to completion but no appreciable decay had occurred) could be determined very accurately and represented $O(^3P)$ produced both by direct photolysis and by $O(^1D)$ deactivation. A single determination of an $O(^3P)$ yield involved back-to-back experiments where the signal at t=t' was determined with N_2 as the dominant $O(^1D)$ quencher (signal $\equiv S_{N_2}$), then with Cl_2 as the dominant quencher (signal $\equiv S_{Cl_2}$), then again with N_2 as the dominant quencher. Signals were normalized for $[O_3]$ and laser power. In addition, it was necessary to correct S_{Cl_2} for absorption of resonance lamp radiation by Cl_2. The procedure for making this correction is described elsewhere.[10] At the highest Cl_2 concentration employed,

absorption of resonance lamp radiation resulted in a 25% drop in signal count rate. Since it is known that $O(^1D)$ deactivation by N_2 produces $O(^3P)$ with unit yield, k_{2c}/k_2 could be determined from the relationship

$$k_{2c}/k_2 = \left(\frac{S_{Cl_2}}{S_{N_2}} - \Phi \right) (1-\Phi)^{-1}, \qquad (IX)$$

where Φ is the quantum yield for producing $O(^3P)$ from O_3 photolysis at 248nm, a quantity which we have previously measured to be 0.093 ± 0.028 [$\beta^*/(1+\beta^*) = \Phi$].[10] Fourteen determinations of S_{Cl_2}/S_{N_2} gave an average value of 0.323 with $2\sigma = 0.060$. According to equation (IX), we obtain for k_{2c}/k_2 the value 0.254 ± 0.097 where the quoted error is 2σ and includes uncertainties in both S_{Cl_2}/S_{N_2} and Φ. Two points are worth noting regarding this result. First, it is unlikely that secondary chemistry involving Cl, ClO, or photolytically produced $O_2(^1\Delta)$ could have influenced the measurement of k_{2c}/k_2; in order to be important, secondary chemistry would have had to occur on a time scale of a few hundred microseconds. Also, in addition to our measurement of Φ, Greenblatt and Wiesenfeld[17] have determined Φ to be 0.06 ± 0.01. Using their value in equation (IX) would have only a minor effect on the result, changing k_{2c}/k_2 from 0.254 to 0.280.

Averaging the results obtained by the two independent methods, and conservatively choosing error bars to bracket the 2σ uncertainties of both methods, gives the result $k_{2c}/k_2 = 0.24 \pm 0.10$. Reaction (2) has generally been assumed to proceed exclusively via the reactive channel (2a).[7,18] Our results, however, indicate that the physical quenching channel is significant.

There is one absolute determination of k_2 reported in the literature. Fletcher and Husain,[7] employing flash photolysis in conjunction with time resolved resonance absorption detection of $O(^1D)$, obtained the value $k_2 = (2.2 \pm 0.2)\times10^{-10}$ cm^3 molecule^{-1} s^{-1}. Husain and co-workers have studied a large number of $O(^1D)$ reactions and, in nearly all cases, report rate coefficients which are about a factor of 2.2 larger than those measured using other experimental techniques; this systematic difference is presumably due to incorrect determination of γ, a parameter which relates the absorbance to the $O(^1D)$ concentration. Interestingly, our value for k_2 is about 25% faster than the value reported by Fletcher and Husain. The reason for this deviation from the trend observed for other reactions is unclear at this time. In addition to Fletcher and Husain's measurement, Freudenstein and Biedenkapp[8] have employed flash photolysis in

conjunction with kinetic absorption spectroscopic detection of ClO to obtain a measurement of k_{2a}, the rate coefficient for the reactive channel which produces ClO, relative to the rate coefficient for the process

$$O(^1D) + O_3 \text{ ----> products.} \qquad (7)$$

Their result was $k_{2a}/k_7 = 0.75 \pm 0.25$. Using our value for $k_{2a}+k_{2b}$, $(2.14 \pm 0.34) \times 10^{-10}$ cm^3 molecule^{-1} s^{-1}, in conjunction with the recommended value[19] for k_7, gives $(k_{2a}+k_{2b})/k_7 = 0.89$. Our results are consistent with those of Freudenstein and Biedenkapp. Although it appears that $k_{2a} >> k_{2b}$, the combined uncertainties of the two studies are large enough that a significant rate for channel (2b) cannot be completely ruled out.

Acknowledgement

This work was supported by the Fluorocarbon Program Panel of the Chemical Manufacturers Association.

REFERENCES

1. F. Kaufman, Proc. Roy. Soc. A247, 123 (1958).

2. M. A. A. Clyne and J. A. Coxon, Trans. Far. Soc. 62, 2175 (1966).

3. H. Niki and B. Weinstock, J. Chem. Phys. 47, 3249 (1967).

4. J. N. Bradley, D. N. Whytock, and T. A. Zaleski, J. Chem. Soc. Far. Trans I 69, 1251 (1973).

5. F. B. Moin, Y. P. Yurkevich, and V. M. Drogobytskii, Doklady Akademii Nank SSSR 226, 866 (1975).

6. M. A. A. Clyne, P. B. Monkhouse, and L. W. Townsend, Int. J. Chem. Kinet. 8, 425 (1976).

7. I. S. Fletcher and D. Husain, Ber. Bunsenges. Phys. Chem. 80, 982 (1976).

8. K. Freudenstein and D. Biedenkapp, Ber. Bunsenges. Phys. Chem. 80, 42 (1976).

9. P. H. Wine and A. R. Ravishankara, Chem. Phys. Lett. 77, 103 (1981).

10. P. H. Wine and A. R. Ravishankara, Chem. Phys. 69, 365 (1982).

11. P. H. Wine, J. M. Nicovich, R. J. Thompson, and A. R. Ravishankara, J. Phys. Chem. 87, 3948 (1983).

12. W. B. DeMore, M. J. Molina, R. T. Watson, D. M. Golden, R. F. Hampson, M. J. Kurylo, C. J. Howard, and A. R. Ravishankara, "Chemical Kinetics and Photochemical Data for Use in Stratospheric Modeling", JPL publiction 83-62, 1983.

13. D. L. Baulch, J. Duxbury, S. J. Grant, and D. C. Montague, J. Phys. Chem. Ref. Data 10, Suppl. 1, 233 (1981).

14. D. D. Parrish and D. R. Herschbach, J. Amer. Chem. Soc. 95, 6133 (1973).

15. J. E. Davenport, B. Ridley, H. I. Schiff, and K. H. Welge, Discuss. Farad. Soc. 53, 230 (1972).

16. S. T. Amimoto, A. P. Force, and J. R. Wiesenfeld, Chem. Phys. Lett. 60, 40 (1978).

17. G. D. Greenblatt and J. R. Wiesenfeld, J. Chem. Phys. 78, 4924 (1983).

18. K. Schofield, J. Photochem. 9, 55 (1978).

TABLE I. Kinetic Data for the Reaction of $O(^3P)$ with Cl_2.*

T(K)	$[O_3]$ (10^{12} cm^{-3})	$[Cl_2]$ (10^{16} cm^{-3})	$10^{-5}\frac{[Cl_2]}{[O(^3P)]_o}$	$k'(s^{-1})$	$10^{14}(k_1 \pm 2\sigma)$** ($cm^3 molecule^{-1} s^{-1}$)
245	4.0	0		11.0	
	2.3	1.94	1.3	196	
	5.7	5.83	1.4	546	
	5.4	7.91	3.3	700	
	5.4	9.93	3.3	873	0.865 ± 0.036
264	2.3	0		6.0	
	1.0	1.20	1.3	169	
	1.2	3.24	4.1	506	
	2.0	4.47	4.5	644	
	1.9	7.09	2.4	1020	
	2.5	9.33	4.7	1260	1.36 ± 0.09
279	2.2	0		6.5	
	1.6	2.41	2.8	495	
	3.1	4.52	4.5	1000	
	2.6	6.33	4.0	1370	
	3.2	7.13	4.5	1560	2.18 ± 0.08
298	470	0		9.9	
	440	1.29	1.3	433	
	450	3.21	5.3	9.1	
	440	4.56	5.2	1420	
	520	7.80	8.7	2140	2.75 ± 0.27

TABLE I (Continued)

T(K)	$[O_3]$ (10^{12} cm^{-3})	$[Cl_2]$ (10^{16} cm^{-3})	$\frac{10^{-5}[Cl_2]}{[O(^3P)]_o}$	k'(s^{-1})	$10^{14}(k_1 \pm 2\sigma)$** (cm^{3}molecule^{-1}s^{-1})
298	300	0		10.4	
	280	0.686	5.4	186	
	340	2.18	4.8	685	
	300	4.90	7.7	1500	
	260	6.67	11	2010	3.03 ± 0.08
298	0.36	0		7.2	
	2.0	1.48	4.0	417	
	0.39	3.37	18	892	
	3.0	5.81	11	1780	3.02 ± 0.38
325	1.6	0		6.6	
	0.92	0		7.9	
	2.0	0.587	0.69	287	
	2.4	1.56	4.3	647	
	0.78	2.01	4.6	875	
	1.6	3.10	5.3	1470	
	0.64	4.40	7.7	2190	
	0.92	5.95	9.8	2890	4.93 ± 0.24
352	1.8	0		8.1	
	0.73	0		8.9	
	1.2	0.415	0.35	314	
	1.8	1.09	0.57	679	
	1.8	1.93	0.97	1300	
	2.1	2.32	1.9	1630	
	0.97	3.25	6.3	2130	
	1.8	3.71	1.7	2310	6.37 ± 0.43

TABLE I (Continued)

T(K)	$[O_3]$ (10^{12} cm^{-3})	$[Cl_2]$ (10^{16} cm^{-3})	$\frac{10^{-5}[Cl_2]}{[O(^3P)]_o}$	$k'(s^{-1})$	$10^{14}(k_1 \pm 2\sigma)$** (cm^{3}molecule^{-1}s^{-1})
371	3.1	0		15.0	
	1.6	.487	0.37	420	
	1.9	1.05	0.66	1020	
	3.1	1.36	1.4	1180	
	1.8	2.64	0.91	2320	8.72 ± 0.54

*All experiments were carried out in N_2 buffer gas at a total pressure of 150 Torr.

** Errors are 2σ and represent precision only.

FIGURE CAPTIONS

1. Typical $O(^3P)$ temporal profiles observed in studies of the reaction $O(^3P) + Cl_2$ ---> products. Experimental conditions: T = 279K; P = 150 Torr; buffer gas = N_2; $[O_3]$ in units of 10^{12} cm^{-3} = (a) 2.2, (b) 1.6, (c) 3.1, (d) 2.6; $[Cl_2]$ in units of 10^{16} cm^{-3} = (a) 0, (b) 2.41, (c) 4.52, (d) 7.13; $[Cl_2]/[O(^3P)]_o$ = (b) 2.8 x 10^5, (c) 4.5 x 10^5, (d) 4.5 x 10^5. Number of laser shots averaged = (a) 18, (b) 350, (c) 700, (d) 1235. Pseudo-first order rate coefficients derived from the data = (a) 6.5 s^{-1}, (b) 495 s^{-1}, (c) 1000 s^{-1}, (d) 1560 s^{-1}.

2. k' versus $[Cl_2]$ plots at four temperatures for the reaction $O(^3P) + Cl_2$ ---> products. Solid lines are obtained from linear least squares analyses and give the bimolecular rate coefficients tabulated in Table I.

3. Arrhenius plot for the reaction $O(^3P) + Cl_2$ ----> products. Dashed line is the recommendation of Baulch, et al. (reference 13) which is based on all previous studies. Solid line is obtained from a linear least squares analysis of our data.

4. Typical $O(^3P)$ temporal profiles observed in studies of the reaction $O(^1D) + Cl_2$ ----> products. Experimental conditions: T = 298K; P = 25 Torr; buffer gas = He; $[O_3]$ = 7 x 10^{12} cm^{-3}; $[Cl_2]$ in units of 10^{13} cm^{-3} = (a) 0, (b) 5.57; laser photon fluence = 10 mjoules per cm^2. Number of laser shots averaged = (a) 700, (b) 2065. Solid lines represent the corrected maxima, i.e. the maximum signal level which would have been attained if $O(^3P)$ did not decay during the

time required for $O(^1D)$ removal to go to completion. The photolysis laser fired at t = 0. The circled point is the extrapolated signal at t = 0. Results derived from the data are (a) k_a = 3890 s^{-1}, β = 0.222 and (b) k_a = 19000 s^{-1}, β = 0.405.

5. k_a versus $[Cl_2]$ plot. The solid line is obtained from a linear least squares analysis and its slope represents the bimolecular rate coefficient for the reaction $O(^1D) + Cl_2$ ----> products.

6. β versus f_{Cl_2} plot. Solid lines represent simulations carried out using a procedure described in the text. Values for k_{2c}/k_2 used in the simulations are shown in the figure.

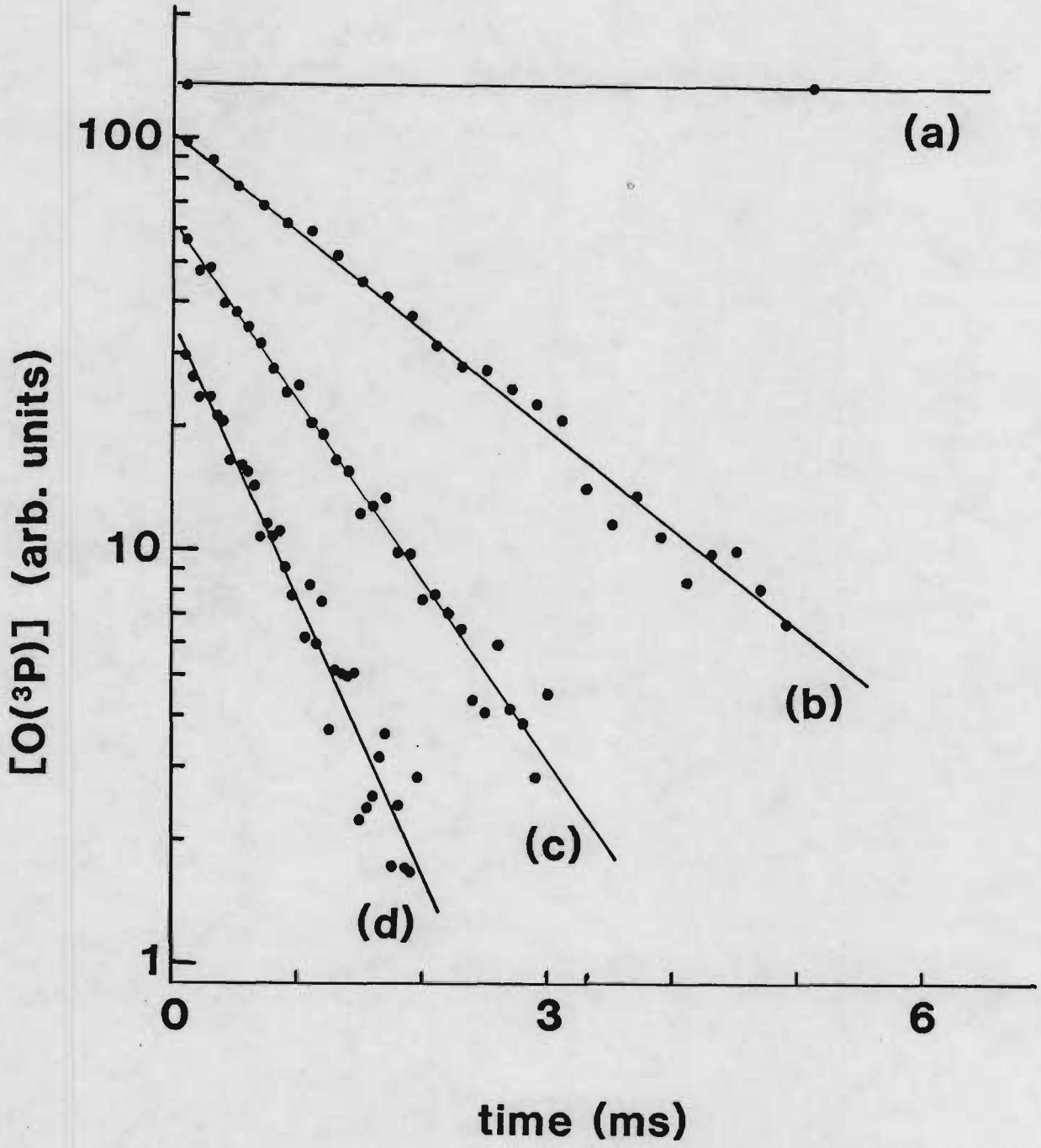
100
10
1
0
3
6
(a)
(b)
(c)
(d)
[O(³P)] (arb. units)
time (ms)

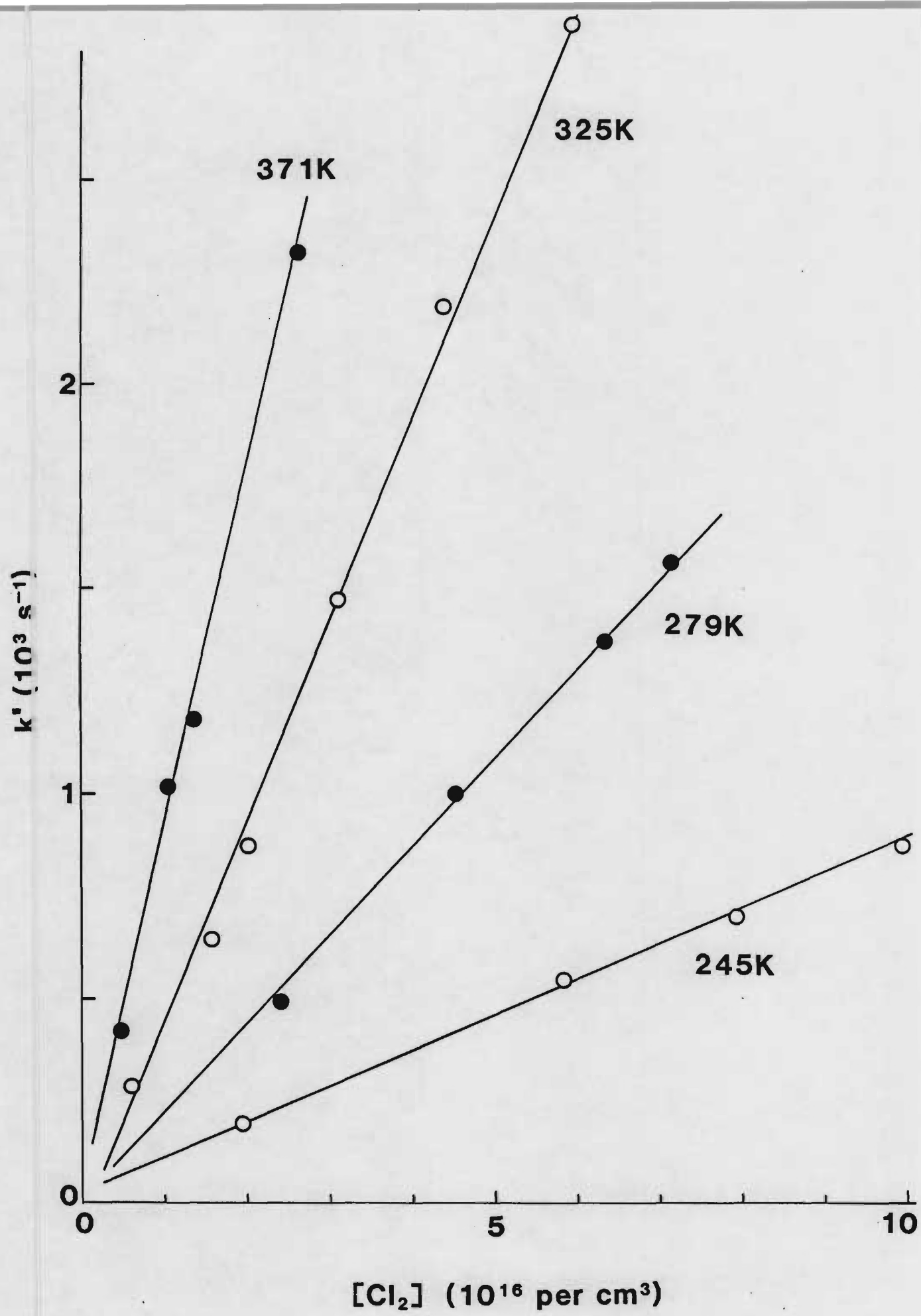
371K
325K
279K
245K
k' (10³ s⁻¹)
0
1
2
0
5
10
[Cl₂] (10¹⁶ per cm³)

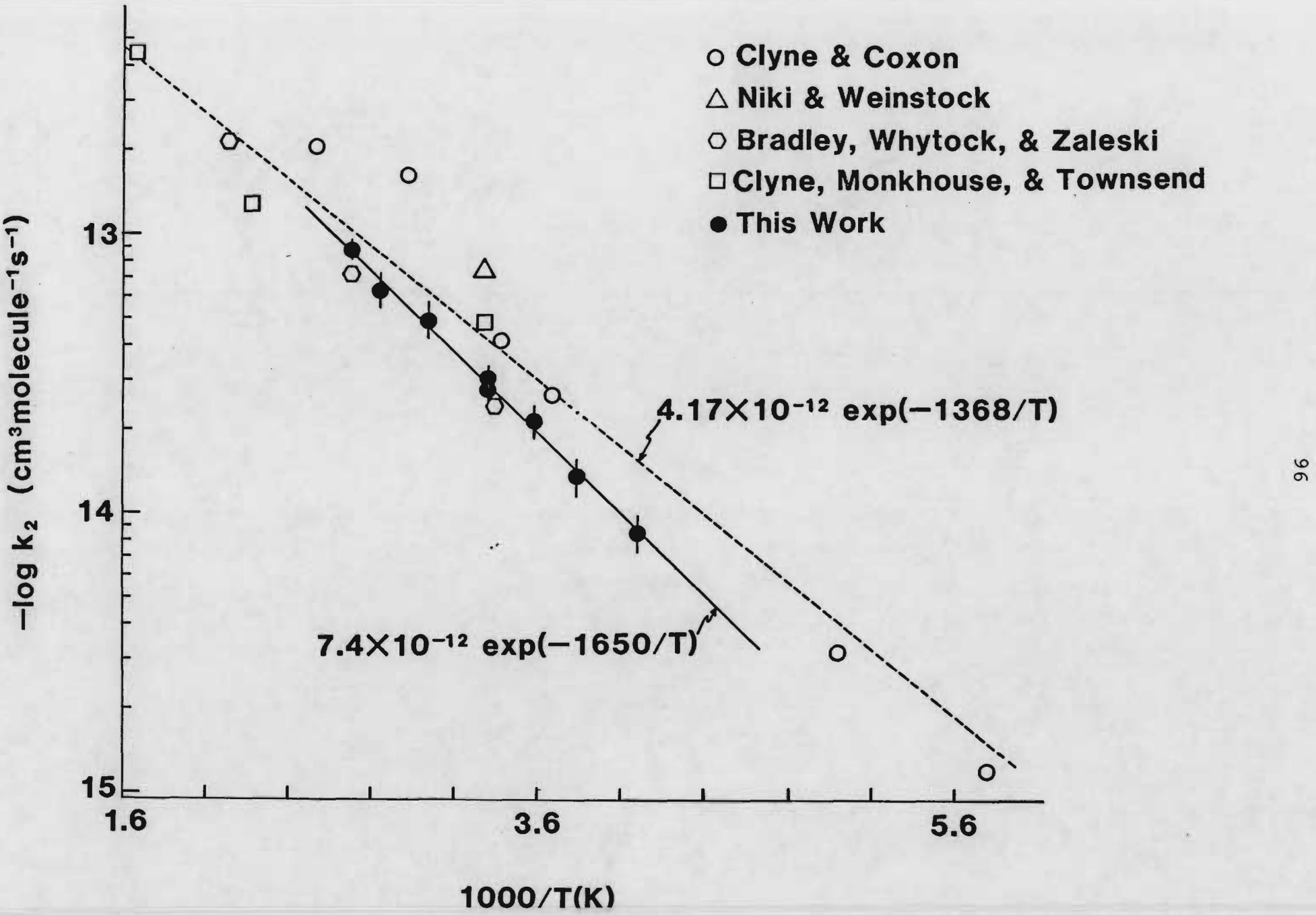
Clyne & Coxon
Niki & Weinstock
Bradley, Whytock, & Zaleski
Clyne, Monkhouse, & Townsend
This Work
4.17X10⁻¹² exp(−1368/T)
7.4X10⁻¹² exp(−1650/T)
−log k₂ (cm³molecule⁻¹s⁻¹)
13
14
15
1.6
3.6
5.6
1000/T(K)

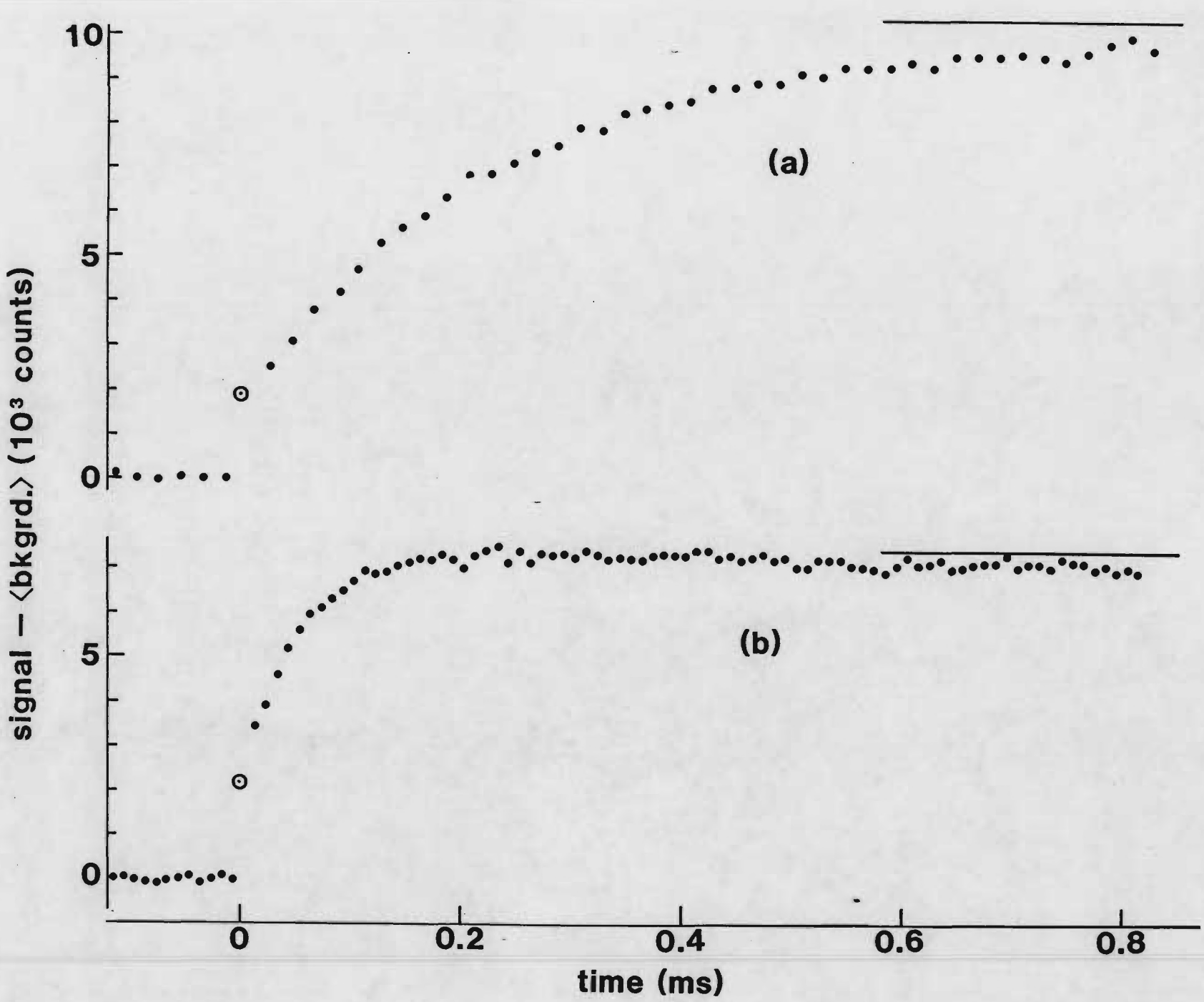
10
5
0
(a)
5
0
(b)
signal − ⟨bkgrd.⟩ (10³ counts)
0
0.2
0.4
0.6
0.8
time (ms)

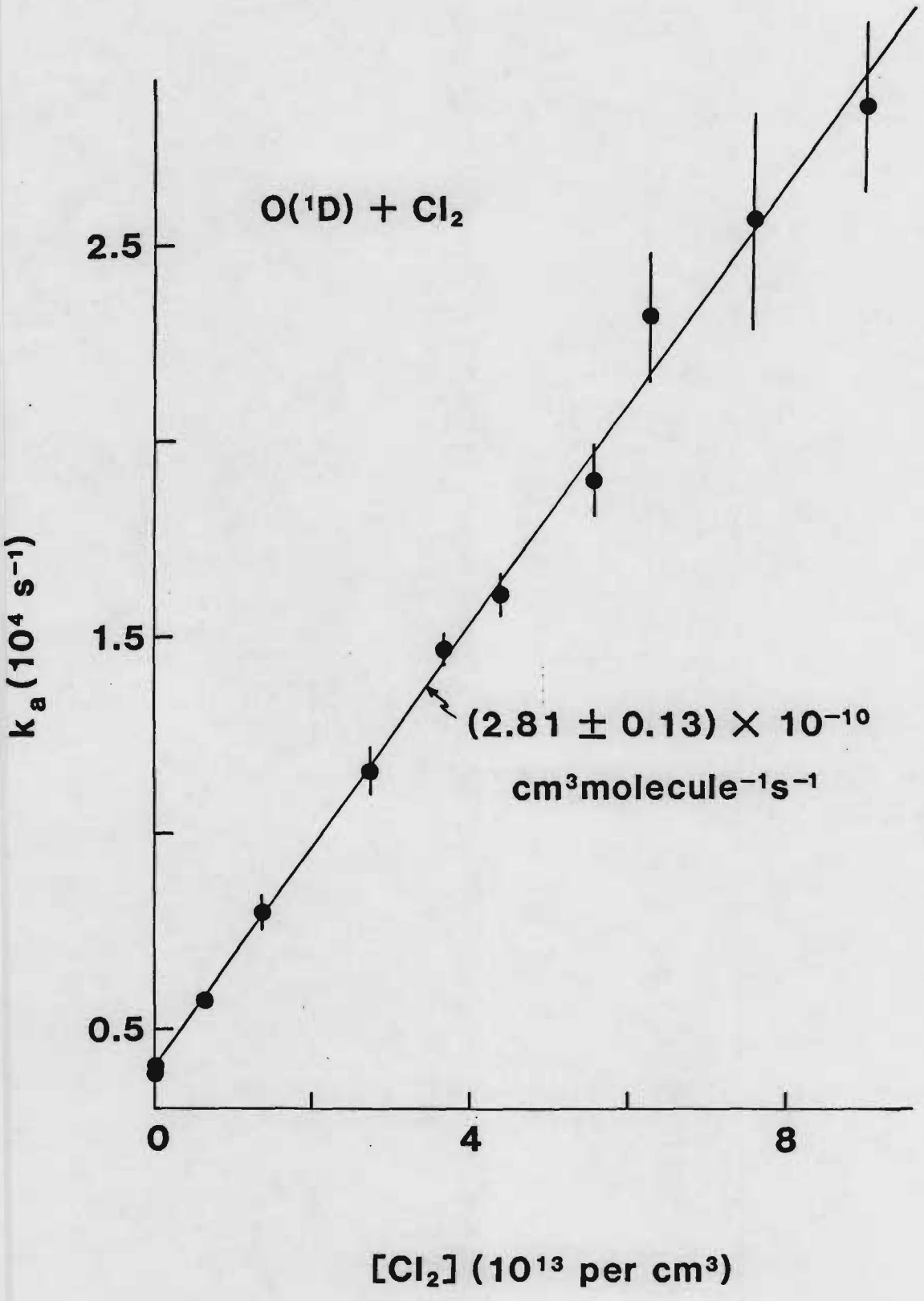
O(¹D) + Cl₂
2.5
1.5
0.5
k_a (10⁴ s⁻¹)
(2.81 ± 0.13) × 10⁻¹⁰
cm³molecule⁻¹s⁻¹
0
4
8
[Cl₂] (10¹³ per cm³)

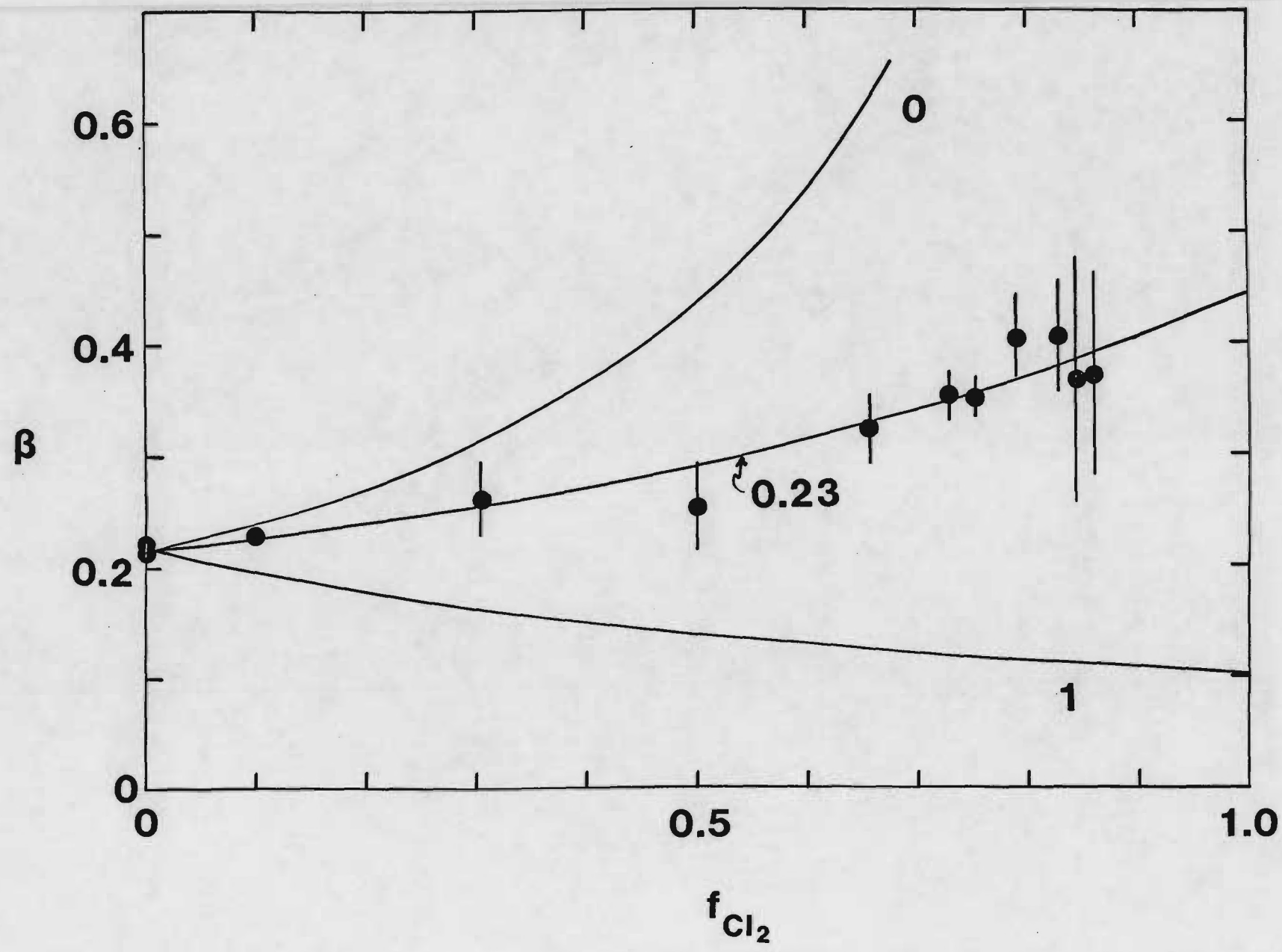
0.6
0.4
0.2
0
β
0
0.5
1.0
f_{Cl_2}
0
1
0.23